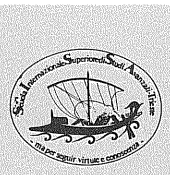

ISAS - INTERNATIONAL SCHOOL FOR ADVANCED STUDIES

DYNAMICAL FRICTION AND THE EVOLUTION OF CLUSTERS OF GALAXIES

Thesis submitted for the attainement of the degree of

"Philosophiae Doctor"

Astrophysics Sector

Candidate:

Vincenzo
Antonuccio

Supervisor:

Prof. D.W. Sciama

TRIESTE

SISSA - SCUOLA INTERNAZIONALE SUPERIORE DI STUDI AVANZATI
TRIESTE
Strada Costiera 11

DYNAMICAL FRICTION AND THE EVOLUTION OF CLUSTERS OF GALAXIES

Thesis submitted for the attainement of the degree of

"Philosophiae Doctor"

Astrophysics Sector

Candidate:

Vincenzo
Antonuccio

Supervisor:

Prof. D.W. Sciama

I dedicate this work to
the memory of my "zia",
COSTANZA TORALDO DI CALIMERA

Acknowledgements

I would like to thank my supervisor, prof. D.W. Sciama, for his support and advice during the years I spent as a student at SISSA and after.
My greatest gratitude goes also to dr. B.J.T. Jones, for his support during one of the worst periods of my life, and for the many talks we had on various subjects related to cosmology.
I am very glad to have the opportunity to thank dr. S. Colafrancesco for many discussions who clarified my ideas. I am also indebted to prof. S. Matarrese, drs. A.B. Romeo, R. Fazio, H. Vedel, J. Hjorth, F. Atrio-Barandela.
Finally, I thank very much all the staff of the Catania Astrophysical Observatory ITALY, and of the Niels Bohr Institute and NORDITA, Copenhagen, DENMARK, where this work was conceived and performed. All the calculations were performed on the CONVEX C210 of the Catania Astrophysical Observatory, ITALY, and I am very glad to thank my local CONVEX system manager, P. Massimino, for having kindly convinced me to commute to the Unix operating system and for his constructive assistance during the calculations. Among the staff of NORDITA, a special thank to the director, prof C. Pethick, and to prof. R. Svensson, for their silent help. The NBI system manager, B. Nilsson, deserves a special thank for his help and advices during the years I spent at NORDITA and NBI.

Abstract

The role of dynamical friction on the formation and evolution of structure on the scale of cluster of galaxies, is reconsidered and discussed. Dynamical friction originates from the fluctuating gravitational field generated by small-scale substructure. The latter is predicted to be abundantly produced in a typical hierarchical clustering model for structure formation, like the standard Cold Dark Matter model. The small random force field of the substructure can significantly affect the formation and dynamics of those large-scale structures whose formation times are long, like clusters of galaxies.

After a review of the main theoretical ideas and observational facts concerning the structure and dynamics of clusters of galaxies (chapters 1 and 2) we investigate the statistical mechanics of the fluctuating gravitational force field component in discrete systems (chapter 3). Our treatment is very general and can be applied to any system where correlations are still in the linear. We show that clustering affects significantly the force probability distribution, through a term proportional to the an integral of the correlation function. We also derive an equation for the probability distribution of the torques' generated by the density peaks of the small scale substructure.

The force probability distribution depends linearly on the correlation function. In turn, it determines the dynamical friction coefficient. In chapter 4 we calculate this coefficient and we study the dynamics of shells of matters within a clustered medium. It turns out that the effects of dynamical friction can be quite large, especially on the infall of the outermost shells. We also study the effect of this modified accretion on the mass spectrum of cosmic structures which should arise. Our results are in qualitative agreement with previous studies.

Finally, we study how dynamical friction affects the evolution of clustering. In chapter 5 a self-consistent self-similar solution of a truncated BBGKY hierarchy set of equations is found. We find that dynamical friction can affect significantly the pairwise velocity distribution, but that the effect on clustering is not very large. Our results are confirmed by some numerical simulations we per-

formed with an N-body code, to which a small scale fluctuating force field has been added to simulate the secular effects of small-scale substructure, which are usually neglected in ordinary N-body codes. A glance at some possible future developments concludes the thesis (chapter 6).

All the original work contained in this thesis is also contained in some papers published or submitted, and in some of these the candidate (**V. Antonuccio**) appears as a co-author. However, after agreement with the other authors, we decided to include in this thesis *only those parts which are entirely original contributions of the candidate.* A comparison with the aforementioned papers can easily allow the reader to identify these contributions.

Contents

1 Structure and Dynamics. 1

1.1 Structure and Substructure. 2

1.2 Mass estimates and Density Profiles. 4

1.3 X-ray Emission. 9

1.4 Structural Relations. 11

1.5 Luminosity Function and Mass Spectrum. 15

1.6 Observational Evidence of Subclustering. 18

2 Evolution of Density Perturbations. 24

2.1 Density and Velocity Fields. 28

2.1.1 Spherical Density Perturbation and Secondary Infall. . . . 31

2.1.2 Early Nonlinear Stages. 33

2.1.3 Late Nonlinear Stages - Numerical Simulations. 34

2.2 Bibliography for Chapters 1 and 2. 42

3 Gravitational Field Fluctuations in Weakly Clustered Systems. 50

3.1 Introduction. 50

3.2 Force Probability Distribution. 56

3.3 Torque Probability Distribution. 62

3.4 Probability Distributions in Protogalactic Structures. 64

3.4.1 Power-law Spectra. 66

3.4.2 Cold Dark Matter Spectrum. 67

3.5 Conclusions. 67

3.6 Appendix A. Asymptotic evaluation of $\Sigma_{cl}(\mathrm{k})$. 69

4 The effect of Dynamical Friction on the Secondary Infall of Matter on Protoclusters. 80

4.1 Introduction. 80
4.2 Dynamical Friction Coefficient. 82
4.3 Dynamics. 85
4.4 Mass Spectrum. 89
4.5 Conclusions. 92
4.6 Appendix 1. 94
4.7 Appendix 2. 97

5 Evolution of Clustering in CDM Models. 106
5.1 Introduction. 106
5.2 BBGKY Hierarchy. 108
5.3 Self-similar Solutions. 112
5.4 Results. 116
5.5 Final Remarks. 119

6 Concluding Remarks and Prospects for Future Work. 126
6.1 Bibliography for Chapters 3, 4, 5 and 6. 128

Chapter 1

Structure and Dynamics.

The study of the dynamics of clusters of galaxies plays for many reasons a central role in contemporary cosmological theories. As Zwicky (1933) and Smith (1936) first discovered there exists a discrepancy between the total amount of mass contained inside the galaxies in a typical cluster and the amount required to ensure that clusters are in stable equilibrium configurations, given the observed velocity dispersions. This observation has led to the idea that the M/L ratio, as determined from the dynamics, is an increasing function of the distance from the center, raising as a consequence the problem of the existence of Dark Matter (see, e.g. Bahcall (1977)) on distance scales $1 - 10h^{-1}Mpc$. This idea has been further confirmed by more recent studies using a variety of tools, such as redshift surveys (Dressler & Schechtman, 1988; Colless, and Hewitt, 1987), analysis of X–ray profiles (Forman & Jones, 1982; Sarazin, 1988; Eyles et al., 1991; Briel et al., 1992; Gerbal et al., 1992), number counts of low–surface brigthness galaxies (Binggeli, Sandage and Tammann (1987)). However, the *quantitative* assessment of the increase of M/L inside clusters and, in general, of other properties like the density profile, the velocity dispersion, the velocity anisotropy, is still far to be complete. Large uncertainties exist in the knowledge of the total M/L and of other quantities even for the nearest and well known clusters like Virgo, Fornax and Coma. The principal reason is the paucity of data on statistically significant samples of galaxies inside these clusters, and of X–ray temperature profiles.
In this chapter we will review the current observational and theoretical knowledge concerning clusters of galaxies. At this point, it would be useful to have a definition of clusters which could unambigously restrict the kind of physical entities we desire to study. This definition should be physically motivated, so

as to make possible a comparison with the results of theoretical studies. More often clusters are defined as objects included in catalogs compiled according to some observational criteria: mostly relying on the galaxy overdensity over some regions of the sky (Abell, 1958; Zwicky et al., 1961–1968). Although it can seem heuristic, it turns out that this definition singles out a sample of objects having some common properties (Sarazin, 1988), like an universal density profile and some features in the velocity dispersion profiles. Our main purpose is to present some background material for the next chapters, so our review does not pretend to be complete. More comprehensive reviews which we have taken into account are those of Bahcall (1977a), Sarazin (1986, 1988), Geller (1990), West (1990), Richstone (1990) and Cavaliere & Colafrancesco (1989).

1.1 Structure and Substructure.

Clusters of galaxies often appear irregular and their distribution is far from being spherically symmetric. In irregular clusters projection effects further complicate the problem of obtaining the intrinsic shape of the matter distribution. However, for most clusters the azimuthally averaged surface luminosity density profile can be adequately described by the surface density law:

$$\mu_L = \mu_{L0} \frac{r_c^2}{r_c^2 + r^2} \tag{1.1}$$

Azimuthally averaged profiles are obtained after having divided the region around the photometric center of the cluster in concentric shells and averaged the number of galaxies in each shell. A density profile which is also often adopted is the De Vaucouleur's law:

$$\mu_L = \mu_{L0} \exp\left[-7.67 \left(\frac{r}{r_c}\right)^{1/4}\right] \tag{1.2}$$

The validity of eq. 1.1 for a sample of 27 Abell clusters has been proved by Dressler (1978b) and Colless and Hewitt (1987) (see also West et al., 1987). One noteworthy feature of the eq. 1.1 is that the space density corresponding to it is given by:

$$\rho(r) = \rho_0 \frac{r_c^3}{[r_c^2 + r^2]^{3/2}}, \tag{1.3}$$

with: $\rho_0 = \mu_{L0}/2r_c$, and King (1962) has showed that this density profile provides an acceptable approximation to the density profile of a system whose distribution

function is a truncated maxwellian:

$$f(\mathbf{r},\mathbf{v}) = \begin{cases} c\exp\left[\frac{\Phi(0)-\Phi(r)}{\sigma_0^2}\right]\left\{\exp\left(-\frac{v^2}{2\sigma_0^2}\right) - \exp\left(\frac{\Phi(r)}{2\sigma_0^2}\right)\right\} & v^2 < \Phi(0) \\ 0 & v^2 \geq \Phi(0) \end{cases} \tag{1.4}$$

In the above equation $\Phi(r)$ and σ_0 are the potential and velocity dispersion, respectively, of a non truncated system with the same total mass. The adoption of the model described by eqs. 1.3– 1.4 implies the assumption that clusters are truncated systems. Observations actually show a rapid decline of the number density of galaxies in many clusters after about $30r_c$(Bahcall, 1977). However, it is very difficult to establish firmly the outer boundary of a cluster, because often clusters are embedded inside superclusters and the contamination due to the background contribution is very difficult to assess (Sarazin, 1986; Dressler, 1978b). Theoretical arguments based on the tidal torques produced by neighbouring substructure on a collapsing protocluster suggest that actual clusters could be tidally limited, bounded systems (Peebles, 1968).

In truncated isothermal models the density distribution is specified by three parameters, namely μ_{L0} or ρ_0, r_c and R_h, the latter being the truncation radius. Bahcall (1975) has observed that the core radius r_c of many rich compact clusters have remarkably comparable values:

$$r_c = (0.25 \pm 0.004)\, h^{-1} Mpc, \tag{1.5}$$

where h is the Hubble constant in units of 100 Km/sec/Mpc. A similar conclusion was reached by Dressler (1978b) who found a larger value for the dispersion , namely: $0.07h^{-1}$. This fact suggests the possibility that the central part of clusters are actually relaxed system: if violent relaxation took place, an universal value for r_c could easily arise. Recently have appeared in the literature claims that the central density profiles of rich clusters has a cusp and increase like r^{-1} (Beers & Tonry, 1986; Merrifield & Kent, 1990). This could indicate that galaxy orbits are more radial near the center, and so the galaxy population in the core of the clusters could not be isotropic and virialized. One must observe, however, that it is very difficult to determine the density and velocity profile for $r \leq r_c$, simply becasue there are very few galaxies (Geller, 1990): so the question of the existence of a central cusp remains open and demands for further study.

If one assumes that clusters are actually relaxed and virialized and that the

distribution functions can be described by the above truncated isothermal laws, the central luminous surface mass density will be given by:

$$\mu_{L0} = \frac{9\sigma_c^2}{2\pi G r_c}. \tag{1.6}$$

Typical observed values for σ_c are 750 Km/sec (Geller, 1990), so using eq. (1.6) and the relation between central density and surface luminosity given above, we get a typical value: $\rho_c \approx 1.4 \times 10^{15} M_\odot h^2/Mpc^3$. A typical value for the central luminosity density is $4 \times 10^{12} h L_\odot/Mpc^3$, and these values give a typical mass–to–light ratio:

$$M/L \approx 300^{+723}_{-166} h M_\odot/L_\odot. \tag{1.7}$$

Similar and somewhat higher values are obtained if one accounts only for total luminosity at blue magnitudes (Rood, 1981; Sarazin, 1988). These numbers show the importance of the dark matter on the scale of clusters of galaxies. For comparison, for single galaxies one has $M/L \approx 1 - 25 h^{-1} M_\odot/L_\odot$. Observe also that the above values for the velocity dispersion have been obtained extrapolating the azimuthally averaged data for galaxies in the central regions, so they are rather free of random scatter, although can be affected by systematic errors due to subclustering. Even larger values of the M/L have been obtained by Colless and Hewitt (1987) for a sample of 25 clusters: $M/L \approx 500 \pm 100 M_\odot/L_\odot$.
From these numbers, one obtains an estimate of the contribution from clusters to the total density of the Universe: $\Omega_{cl} \approx 0.2 e^{\pm 0.2}$, which can be compared to the upper limit for baryons from nucleosynthesis, $\Omega_b \approx 0.0016$.

1.2 Mass Estimates and Density Profiles.

The estimates of the value of the M/L ratio for clusters are not free from uncertainties connected with the model assumptions. The hypothesis underlying the derivation of eq. (1.7) is that the matter generating the gravitational potential is distributed in the same way as the visible matter, i.e. that there is no **segregation** between dark and baryonic matter, an hypothesis which could be tested by detailed comparison between theoretical models and observed galaxy distribution functions (Kent & Gunn, 1982; Kent & Sargent, 1983).
The total gravitating mass in a cluster can be estimated by means of the virial

theorem. Assuming spherical symmetry and that time averages and phase-space averages coincide, the virial theorem gives:

$$\langle \frac{M(r)}{r} \rangle = \frac{1}{G} \langle v^2 \rangle \tag{1.8}$$

the brackets indicating phase-space averaging. In practical applications one identifies the above averages with averages over all the galaxies in the sample: this amounts to assume that galaxies represent a fair sample of the underlying phase-space distribution, i.e. that they are a well-mixed population and, more important, that the galaxy distribution traces the total mass distribution. Both these hypotheses must not be necessarily true if galaxies inside a cluster form only at local peaks of the density field, as predicted by biased galaxy formation theories (Kaiser, 1984). Under the additional hypothesis of energy equipartition the intrinsic mean squared velocity is simply connected to the observed projectec total velocity: $\langle v^2 \rangle = 3 \langle v^2 \rangle_{obs}$. Assuming then an uniform mass distribution one obtains an estimate for the total mass:

$$M_{virial} = \frac{\langle v^2 \rangle}{G \langle r^{-1} \rangle} \tag{1.9}$$

However, we had to introduce a number of significant hypotheses.
The virial theorem allows one also to get lower and upper limits of the total mass of a cluster, as was shown by Merritt (1987). Following, this latter paper, let us write: $M_{tot}(r) = M_T F(r), 0 \leq F(r) \leq 1, 0 \leq r \leq R_h$, where M_T is the total mass of the cluster. Then from eq. (1.8) one gets:

$$M_T = \frac{\langle v^2 \rangle}{G \langle F(r) r^{-1} \rangle} \tag{1.10}$$

The numerator is obtained from the observed galaxies' velocities and is then fixed. The denominator, on the other hand, is model dependent, and it is clear that a minimum value for M_T can be obtained by maximizing it. Taking into account the limit on $F(r)$ one then obtains:

$$M_{min} = \frac{\langle v^2 \rangle}{G \langle r^{-1} \rangle} \tag{1.11}$$

The maximum value of M_T can be obtained by minimizing $F(r) r^{-1}$; for instance, one could imagine to put all the mass near the outer boundary $r \approx R_h$. But this correspond to an unrealistic density distribution, increasing with distance

from the center. On the other hand, if we impose the additional constraint that the density must be a non-increasing and continously differentiable function of r, then $F(r)$ must verify the additional condition:

$$\frac{d}{dr}\left(\frac{1}{r^2}\frac{dF}{dr}\right) = 9x^2\frac{d^2F}{dx^2} \leq 0, \tag{1.12}$$

where $x \equiv r^3$. The function $F_1(x) = x/R_h^3$ is the maximal function satisfying the above inequality under the proper constraint, i.e. any other function verifying the boundary cconditions: $F(0) = 0, F(R_h^3) = 1$ is necessarily smaller than F_1 at some point in the interval. One the concludes that the maximum mass can be written as: $M_{max} = R_h^3\langle v^2\rangle/G\langle r^2\rangle$, and this produces a minimum central density:

$$\rho_{min} = \frac{3}{4\pi G}\frac{\langle v^2\rangle}{\langle r^2\rangle} \tag{1.13}$$

Applying eqs. (1.11- 1.12) to the Coma cluster and using the galaxy density profile $F(r)$ favored by Kent & Gunn (1982), which corresponds to a truncated King model, one obtains the following limits (Merritt, 1987):

$$M_{min} = 0.19M_{virial}, \qquad \rho_{min} = 10^{-3}\rho_{virial}. \tag{1.14}$$

One concludes that the estimates of M and consequently of the total M/L based on the virial estimators can be subject to rather large uncertainties.
Apart for these problems, the use of virial mass estimators to determine the mass of clusters and groups of galaxies has been criticized on purely statistical bases (Neymann, 1961; Bahcall & Tremain, 1981; Heisler et al., 1985). As we noticed above, the virial theorem involves some averages taken over the sample. One can then ask which is the statistics of the quantities $\langle v^2\rangle$ and $\langle r^{-1}\rangle$ introduced above, for various possible distributions, and how the statistical uncertainties affect the probability of getting values of the mass very far from the median ones. Bahcall & Tremaine (1985) showed that the virial theorem mass estimator can be regarded as a poor statistic estimator, being *biased* and *inefficient*. We try to summarize shortly their arguments:

- *Bias*: The harmonic sum $\langle r^{-1}\rangle = \sum_{i=1}^{N}\sum_{j\leq i} r_{ij}^{-1}$ is strongly affected by the presence of a few pairs having a small separation. The paradoxical case would be a system where all particles lie in short–distance pairs rather than being randomly distributed.

- *Inefficiency.* It can be easily shown that the variance of the quantity $\langle r^{-1} \rangle$, i.e. the difference: $\langle r^{-2} \rangle - \langle r^{-1} \rangle^2$ diverges for an isotropic sample. This implies that the standard deviation of the virial mass is not lesser than $\pi^1 \, (2 \ln N)^{1/2} \, N^{-1/2}$, and so it converges slower than $N^{-1/2}$, which is the usual decrease of a statistical estimator having a Poisson statistics.

In the same paper Bahcall & Tremaine (1985) suggest another estimator which, for systems having a velocity distribution enough anisotropic, should give a better estimate of the total mass:

$$M_{BT} = \frac{24}{\pi G N} \sum_{i=1}^{N} v_{zi}^2 r_i \tag{1.15}$$

In eq. (1.15) N is the total number of galaxies and v_z the line-of-sight velocities. Moreover, they show that for reasonable small samples ($N \leq 20$) this statistical indicator has a variance diminishing enough rapidly with the size of the sample. The problem with M_{BT} is that the average distribution of anisotropy should be known *a priori*, or at least one should be enough sure that in no part of the cluster the orbits are predominantly circular, otherwyse the estimates base on M_{BT} are grossly in error. The arguments by Bahcall & Tremaine (1985) are then very relevant for the determination of mass in groups and poor clusters for which the number of redshifts determined is not very high, or for those clusters like Coma for which most velocity determinations are mostly restricted to the central part of the cluster, so that an unbiased estimator should be preferred. Recent confirmation of the merits of Bahcall & Tremaine's (1985) estimator come both from observational (Malumuth et al, 1992) and theoretical (Thomas & Couchman, 1992) studies.

All the estimates based on the virial theorem are global estimates, because involve averages of quantities over all the extension of the cluster. It seems then reasonable to suspect that a detailed self-consistent modelling of the density and velocity dispersion profiles could set more stringent limits on the dark matter distribution and the M/L ratio, at least inside spherical, relaxed clusters. In order to reliably perform such an anlysis, positions and velocities for a large subsample of galaxies inside the cluster are required. Although the number of known redshifts of galaxies in clusters has been increasing in the last years, the

analysis of these data is still subject to large uncertainties. The main reason lies in the fact that also in apparently relaxed, spherical clusters like Coma the data are scattered over a large region and this makes a quantitative evaluation of the velocity dispersion profile subject to rather large uncertainties (Kent & Gunn, 1982). Moreover, from the observations one can determine two quantities, namely the surface density $\Sigma(r)$ and the line-of-sight velocity dispersion $\sigma_{ls}(r)$. The latter is connected to the radial and tangential velocity dispersion through a simple geometrical relation:

$$\Sigma(r)\sigma_{ls}^2(r) = 2\int_r^\infty d\lambda \frac{\lambda\rho_g(\lambda)}{\sqrt{\lambda^2 - r^2}}\left[\sigma_r^2 - \frac{\lambda^2}{r^2}\left(\sigma_r^2 - \sigma_t^2\right)\right] \tag{1.16}$$

where $\rho_g(r)$ is the galaxy density and σ_r, σ_t are the radial and tangential velocity dispersions, respectively. These latter quantities are connected through the Jeans' equation:

$$\frac{d}{dr}\left(\rho_g\sigma_r^2\right) + \frac{2\rho_g}{r}\left(\sigma_r^2 - \sigma_t^2\right) = -\frac{G\rho_g M_{tot}(r)}{r^2} \tag{1.17}$$

The mass M_{tot} is the total gravitating mass: it includes the contribution of the dark component. We have now 2 equations in the three variables, namely σ_r, σ_t and $M_{tot}(r)$. The problem is clearly underconstrained, but if one adds some additional constraint, as for example the condition that the dark matter density is a decreasing function of the distance:

$$\frac{d}{dr}\left(\frac{1}{r^2}\frac{dM_{tot}}{dr}\right) \leq 0,$$

or that the anisotropy $\beta = 1 - \sigma_t^2/\sigma_r^2$ should increase with distance (consistently with theoretical sufggestions from N–body simulations) one could hope to restrict significantly the range of possible dark matter distributions. It is however clear now that the situation is different (Merritt, 1987; Kent & Gunn, 1982): presently available data sets do not allow one to put firm constraints on the range of possible models. For example, the data by Kent & Gunn (1982) on Coma can be well fitted by models with an increasing anisotropy as well as by isotropic models, and anyhow both these models could be rejected with confidence limits higher than 85% (Merritt, 1987).

Another interesting tool to constrain the mass distribution is the spatial derivative of the cumulative distribution function of the line-of-sight velocities $N(v_{ls})$. If one

assumes a lowered truncated maxwellian as a model for the distribution function (eq. 1.4), then Merritt (1987) has shown that $N(v_{ls})$ verifies an equation:

$$\frac{dN}{dv_{ls}} = 16\pi^2 \int_0^{r_{max}(v_{ls})} dr r^2 \int_{v_{ls}}^{v_{max}(r)} dv v f\left[\frac{v^2}{2} + \Phi(r)\right] \qquad (1.18)$$

where $r_{max}(v_{ls})$ is the maximum distance a galaxy can travel, given the observed projected velocity v_{ls} and the (real) distance from the center r. One easily understands that r_{max} is determined by inverting the energy conservation equation: $2\left[\Phi(0) - \Phi(r_{max})\right] = v_{ls}^2$. The quantity on the left-hand side of eq. (1.18) can be estimated by binning the data in concentric shells at given distances from the center, once the functions $v_{max}(r)$ and $r_{max}(v_{ls})$ is known from a model density-potential distribution. However, the observed distribution of dN/dv_{ls} for the Coma cluster is clearly skewed, so that no isotropic model as the truncated isothermal one on which the deduction of the right-hand side of eq. 1.18 was based can ever be a good model. This skewness is an indication of subclustering, whose occurrence in Coma has been recently confirmed by ROSAT observations (Briel et al., 1992). From this example one concludes that oversimplified studies which do not take into account the real spatial and velocity structure of the galactic population can lead to large uncertainties in the determination of the intrinsic properties of a cluster.

1.3 X-ray Emission.

Clusters of galaxies show a diffuse X–ray emission which has been broadly investigated since its discovery in the seventies' (Cavaliere et al., 1971; Giacconi et al., 1972, 1974; Sarazin, 1986). It is now acknowledged that a large fraction of this emission in the range $3 - 30 kev$ comes from bremsstrahlung electron radiation emitted by high temperature intracluster gas (Felten et al., 1966; Sarazin, 1986). Simple calculations show that the cooling time of this gas is much larger than the typical dynamical time for most clusters, so it in dynamical equilibrium within the gravitational potential generated by the Dark Matter distribution. From the shape of the spectrum one can get an average electronic temperature of this intracluster plasma, and measurements of the total integrated emission provide values for the electronic density, so that the total mass of this emitting plasma can be estimated. Simple calculations show that this mass is at least

comparable with the total mass of the galaxies inside the cluster, and that the gas is not self-gravitating (except maybe near the center and in those regions where a cooling flow is seen), so that the dominant gravitational field is that of the dark matter component. The intracluster plasma is then expected to relax into the gravitational field of the dark matter, and for this reason it is believed to trace the gravitational potential of the cluster. A full review of the X–ray cluster emission is well beyond the purposes of this thesis: here we will only report on few aspects more directly connected with the mapping of the cluster gravitational potential and the dynamics.

Mapping of the X-ray spectrum of the intracluster gas at different points can provide the local density and temperature distribution of the dark matter inside a cluster. Moreover, many clusters at high redshift are not easily resolvable at optical wavelemgths but can be easily detected as X-ray sources, so that one can obtain data and statistics for many more clusters than those in the catalogues (Cavaliere & Colafrancesco, 1989). Until now, however, the detectors used on-board the X-ray satellites had not enough resolving power to allow detailed maps of the temperature and electroni density distributions across a cluster, which is necessary to get a detailed density profile of the gas and of the dark matter.

Most of the analyses of the X–ray emission from clusters performed until now agree on finding very high values for the total clusters' mass, consistently with the results of the optical studies (Sarazin, 1986). For example, Hughes (1989) finds a total mass for the Coma cluster of $M_{tot} \approx 55 - 150 \times 10^{13} M_{\odot}$ within a radius of $2.5 h^{-1}$ Mpc. Recent investigations have however cast some doubts on some old ideas about the distribution of dark matter and the total amount of X-ray emitting gas in clusters. Eyles et al. (1991) performed observations of the Perseus cluster with the SL2 XRT facility onboard the *SPACELAB 2* mission. In the broad range of energy they scrutinized ($2.5 - 25$ kev) this instrument was able to map the variation of the spectrum with distance from the cluster center. Sound speed is usually high enough in the intracluster gas, so one can assume that transport mechanisms are efficient and the gas is described by an ideal equation of state. Under the hypothesis that the intracluster gas is spherically symmetric distributed, the gravitational mass generating the potential in which it lies can be obtained from the Jeans' equation and from the equation of hydrostatic

equilibrium:

$$M_{tot}(r) = -\frac{kT_X(r)}{G\mu m_p}\left[\frac{d\ln\rho_X(r)}{d\ln r} + \frac{d\ln T_X(r)}{d\ln r}\right] \tag{1.19}$$

where m_p is the proton mass and μ the mean molecular weight. Eyles et al. (1991) modelled the total density with an Hubble profile:

$$\rho_X(r) = \frac{\rho_{0X}}{[1+(r/r_c^2)]^{3/2}} \tag{1.20}$$

with different values of the four parameters in eqs 1.19– 1.20 and temperature profiles. Their best fit model has a core radius $r_c = 0.26$ Mpc, $\beta = 1.12$ and a central $M/L = 100 M_\odot/L_\odot$ (assuming $H_0 = 50$ Km/sec/Mpc, considerably lesser than the quoted median values given above. The total gravitating mass within $1.3 Mpc$ of the center amounts to $5.7^{14} M_\odot$, compared to the value $2^{15} M_\odot$ found from the virial mass estimate by Kent & Sargent (1983). Moreover, the total mass contributed by the gas is about 80 times larger than the mass contained inside galaxies. Similar results have been obtained by Gerbal et al. (1992) from an analysis of the IPC Einstein data of two apparently relaxed clusters of galaxies. However, in the light of the comments by Cavaliere & Colafrancesco (1989), these results could also indicate toward an intrinsic variance in the average cluster properties originated from unresolved substructure. It is evident that no firm conclusion can be established before new extensive analyses will be completed and data from ROSAT and AXAF will be available. It is interesting to observe that the variance in observed global cluster parameters can be used to constrain hierarchical clustering models of cluster formation (Cavaliere & Colafrancesco, 1989), as has been recently done by Henry & Arnaud (1991)
It is then evident the importance of detailed large–band X–ray observations of clusters, and of the detailed comparison with the results of optical studies.

1.4 Structural Relations.

One can expect to gain information about the mechanism of cluster formation from observed correlations among different physical parameters characterizing the clusters. If they exist, these correlations should at least be the targets of any physically motivated theory of cluster formation. Here we will only mention those observed relationship among dynamical and structural parameters.
The existence of a proportionality between the total X–ray luminosity L_X and the

velocity dispersion was suggested long time ago by Solinger & Tucker (1974), who used EINSTEIN data for Virgo Cluster. Although a large amount of the X-ray emission from Virgo comes from the Cd galaxy M87, which has an extended X–ray halo, recent observations with the LAC counter on GINGA in the range $1.5 - 38$ kev show that the X–ray emission is diffuse and comes from an extended, non-isothermal intracluster halo (Takano et al, 1989; Koyama et al, 1991) . Further studies employing a larger set of data for more clusters confirmed the existence of this relation, which reads:

$$L_X \approx 4.2 \times 10^{44} \left[\frac{\sigma_c^4}{10^3 Km/sec}\right] \tag{1.21}$$

(Quintana & Melnick, 1982) where L_X is expressed in erg/sec, and σ_c is the central velocity dispersion. Eq. (1.21) was obtained from data in the spectral range $2 - 10$ kev.

If the temperature of the intracluster gas is constant, this relation could be interpreted as a relation between the total gas mass and the central potential of the cluster. However, there exists also a correlation between gas temperature and velocity dispersion (Mithchell et al, 1979; Smith et al., 1979):

$$T_X\,(K^\circ) \approx 6 \times 10^7 \left[\frac{\sigma_c}{10^3 Km/sec}\right]^2 \tag{1.22}$$

A relation between T_X and σ_c^2 is expected if the galaxies and the gas have the same isothermal distribution inside the cluster and the gas is isothermal (Cavaliere & Fusco–Femiano, 1976, 1978). From the hydrostatic equilibrium equation, under the hypothesis of an isothermal distribution for the gas, one obtains:

$$\frac{d\ln\rho_g}{dr} = -\frac{\mu m_p}{kT_X}\frac{d\Phi}{dr} \tag{1.23}$$

and, if the density distribution generating the potential $\Phi(r)$ is approximated by a truncated King model one obtains a density profile for the gas:

$$\rho_g(r) = \rho_{g0}\left[1 + \left(\frac{r}{r_c}\right)^2\right]^{-\frac{3\beta}{2}}, \tag{1.24}$$

where the coefficient β is given by:

$$\beta = \frac{\mu m_p \sigma_c^2}{kT_X} \tag{1.25}$$

Jones & Forman (1984) report an average value for $\beta_{obs} \approx 0.65$, while the observed relation would rather give a value about twice as large (Sarazin, 1986). This discrepancy between the observed and predicted values of β can be explained in various ways, all of which point to the weakness of some of the assumptions underlying the simplified model which has been adopted. It seems that making more detailed, non–isothermal models of the gas distribution one does not improve substantially the situation, while if one supposes that the dispersion velocity of galaxies has been in some way overestimated the situation can sensibly improve. A clear example of this fact has been given by Kent & Sargent (1983), whose detailed dynamical modelling of Perseus cluster has sensibly reduced the discrepancy. As Sarazin (1986) has observed, the approximation to the density distribution of the King models fail to be a good one at large distances from the cluster where most of the emitting gas is found. A better approximation gives a value for β which is 2/3 of the one given in eq. (1.25), and is in far better agreement with the observations (considering also the large scatter in the observed relation).

A relation between the total gas mass deduced from the modelling of the X-ray emission X-ray and the total luminous mass, was recently found by Arnaud et al. (1992):

$$M_{gas} \propto L_v^{1.9\pm0.3} \tag{1.26}$$

This is a 1σ result obtained collecting together optical data for 27 clusters from different sources: the rather large scatter in the relation could be due to this reason. However, this relation shows that the gas content increases with total mass, assuming that L_v increases also with the total mass, and this means that rich clusters of galaxies have a larger fraction of gas than poor clusters and groups (David et al, 1990). Galaxy and star formation could then be less efficient in rich clusters than is poor one. This fact is ultimately consistent with the recent findings of a large amount of very blue, low-luminosity, dwarf and low-surface-brigthness galaxies in nearby clusters (Binggeli et al., 1984, 1987, 1991; Ferguson, 1989; Davies et al, 1988). Altough in the present thesis we are only concerned with dynamical aspects and not with problem related to galaxy population in clusters, it is clear that the problem of the global M/L contributed by low-surface-brigthness galaxies is a very interesting one also for purely dynamical

reasons. Unfortunately these objects are too faint for the present technological possibilities to allow determinations of redshift, so their dynamics within the cluster environment has not yet been determined.

Other interesting relations exist among parameters derived from fits to the optical data. West et al (1989) deduced a relation between the optical radius (defined as the radius of the isopleth containg half of the integrated luminous emission) and the totical optical luminosity, derived from an analysis of a sample of 29 clusters:

$$R_{50} \propto L_v^{0.51 \pm 0.007} \qquad (1.27)$$

West et al. (1989) show that this relation is consistent with the expectations of an hierarchical clustering model. In a cosmologically flat Universe the turnaround time t_c scales with the average overdensity of a typical perturbation as $t_c \propto \bar{\delta}^{-3/2}$, and if the density fluctuations are gaussian distributed and generated by a power spectrum of index n the density variance will be given by (Peebles, 1980, §26):

$$\left(\frac{\delta M}{M}\right)^2 \propto Vk^3 \cdot AK^n \propto x^{-(3+n)},$$

where $x \propto k^{-1}$ is the comoving length and V is the volume of the region. During the linear phase of the growth the density contrast grows with time as $(\delta M/M)^2 \propto x^{-(3+n)}t^{4/3}$, so the collapse time t_c, determined from the condition $(\delta M/M)^2 \approx 1$ will scale with comoving length as:

$$t_c \propto x_c^{3(3+n)/4}$$

The background density varies as: $\rho \propto a^{-3} \propto t^{-2}$, and the proper critical length as: $r_c \propto a x_c \propto t_c^{2/3} x_c \propto x_c^{\frac{n+5}{2}}$, so finally the mass of the collapsed structures will scale as:

$$M \propto \rho \bar{\delta} r_c^3 \propto t_c^{-4/3} r_c^3 \propto r_c^{-\frac{2(3+n)}{(5+n)}+3} = r_c^{\frac{(9+n)}{(5+n)}},$$

giving:

$$r_c \propto M_{tot}^{\beta}, \qquad \beta = \frac{5+n}{9+n} \qquad (1.28)$$

For $n = 0, -1, -2$ one gets $\beta = 0.56,\ 0.5,\ 0.43$, respectively. The empirical relation (1.27) is approximately consistent with an hierarchical clustering picture with an index varyin in the range $-2 \leq n \leq 0$. The upper value is more cosnsistent with the standard CDM model (Efstathiou et al., 1988).

Finally, Kashlinsky (1983) found another relation between gravitational radius and central velocity dispersion:

$$R_{gr} \propto \sigma^{1.55\pm0.45} \tag{1.29}$$

with a correlation χ^2 coefficient $r = 0.65$. As Kashlinsky (1983) notes, given the large uncertainty this relation could be consistent either with an universal constant density or an universal surface density.
The difficulty of establishing reliable empirical corrrelations among the physical parameters describing a cluster could also be ascribed to the current rather uncertain definition of cluster (Cavaliere et al., 1992) and, in general, is a signal of the large observational uncertainties. One hopes that the situation will become better in a few years, after the completion of deeper and more detailed surveys of clusters.

1.5 Luminosity Function and Mass Spectrum.

The luminosity function of groups and clusters of galaxies is enough well determined observationally (Bahcall, 1979) and can be described by a Schechter (1976) relation:

$$\eta\left(L\right)dL = \eta_0 \left(\frac{L}{L_0}\right)^{-\alpha} \exp\left(-\frac{L}{L_0}\right) dL \tag{1.30}$$

with $\alpha = 2.05 \pm 0.1$, $L_0 = (1.05 \pm 0.2) \times 10^{13} L_\odot$, $\eta_0 = 1.2 \times 10^{-7} \left(10^{12} L_\odot\right)^{-1}$. This equation is valid over a large interval: $10.2 \leq \log\left(L/L_\odot\right) \leq 13.8$, ranging aprroximately from Gott & Turner (176) groups up to rich clusters. Its mathematical form should be consistently explained by any theory of cluster formation. A very simple approach to this problem was devised by Press & Schechter (1974, hereafter PS). It involves three main hypothesis: a) the statistics of the sites of clusters' and groups' mass distribution is gaussian; b) clusters form at theose regions where the average density, smoothed with a window function, is larger than than a critical value δ_c. Smoothing is a necessary tool to filter substructure: its use is predicated on the basis that low mass substructure has very little influence on the gravitational evolution of larger mass scales in hierachical clustering models. However, the precise mathematical form of the window function is usually chosen in a rather *ad hoc* way. The most popular choices are the *sharp space filtering*: $W \propto H\left(1 - R/R_f\right)$, the *k-space filtering*: $\widetilde{W}\left(k\right) = H\left(1 - k/k_{up}\right)$

and the *gaussian filtering*: $W \propto \exp\left(-R^2/2R_f^2\right)$ (we have denoted with a ˜ the Fourier transform, and by $H()$ the Heaviside function). More physically motivated choices have been given by Appel & Jones (1990).
If $\rho(\mathbf{r},t)$ denotes the unfiltered density field, the smoothed field will be given by:

$$\rho_c(\mathbf{r},t) = \int d^3\mathbf{r}'\rho(\mathbf{r},t)\, W(\mid \mathbf{r}-\mathbf{r}' \mid) \tag{1.31}$$

and the variance of the mass density fluctuations will be given by:

$$\sigma^2(R_f,t) = \int d^3\mathbf{k}\widetilde{W}^2(k,R_f)\, P(k,t) \tag{1.32}$$

where $P(k,t)$ denotes the power spectrum. The third hypothesis in the PS argument is that: c) the probability of forming an object at a given point is proportional to the probability for the point of lying in a region of overdensity larger than the critical one:

$$P(\delta,\delta_c) = \int_{\delta_c}^{\infty} d\delta \frac{1}{(2\pi)^{1/2}\sigma} \exp\left(-\frac{\delta^2}{2\sigma^2}\right) \tag{1.33}$$

The characteristic mass associated to a filter with radius R_f will be given by $M \approx 4\pi\rho_b R_f^3/3$; the critical overdensity will be given by $\delta_c \approx \sigma(M_c)$, and the number density of regions whose density exceeds this value will be given by:

$$n_{PS}(M) = -\frac{\bar{\rho}}{M}\frac{dP}{dM} =$$

$$= -\frac{\bar{\rho}}{(2\pi)^{1/2}}\frac{\delta_c}{\sigma^2}\exp\left(-\frac{\delta_c^2}{2\sigma^2}\right)\frac{1}{M}\frac{d\sigma}{dM} \tag{1.34}$$

For instance, for a power-law spectrum one has: $\sigma^2(R_f) \propto M_c^{-(3+n)/3}$ and we obtain:

$$n_{PS}(M) = \left(\frac{2}{\pi}\right)^{1/2}\bar{\rho}\frac{n+3}{6}\frac{1}{M^2}\left(\frac{M}{M_c}\right)^{-\frac{3+n}{6}}\exp\left[-\left(\frac{M}{M_c}\right)^{\frac{3+n}{3}}\right] \tag{1.35}$$

where $M_c = M_c(0)\,(1+z)^{-\frac{6}{3+n}}$ is the characteristic mass which goes nonlinear at redshift z.
Eq. (1.35) is not the actual PS equation: the actual one can be obtained from this multiplying by 2.This latter step is necessary to give the correct normalization and it means that the PS way of counting objects underestimates the real number, excluding objects which, although contained inside underdense regions,

eventually coome into overdense ones.

The problem of the factor "2" problem in the original PS derivation has produced various attempts toward a solutions. It seems to have been recently partially solved (Cole & Kaiser, 1989; Bond et al., 1991), at least when some filter functions are adopted.

Apart for the normalization problems, the PS approach gives a "static" treatment of the statistics of structure formation, i.e. the dynamics of the density perturbations is not taken into account: in the PS scheme regions of given overdensity collapse altogether at the same time. When one takes more realistically into account the dynamics and the kinetics of the process, i.e. secondary infall and some prescriptions on the rates of production and destruction of objects on a given mass scale, the original PS spectrum turns out to be modified and a steeper profile for higher mass is obtained (Cavaliere et al., 1991). However, the real situation can be even more complex. Consider what happens to a region which at some epoch t_i is surrounded by, but external to, some overdense regions which are entering a nonlinear stage. Secondary infall on these regions will poor the background on which the linear region is growing, and Rozgacheva (1988) has shown that this act to accelerate the further collapse of the linear region: the most probable temporal evolution will be: $\delta \propto t^{5/3}$. Overdense regions are not static: they move through the background, and one can see that there exists a finite probability for a given region to enter an underdense region and to speed up in this way the collapse. We quoted this example only to show that a proper dynamical theory of structure formation could reveal many more subtleties (Lucchin, 1988, Cavaliere et al., 1992). Other possible deviations from the PS prediction could arise when the peculiarities of galaxy formation in the overdense environments of clusters are taken into accoun (Bardeen et al, 1986; Bower, 1991; David & Blumenthal, 1992).

Another theoretical approach to the problem of the mass function of clusters relies on the idea that these structures form only at the peaks of the density field, rather than only in overdense regions (Doroshkevich, 1970; Peacock & Heavens, 1985). After having smoothed the density field with a filter of scale R_f the number density of highly overdense ($\nu = \delta/\sigma \ll 1$) peaks of mass m, computed by

Bardeen et al. (1986) is:

$$n_{peaks}\left(m,\nu\right)=\left(\frac{3+n}{6}\right)^{3/2}\frac{\bar{\rho}}{\left(2\pi\right)^{1/2}m^{2}}\nu^{2}\exp\left(-\frac{\nu^{2}}{2}\right) \tag{1.36}$$

asuming a power-law spectrum of density perturbations. The problem here is that this equation overestimates the number of small (low ν) objects, because these latter have very diffuse mass distributions and tend to overlap: so they should not be counted as single objects. On the onther hand, the number density of massive (high ν) objects will be underestimated, because the objects do not precisely coincide with single peaks. For high peaks, one has approximately:

$$n_{peaks}\approx\frac{1}{2}\left(\frac{3+n}{6}\right)^{3/2}\nu^{3}n_{PS} \tag{1.37}$$

(Thomas & Couchman, 1992).

Both the PS and the peaks' approach are based on the assumption of a gaussian amplitude distribution of the density perturbations; deviations from this behaviour however necessarily arise during the nonlinear evolution and, more importantly, could be generated by some specific primordial seeds like cosmic strings. Lucchin & Matarrese (1988) have shown that the mass distributions of various non gaussian density perturbations deviate significantly from the PS distribution at high masses, typical of rich clusters: this fact could be a tool to discriminate among different cosmological scenarios for the primordial density perturbations.

It has to be said that numerical simulations from gaussian initial conditions have generally tended to confirm the validity of the PS approach (Efstathiou et al., 1988). Recent work by Brainerd & Villumsen (1992) casts some doubts on this conclusion: the authors find that the high mass decrease of their numerical mass function is much much lesser pronounced than in the PS approach.

1.6 Observational Evidence of Subclustering.

The issue of subclustering has arisen in the last years as one of the central issues in the study of the origin and evolution of clusters of galaxies. In this chapter we will only review the observational situation, leaving to the next chapter a short review of the theoretical results.

After the seminal work of Baier (1977) many authors have claimed to detect

a substantial amount of subclustering in the spatial distribution and/or X–ray images of clusters (Geller & Beers, 1982; Gioia et al., 1982; Baier, 1983, 1984; Baier & Oleak, 1984; Bothun et al., 1983; Fitchett & Webster, 1987; Fitchett & Merritt, 1988; Fabricant et al., 1986; Binggeli et al., 1987; Malumuth et al., 1992). On the other hand, other authors have seen little or no subclustering (West et al., 1988; Rhee et al., 1991). Part of the reason for this lies in the different definitions of subclustering adopted. Baier (1983, 1984), Baier & Oleak (1984) and Geller and Beers (1982) look at density contours obtained by smoothing the number counts histograms, and look at asymmetries of the isopleths. The level of subclustering detected depends on the smoothing length, and the method seems successful in identifying large clumps in the galaxy projected distribution, rather than low level fluctuations. These asymmetries are taken as evidence of ongoing merger events, and morphologically these clusters are not very much different from the "double clusters" like Abell 1750 and SCo 627–54 (Forman et al, 1981), which show two main lumps in X–ray and in the galaxy distribution: the only difference is in the scale of linear separation between the centroids of the clusters. Generally speaking, there are at least three main motivations behind a detailed study of subclustering:

- To determine the real M/L ratios. As Bothun et al. (1983) have shown for the case of the Cancer cluster, the resolution into subgroups which proved to be not gravitationally bound together has forced to review the estimated M/L from ≈ 700 (from virial mass arguments) to ≈ 250, consistent with the M/L of groups of galaxies.

- Relaxation. Any subclustering should be erased if the cluster were completely relaxed. On the other hand, the detection of suclustering inside the core regions of apparently spherical and relaxed clusters suggests that this could not be the case (Beers & Geller, 1982; Fabricant et al., 1986; Fitchett & Webster, 1987; Fitchett & Merritt, 1987).

- Connection with initial conditions. In CDM models for galaxy and clusters formation a substantial amount of substructure is predicted to occur, while in HDM models any structure on scales lower than $10^{13} M_{\odot}$ is erased by neutrino free streaming. So the presence and amount of substructure inside

clusters could be important to discriminate among different cosmological models on scales on which the Universe is nonlinear.

In order to show the conceptual and practical difficulties of an analysis of subclustering, we will study in some detail a statistically precise definition of subclustering and a method of measuring it that have been proposed by Fitchett (1988) and since then have been adopted in many other studies (e.g. West et al., 1988; Fitchett & Merritt, 1988; Rhee et al., 1992). Fitchett distinguishes between sublustering detected in the projected distribution of galaxies and in the combined 2–D and line–of–sight velocity distribution. Projection effects can mask subclustering: a cluster could be made of two or more clumps which, if seen in projection along the same line of sight, could appear as only one cluster with a smooth density profile (also at X–ray wavelengths, because the gas could be distibuted symmetrically around the axis). Then the only way to detect the real structure is to analize the projected velocity distribution of the galaxies and check whether they came from the same distribution, i.e. from the same clump. The best statistical tool to detect subclustering would be a maximum likelihood test for group membership: given a sample of N_p galaxy positions and line–of–sight velocities $\left\{x_{(i)}, v_{ls(i)}\right\}_{i=1}^{N}$, one divides this sample in n_g groups and defines a likelihood function and a null hypothesis for subclustering (e.g. that the fluctuations in number counts are Poissonian). This likelihood function is proportional to a cumulative probability distribution for the partitions, and must be found by computing its value for some given theoretical distribution (Fitchett uses a Gaussian distribution of $\left\{x_{(i)}, vls(i)\right\}_{i=1}^{N}$. The partition which maximizes the likelihood function will be the best choice, and from the value of the likelihood function one can deduce a significance level for the detected substructure. In practical applications this program can hardly be accomplished for real clusters, for two main reasons:

1. The calculation of the likelihood function is a formidable problem. For example, for $N_p = 19$ and $n_g = 9$ one has $\approx 1.7 \times 10^{12}$ different partitions! This would require a very large computer time.
2. The search for the maximum of the likelihood function can be a very difficult problem. Often this function has many local maxima very near to the absolute maximum, and only recently strategies like *Simulated*

Tempering (Marinari & Parisi, 1992) have been introduced to deal with this kind of problems.

A more viable method is offered by the **Lee Statistics** (Lee, 1979): we will illustrate it for 2–D data. Suppose to draw a line trough the cluster and to project all the positions vectors of the galaxies along this line. Choose one of the projected positions as the origin and partition all the other projections data in two sets, respectively to the left and to the right of the origin. Compute then the quantity:

$$L(\phi) = \frac{n_l \left(\mu_l - \mu_T\right)^2 + n_r \left(\mu_r - \mu_T\right)^2}{n_l \Sigma_l + n_r \Sigma_r} \tag{1.38}$$

where: n_l, n_r are the number of points to the left and to the right of the origin, respectively, μ_l, μ_r the averages and Σ_l, Σ_r the variances to the left and to the right of the origin, respectively. μ_T is the average for all the sample. The estimator $L(\phi)$ depends on the position angle of the line, ϕ (measured w.r.t. some arbitrary reference line inside the cluster), because the averages and the variances depend on ϕ. One then evaluates:

$$L_{max} = max_{\phi} L(\phi) \tag{1.39}$$

and the angle such that $L(\phi_*) = L_{max}$ defines the value of the orientation for which substructure is significant. Lee (1979) showed that the statistics of the indicator given by eq. (1.39) is equivalent to the maximum likekihood statistics (under some conditions on the sample), and here lies the importance of the Lee statistics: it is a 1-dimensional equivalent of the maximum likelyhood. Also the local extrema of the function $L(\phi)$ different from the absolute maximum are connected with substructure, although in applications to clusters the Lee statistics proves to be more efficient in cases where only two clumps dominate the overall subclustering (Fitchett & Webster, 1987; Rhee et al, 1991). Before using this statistics (as any other statistics), one has to perform Montecarlo simulations to fix the relevant probabilities (see, e.g. Lindgren, 1976), but this is a task much more feasible for this statistcs, because there are only 2 groups, i.e. the left and the right. Another interesting feature of the Lee statistics is the fact that it deals on an equal level with position *and* velocity information.

Other statistics can be introduced to characterize some aspects of subclustering which proved to be difficul to detect with the Lee statistics (Fitchett & Webster,

1988; Rhee et al., 1991). The usefulness of these studies can be seen in the applications: substructure has been detected also in those clusters like Coma and Hydra 1 whose X–ray map suggested a relaxed configuration (however, concerning Coma see the recent ROSAT observations of Henry & Briel, 1992). As an example, consider the Coma cluster: Fitchett & Webster (1988) use position and redshift data coming from three different samples, namely Kent & Gunn,(1982) (94 galaxies, complete to $m_v \leq 15.7$) and Godwin & Peach (1977). Applying the Lee statistics to projected positions (2–D) data, they are able to show that there exist two main subclumps and our line of sight passes very near to the center of them. The subclumps have characteristic virial masses 2.6 and $4.6 \times 10^{14} M_{\odot}$, and are centered about the galaxies NGC 4874 and NGC 4889, respectively.
In a similar way, Fitchett & Merritt (1988) analysed the Hydra 1 cluster. Although the overall velocity histogram for the galaxies within $0.995 h^{-1} Mpc$ of the cluster center is gaussian, the velocity histogram in the central $0.40 h^{-1} Mpc$ is flat. An analysis based on the Jeans' equations (1.17) shows that the data are inconsistent with equilibrium models at a high significance level, namely 2.4σ. Models including susbtructure are in much better agreement with observations, and the authors use 5 more tests other than Lee statistics to check this hypothesis. On the other hand, Rhee et al (1991), using the same statistical tests, found much lesser evidence for substructure. However, as the authors themselves admit, they analysed only positional data, and one must remember that the evidence from Fitchett & Webster (1988) and Fitchett & Merritt (1988) comes from position–velocity data.
One weak point of all these studies is that the substructure is put in a completely *ad hoc* way. For example, Fitchett & Merritt (1988) consider three possible models for substructure in Hydra 1: one in which groups of galaxies are distributed according to a De Vaucouleur's profile near the center, a second in which a virialized region is surrounded by infalling subgroups randomly distributed, and a third one in which symmetrically displaced groups are distributed within the inner relaxed region of the cluster. The third model seems to be favored by the tests. However, none of this models comes as a natural output of a scenario of galaxy formation, e.g. the CDM. It could be interesting to see how the predictions in the highly nonlinear regimes coming from the self–similar solutions (Davis & Peebles, 1978) or from numerical simulations (Efstathiou et al., 1988;

Antonuccio–Delogu, 1992) compare with observations.

A final point to notice is that X–ray observations are now revealing an increasing amount of subclustering, particularly in poor, non–centrally–dominated clusters (Bechtold et al., 1983). Recently, Henry & Briel (1991) discovered 23 new point sources in the Coma cluster which do not seem to be associated with any visible galaxy. Whether this emission comes from populations of OB stars inside blue compact dwarf galaxies or from shocks originating from gas trapped inside residual density perturbations which did not attracted enough mass to excite a starburst episode and/or form galaxies, it is evident that they are associated with substructure and this shows once again the importance of substructure inside clusters.

Chapter 2

Evolution of Density Perturbations.

As we saw in the preceding chapter, there is some observational evidence that some clusters of galaxies could be structures not completely formed, with an inner core already collapsed and virialized and outer parts showing evidence of being still in the linear phase of evolution. It is then interesting to investigate what theory can tell about the development of clustering inside a density fluctuation which is going to originate a structure of the size of a cluster by the present epoch. Most of the exact results which have been obtained describe the evolution of slightly overdense, isolated density perturbations in homogeneous, isotropic cosmological models (see e.g. Peebles, 1980; Efstahiou, 1990). In this case the equations describing the evolution of the density and velocity field are linear and can be solved exactly (§2.1). Being isolated, the fluctuations keep the same aplitude distributions they had at the beginning of their evolution: if they had a gaussian distribution, this will be preserved during the linear phases of the evolution. The next step is to consider the nonlinear interactions among density perturbations on different scales, and how the gravitational interactions modify the amplitude distribution (§2.1.2). We will see that deviations from a gaussian distribution appear during this phase, induced only by gravitational effects (§2.1.3). Finally, we will consider the evolution during the nonlinear phases, commenting the results of previous N–body simulations of clusters' formation and the theoretical work on the solution of the BBGKY hierarchy for the evolution of correlations in a self-gravitating cosmological background.
In the rest of this thesis, we will restrict ourselves to an homogeneous, isotropic

cosmological model described by the Friedmann equations:

$$\frac{d^2a}{dt^2} = -\frac{4\pi G\rho_b a}{3} + \frac{\Lambda}{3}a, \tag{2.1}$$

$$\frac{d}{dt}\{\rho_b a^3\} = 0. \tag{2.2}$$

The cosmological expansion factor $a(t)$ describes the evolution of the metric coefficients and connects the proper and comoving distances:

$$\mathbf{r} = a(t)\mathbf{x}. \tag{2.3}$$

Taking the time derivative of the above equation we obtain the proper velocity:

$$\mathbf{V} = \frac{d\mathbf{r}}{dt} = a(t)\mathbf{u} + \dot{a}(t)\mathbf{x}, \tag{2.4}$$

where $\mathbf{u}$ is the peculiar velocity, which measures the deviation from the Hubble flow: $\mathbf{v}_{Hubble} = \dot{a}(t)\mathbf{x}$.

We now recall some ideas and definitions concerning the statistics of density perturbations in a cosmological background. One of the main assumptions in cosmology is that the sample of Universe we can see is a "fair sample": its statistical properties reflect the statistical properties of all the Universe. There are however different methods of describing the statistics of a sample of objects, e.g. correlation analysis (Peebles, 1980), percolation (Shandarin & Zeldovich, 1989), fractal sets (Pietronero, 1987; Jones et al., 1988) among others. Here and in the rest of this thesis we will consider the correlational analysis which has become a standard tool.

If the universe around us is only one out of many possible realizations, then it is convenient to look at the density field $\rho(\mathbf{r}, t)$ as a stochastic variable. We will also assume that the Universe is everywhere isotropic (and then, as a consequence, homogeneous, see e.g,. Weinberg (1972)), so the zero–order moment of $\langle\rho(\mathbf{r}, t)\rangle$ will not depend on position. All the other quantities derived from density which we will introduce later, like the overdensity δ, will always be meant to be average values of stochastic variables and the deterministic equations we will write should always be meant as involving averages over the ensemble of possible realization of the field.

One of these averages, the **two point correlation function** is of particular importance. It is defined as the combined probability of finding a given overdensity

at two different positions in space:

$$\xi(\mathbf{r},t) = \langle \delta(\mathbf{x},t)\delta(\mathbf{x}+\mathbf{r},t)\rangle \tag{2.5}$$

where: $\delta = \rho(\mathbf{x},t)$ is the overdensity. If the sample is discrete and the density is independent of position, ξ can be expressed as the excess probability over the average of finding two objects separated by a distance $\mathbf{r}$:

$$\delta P = n^2\,[1+\xi(\mathbf{r},t)] \tag{2.6}$$

Generalizing this definition, one can analogously define the $n-point$ correlation functions $\xi^{(n)}$. The correlation functions are determined by a set of equations which can be obtained from moments of the collisionless Boltzmann equation, and define the so-called Bogolyubov-Born-Green-Kirkwood-Yvon hierarchy (Davis & Peebles, 1978; Peebles, 1980). We will deal with these equations in chapter 5. The correlation functions describe the clustering of the density field. Suppose we are considering a region of the Universe of volume V, containig a discrete population of objects, so that one can write: $\rho(\mathbf{r}) = \sum_i n_i \delta(\mathbf{x_i})$ (where δ here denotes the Dirac's delta distribution). This density field can now be decomposed into Fourier harmonics:

$$\rho(\mathbf{r}) = \sum_{\mathbf{k}} \delta_{\mathbf{k}} e^{-i\mathbf{k}\cdot\mathbf{r}},$$

so the average in eq. 2.5 becomes:

$$\xi(\mathbf{r}) = \frac{V}{(2\pi^3)} \int d^3\mathrm{k}\delta_{\mathrm{k}}\delta^*_{\mathrm{k}} e^{i(bfk'-\mathbf{k}\cdot\mathbf{x}-i\mathbf{k}\cdot\mathbf{r})} \tag{2.7}$$

where the asterisk means complex conjugation. But the density field is real, so: $\delta^*_{\mathbf{k}} = \delta(-\mathrm{k})$, and in the limits in which V is much larger than the typical correlation length of the field, we can see the average of eq. (2.5) as an integration over all the wavenumbers:

$$\xi(\mathbf{r}) = \frac{V}{(2\pi)^3} \int d^3\mathrm{k}' \mid \delta\,(\mathrm{k}') \mid^2 e^{-i\mathbf{k}'\cdot\mathbf{r}} \tag{2.8}$$

The function $P(\mathrm{k}) = \mid \delta(\mathrm{k}) \mid^2$ is the **power spectrum**: its Fourier transform is the correlation function (eq. 2.8). All the statistical averages over the ensemble in an isotropic Universe depend only on $r = \mid \mathbf{r} \mid$, and as a consequence also the power spectrum will depend on $k = \mid \mathrm{k} \mid$. One can then easily verify that under this further constraint eq. (2.8) becomes:

$$\xi(r) = \frac{V}{(2\pi)^3} \int dk' 4\pi k'^2 P(k') \frac{\sin k'r}{k'r} \tag{2.9}$$

The power spectrum is the spectral density of the Fourier amplitudes of the density field. However, its specification is generally not sufficient to predict the subsequent evolution of the density fluctuations: only a knowledge of all the higher order correlation functions makes this knowledge possible. The reason can be seen already from eq. (2.8) and from the definition of power spectrum: both involve only the moduli squared of the density field's Fourier transforms. But in general the $\delta_{\mathbf{k}}$ are complex quantities and a full specification involves also the determination of a **phase factor** $\theta_{\mathbf{k}}$. If the phase factors are uniformly randomly distributed then in the limit of high wave density (i.e. large volumes) their contributions mutually cancel each other, and the average density fluctuation squared is the sum of all the modes ($\mid \delta \mid^2 = \sum_k \mid \delta_{\mathbf{k}} \mid^2$). If this *random phase hypothesis* is verified then the Large Number Theorem hold, and the probability distribution of any quantity involving the sum of many independent quantities like $\mid \delta \mid^2$ approaches a gaussian distribution:

$$P(\mid \delta \mid) \propto \exp\left(-\frac{\delta^2}{\sigma^2}\right) \tag{2.10}$$

The variance of the density field σ is connected to the correlation function:

$$\sigma^2 = \frac{V}{(2\pi)^3} \int P(k) d^3k \tag{2.11}$$

As Efstathiou (1990) noticed, one can see already from eq. (2.10) that the approximation of gaussian distributed density perturbations can only hold in the linear regime, i.e. when $\xi \ll 1$ and $\sigma \ll 1$, because by definition $\mid \delta \mid \leq 1$ and we cannot have a finite probablity of having $\mid \delta \mid > 1$. Present–day nonlinear perturbations cannot be gaussian: correlations develop during their development which tend to create phase correlations and increase the clustering. The Fourier transforms of the density field are no longer inedependent: cross correlation terms become comparable in magnitude to the two–point correlation function. Howaver, a gaussian field has a very important distinctive feature: all the higher order correlation functions are either identically zero (the odd ones) or explicitly dependent on $\xi(r)$ (the even order components). This simplifies enormously the calculations and allows one to completely specify many characteristics, like for instance the statistics of extremal points (Bardeen et al., 1986). A complete presentation of the properties of gaussian density field would take too much time and would bring us away from our main purpose, so we will not attempt it here.

2.1 Density and Velocity Fields.

We will first of all obtain the equations describing the evolution of a density perturbation within an homogeneous background. If gravitational forces dominate over other kind of interactions (a plausible hypothesis at the rather late epochs of evolution, see e.g. Kolb & Turner, 1989), then one can suppose that the medium is collisionles and its distribution function $f(\mathbf{x}, \mathbf{u}, t)$ obeys the cosmological collisionless Boltzmann equation:

$$\frac{\partial f}{\partial t} + u^\alpha \frac{\partial f}{\partial x^\alpha} + \frac{1}{ma}\frac{d\Phi}{dx^\alpha}\frac{\partial f}{\partial u^\alpha} = 0. \tag{2.12}$$

We recall that this equation is obtained by applying the Liouville theorem to the probability density $d\mu = f d^3\mathbf{x} d^3\mathbf{u}$ over a bounded region of the phase space of the collisionless system:

$$\frac{d}{dt} d\mu = 0, \tag{2.13}$$

The time derivative appearing in eq. (2.13) is a total time derivative. The equation of motions for the particles of the collisionless fluid are:

$$\frac{d\mathbf{x}}{dt} = a\mathbf{u}, \quad \frac{d\mathbf{u}}{dt} = \frac{1}{ma}\nabla_{\mathbf{x}}\Phi \tag{2.14}$$

Putting eqs. (2.14) into eq. (2.13) one gets eq. (2.12).

The probability density $f(\mathbf{x}, \mathbf{u}, t)$ cannot be deduced directly from the observations in real cases. For example, in the case of a cluster of galaxies, also if we had all the velocities and position for all the galaxies gravitationally bound to the cluster, which in the best case are about few hundred, we could sample a very limited region of the entire phase space of the cluster. The best we can do is to admit our ignorance and to use some averaged integral quantities which can be more reliably determined from the observations. The moments of the distribution function like the density, average velocity, velocity anisotropy tensor seem to be suitable to this purpose, because they can be easily determined from the observations, at least in principle.

The zero order moment of eq 2.12 gives the continuity equation:

$$\frac{\partial \rho}{\partial t} + \frac{1}{a}\nabla\{\rho\mathbf{u}\} = 0 \tag{2.15}$$

Multiplying eq. (2.12) by $\mathbf{u}$ and integrating over velocities we get an equation for the average velocity:

$$\mathbf{v} \equiv \frac{\int d^3\mathbf{u} f \mathbf{u}}{\int d^3\mathbf{u} f}$$

This equation is easily found:

$$\frac{\partial v^\alpha}{\partial t} + \frac{\partial}{\partial x^\beta}\langle u^\alpha u^\beta \rangle + \frac{1}{ma}\frac{\partial \Phi}{\partial x^\alpha} = 0, \tag{2.16}$$

where we have defined the velocity anisotropy tensor:

$$\langle u^\alpha u^\beta \rangle = \frac{\int d^3 f \mathbf{u} u^\alpha u^\beta}{\rho}. \tag{2.17}$$

In this equation $\Phi(\mathbf{x}, t)$ is the gravitational potential generated by the local density excess, which verifies the equation:

$$\Delta_x \Phi = 4\pi G \left[\rho(\mathbf{x}, t) - \rho_b(t)\right] \tag{2.18}$$

As is well known, each new moment of the collisionless Boltzmann equation introduces a new set of unknowns; in the latter equations the new unknowns are the components of the velocity correlation tensor, $\langle u^\alpha u^\beta \rangle$. It is then necessary to truncate at some point the hierarchy of moment equations by making some physical approximations which take into account the proper spatial and temporal scales of the problem in hand (Davis & Peebles, 1977; Bouchet & Pellat, 1984). We will come back to this problem later.

Let us now linearize the above equations by introducing the density perturbation:

$$\rho(\mathbf{x}, t) = \rho_b(t)\left(1 + \delta(\mathbf{x}, t)\right). \tag{2.19}$$

Here $\rho_b(t)$ is the background density which according to eq. (2.2) changes as: $\rho_b \propto a^{-3}(t)$. Introducing eq. (2.19) into the continuity equation, assuming that the unperturbed peculiar velocity field is zero and keeping only terms of the first order in δ one gets the perturbed continuity equation:

$$\rho_b \frac{\partial \delta}{\partial t} + \frac{1}{a}\nabla \cdot (\rho_b \delta \mathbf{v}) = 0 \tag{2.20}$$

Here $\delta\mathbf{v}$ denotes the linearized peculiar velocity. However, because the unperturbed peculiar velocity field is assumed to be identically zero, hereafter we will drop the perturbation symbol "δ" from the notation for the peculiar velocity.

Proceeding in a similar way, we obtain the linearized first order moment equation:

$$\frac{\partial v^\alpha}{\partial t} + \frac{\dot{a}}{a}\mathbf{v} + \frac{\partial}{\partial x^\beta}\left(1 + \delta\right)\langle u^\alpha u^\beta \rangle + a^3 \rho_b \frac{\partial \Phi}{\partial x^\alpha} = 0 \tag{2.21}$$

After having introduced this equation into equation 2.13 and having performed some algebra, one finds a second order differential equation for the density perturbation:

$$\frac{\partial^2\delta}{\partial t^2} + 2\frac{\dot{a}}{a}\frac{\partial\delta}{\partial t} = \frac{1}{a^2}\nabla_x \cdot \left[(1+\delta)\,\nabla_x\Phi\right] + \frac{1}{a^2}\frac{\partial^2}{\partial x^\alpha x^\beta}\left[(1+\delta)\,\langle u^\alpha u^\beta\rangle\right]. \qquad (2.22)$$

Before proceeding to discusse the solutions of this equation, we should be able to specify the form of the peculiar velocity anisotopy tensor $\langle u^\alpha u^\beta\rangle$. In the above equation (2.22) this term plays the role of a stress tensor, and its gradients play the role of pressure forces. If the density perturbation is not isolated, tidal forces from neighbouring density irregularities can induce shear through quadrupole and higher order moments, and so they can make this tensor different from zero. However, for an isolated, spherically symmetric and linear density perturbation having a coherence length of the density field d such that: $\left(v/\sqrt{G\rho_b}d\right)^2 \ll 1$ one can suppose that velocity asymmetries, if eventually present at the origin, had not yet had time to grow sensibly, and we can simply ignore the velocity anisotropy tensor. Later in this thesis we will however remove this limitation and we will consider some more realistic possibilities.
With this simplification eq. (2.22) reduces to:

$$\frac{\partial^2\delta}{\partial t^2} + 2\frac{\dot{a}}{a}\frac{\partial\delta}{\partial t} = 4\pi G\rho_b\delta \qquad (2.23)$$

For the $\Omega = 1$, $\Lambda = 0$ Universe we are considering in this thesis one has $a(t) \propto t^{2/3}, \dot{a}/a = 2/3t$ and eq. 2.23 admits two possible solutions:

$$\delta_+(\mathrm{x},t) = A_+(\mathrm{x},t)t^{2/3}, \quad \delta_-(\mathrm{x},t) = A_-(\mathrm{x},t)t^{-1/3}. \qquad (2.24)$$

The second solution describes a decaying mode, while the first one is the most interesting one and tells us that the density contrast grows as the expansion factor. Observe that the spatial and temporal parts are separated: this is a consequence of the spatial homogeneity of the background over which the density perturbation grows.
We can also determine the velocity field by linearizing eq. 2.21, so as to obtain:

$$\frac{\partial v^\alpha}{\partial t} + \frac{\dot{a}}{a}v^\alpha = \frac{1}{a}\frac{\partial\Phi}{\partial x^\alpha} = G\rho_b a\int d^3\mathrm{x}'\delta(\mathrm{x}',t)\frac{\mathrm{x}'-\mathrm{x}}{|\,\mathrm{x}'-\mathrm{x}\,|}. \qquad (2.25)$$

Using eq. (2.24) into the latter equation one verifies that the term in the right-hand side is also a product of a function of position and time variables, so one

can also look for a solution of the form of eq. (2.23) for the velocity field: $\mathbf{v} = \mathbf{V}_+(\mathbf{x},t)t^p$. Subsituting into eq. (2.25), and taking into account the time dependence in the acceleration:

$$G\rho_b a \int d^3\mathbf{x}'\delta(\mathbf{x}',t)\frac{\mathbf{x}'-\mathbf{x}}{\mid \mathbf{x}'-\mathbf{x} \mid} \propto t^{-\frac{4}{3}+p}$$

one finally gets $p = 1/3$ for the growing mode. The decaying mode has $p = -4/3$ and a negative sign for the peculiar velocity field (Peebles, 1980), corresponding to a velocity field directed in the opposite direction to the density perturbation and tending to erase it. The final solution for the velocity field then reads:

$$v^\alpha = \frac{Ha}{4\pi}\frac{\partial}{\partial x^\alpha}\int d^3\mathbf{x}'\frac{\delta(\mathbf{x}')}{\mid \mathbf{x}'-\mathbf{x} \mid}. \tag{2.26}$$

This linear result is of great interest on scales larger than $8h^{-1}$ Mpc, on which the present Universe is believed to be still linear.

2.1.1 Spherical Density Perturbation and Secondary Infall.

The linear theory predicts the existence of growing density perturbations, but the evolution of each perturbation depends on its detailed shape and density distribution. The simplest case to analise is that of a spherical homogeneous shell, a case which can be relevant for the secondary infall of matter on some given seed perturbation, or on an already collapsed and virialized region (Gunn & Gott, 1972; Bertschinger, 1985).

The evolution of a shell enclosing a mass M inside a given radius r is given by the equation:

$$\frac{d^2r}{dt^2} = -\frac{GM}{r^2} \tag{2.27}$$

where $r(t)$ is the proper distance from the center. If shells do not cross during the evolution the mass inside a given radius $r(t)$ is conserved and constant. If one now writes: $r(t) = a(r_i,t)r_i$, one can easily check that the density will be given by:

$$\bar{\rho}_i(r,t) = \frac{3M}{4\pi a^3(r_i,t)r_i^3} \tag{2.28}$$

Substituting into eq. (2.27) and taking into account eq. (2.2) one gets an equation for the expansion parameter $a(r_i,t)$:

$$\frac{d^2a(r_i,t)}{dt^2} = -\frac{4\pi G}{3}\frac{\bar{\rho}_i(r_i,t_i)}{a^2(r_i,t)}. \tag{2.29}$$

This equation can be integrated once to give:

$$\left(\frac{da}{dt}\right)^2 = \frac{8\pi G\rho_i}{a} + \Gamma \tag{2.30}$$

where Γ is an integration constant. We will look for a parametric solution of this equation. Let us introduce a new quantity $\theta(t)$ such that:

$$\left(\frac{d\theta}{dt}\right)^2 = \frac{1}{a(t)}\sqrt{\frac{8\pi G\rho_i}{3}}. \tag{2.31}$$

If we now rewrite eq. 2.30 in terms of the new variable θ we obtain:

$$\left(\frac{da}{d\theta}\right)^2 = H_i^2\left(\frac{\beta}{a} + \gamma\right) \tag{2.32}$$

where one has defined:

$$\beta = \frac{\rho_i}{\rho_c}, \gamma = \frac{\rho_c - \bar{\rho}_i}{\rho_c}.$$

Here ρ_c is a critical density. Now, it is easy to check that in terms of this new independent variable, the expansion factor a verifies the equation:

$$\frac{d^2a}{d\theta^2} = \gamma a + \frac{\beta}{2} \tag{2.33}$$

This equation has a simple solution:

$$a(\theta) = \begin{cases} \left(a_{min} + \frac{\beta}{2\gamma}\right)\cos([-\gamma]^{1/2}\,\theta) - \frac{\beta}{2\gamma} & \gamma < 0 \\ \left(a_{min} + \frac{\beta}{2\gamma}\right)\cosh(\gamma^{1/2}\theta) - \frac{\beta}{2\gamma} & \gamma > 0 \end{cases} \tag{2.34}$$

Using eq. 2.32 we can also obtain the equation for the time dependence:

$$H_i t = \begin{cases} \frac{1}{[\gamma]^{1/2}}\left(a_{min} + \frac{\beta}{2\gamma}\right)\sin(\mid\gamma\mid^{1/2}\,\theta) - \frac{\beta}{2\gamma}\theta & \gamma < 0 \\ \frac{1}{\gamma^{1/2}}\left(a_{min} + \frac{\beta}{2\gamma}\right)\sinh(\mid\gamma\mid^{1/2}\,\theta) - \frac{\beta}{2\gamma}\theta & \gamma > 0 \end{cases} \tag{2.35}$$

Observe that these equations (2.32- 2.34) are sligthly different from those og Gunn & Gott (1972): putting $a_{min} = 0$ one easily recovers their set of equations. The parameter γ measures the mean overdensity of the shell, i.e. the excess fractional density w.r.t. the critical density which marks the transition between the regimes of infinite expansion and recollapse. Eq. (2.27) is symmetric w.r.t. time: it describes a reversible process, involving only the mean–field component

of the gravitational field. In chapter 4 we will take into account the first–order corrections produced by dynamical friction effects, which are a byproduct of the discrete nature of the phase space of a perturbations. We will see that these modifications are really important only for **hierarchical clustering models** of galaxy and clusters' formation, like the CDM models, while in models predicting a small amount of substructure on these scales, like the Hot Dark Matter cosmologies, these corrections are quantitatively irrelevant.

2.1.2 Early Nonlinear Stages.

The linear solutions found in the preceding paragraph were obtained by expanding the density up to the first order in δ and truncating the velocity hierarchy at the zero–order, i.e. putting simply: $\langle u^\alpha u^\beta \rangle = 0$. The equations found in the preceding section involve only the time as independent variable: if we take the Fourier transform of the solutions we notice that each single component of the Fourier transformed density field evolves independently of the others. Correlations, if initially present, grow like the density field, i.e. $\xi(r) \propto (1+z)^{-2}$ (because the correlation function grows as δ^2).
However, as the amplitude of the fluctuations on a given scale grows, nonlinear coupling of modes of different wavenumbers modifies the power spectrum and, in general, phase coupling induces the growth of higher order correlations. The density field can generally be expanded in a perturbative series:

$$\delta(\mathrm{k}) = \delta^{(1)}(\mathrm{k}) + \delta^{(2)}(\mathrm{k}) + ..., \tag{2.36}$$

where $\delta^{(1)}(\mathrm{k})$ is the Fourier transform of linear solution of the preceding section. Evolution of second order perturbation has been considered by a number of authors (Peebles, 1980, §18; Juskiewicz, 1981; Vishniac, 1983; Juskiewicz et al., 1984; Coles, 1990). Inserting the expansion (2.36) into eqs. (2.20),(2.21) and eq. (2.18), expanding all the other quantities and performing some reduction one arrives at a separable second order equations for $\delta^{(2)}(\mathrm{k})$. The expansion up to the second order of the averaged density perturbation squared now reads:

$$\mid \delta(\mathrm{k}) \mid^2 = \mid \delta^{(1)}(\mathrm{k}) \mid^2 + \mid \delta^{(2)}(\mathrm{k}) \mid^2 + 2\Re\langle \delta^{(1)}(-\mathrm{k})\delta^{(3)}(\mathrm{k})\rangle \tag{2.37}$$

The mixed average on the right–hand side does not cancel out after averaging over phases: this important fact, noted by Vishniac (1983), complicates enough the

analysis, because it brings into the game also $\delta^{(3)}$. After some tedious calculations (Juskiweicz et al., 1984), one can show that the power spectrum will be given by:

$$P(\mathrm{k},t) = P(k)\left(\frac{t}{t_{rec}}\right)^{4/3} + [I_1(k) + I_2(k)]\left(\frac{t}{t_{rec}}\right)^{8/3} \tag{2.38}$$

and the correlation function will now be given by:

$$\xi(r) = 4\pi \int_0^\infty dk k^2 \frac{\sin(kr)}{kr} [P(k) + I_1(k) + I_2(k)], \tag{2.39}$$

where $I_1(k), I_2(k)$ are two functions depending on $P(k)$. The precise behaviour of $\xi(r)$ now depends on the shape of the power spectrum. Coles (1990) has shown that for the CDM spectrum and a gaussian window function of radius R_f one has:

$$P(k) = AkT_f^2(k)\exp\left(-k^2R_f^2\right),$$
$$T_f(k) = \frac{\log(1+2.34q)}{2.34q}\left[1 + 3.89q + (16.1q)^2 + (5.46q)^3 + (6.71q)^4\right]^{-1/4} \tag{2.40}$$

where: $q = k/\Omega_{CDM}h^2 Mpc^{-1}$ the modified spectrum is in general steeper for small r and has a crossing point larger. The modification depend sensibly on the value of the bias parameter adopted, however. The steepening of $\xi(r)$ can be physically interpreted as a consequence of the transfer of power from low to large k. About the eventual shortening of the correlation length there is no general consensus: the point where $\xi \approx 0$ marks the transition to the linear regime, and in this region a competition between transfer of power from larger regions and the shrinking due to gravitational contraction, which have almost the same magnitude, make an interpretation of the ongoing physics rather subtle and circumstantial.

In conclusion, the inclusion of nonlinear effects modifies the spectrum inducing a steepening and a fast transition to the nonlinear regime. Quantitatively, the effect depends on the shape of the power spectrum. Nonlinear terms grow much faster than the linear ones, and the time interval in which a linear approximation can be reasonably adopted is quite limited.

2.1.3 Late Nonlinear Stages - Numerical Simulations.

The nonlinear evolution of density perturbations should provide the final answer to the problem of clusters' formation and evolution. As we saw in chapter 1,

there is evidence that the central regions of rich clusters have typical overdensities $\bar{\delta} \approx 100$ and have already turned around. A solution of the nonlinear BBGKY hierarchy has been found only under some approximations (Fry, 1984; Hamilton, 1988). Numerical simulations could in principle provide the answer to the problem of nonlinear evolution. In practice, the simulations peformed until now proved to have a limited dynamical and mass range to reach the target. More specifically, the problem is that clusters of galaxies are very inhomogeneous systems, with dense central cores having typical radii $400 - 700h^{-1}$ Kpc and extended outskirts where the overdensity drops by 2-3 orders of magnitude. In typical simulations like those performed by Thomas & Couchman (1992) one has 32^3 particles inside a cubic region of $50Mpc$ size; the softening parameter is usually taken enough small to increase the dynamical range, but must also be large enough to minimize relaxation problems. As an example, Thomas and Couchman (1992) choose $s \approx 40h^{-1}Kpc$. The 2-body relaxation time is then given by:

$$\frac{t_r}{t_0} \approx 0.03 \times \frac{(R/s)^{3/2}}{\ln(R/s)} N^{1/2} \left(\frac{N_p}{32^3 \Omega_p}\right)^{1/2} \tag{2.41}$$

where Ω_p is the particle number density, t_0 the age of the Universe and R the core radius. At the end of the simulation, they find typical cor sizes $R \approx \sqrt{e}s$: the relaxation time is then quite short in the core, because N is small (≈ 40). On the other hand, the outer parts of the cluster are free from this problem because there $N \ll 1$. This shows that the interpretation of the results of numerical simulations must be done carefully.

Two main methods have been adopted in the numerical studies of clusters: Montecarlo and N-body simulations. The essence of the Montecarlo method is the generation of a stochastic process obeying a set of laws which describe the different physical interactions among the different components of the cluster (i.e. dark matter, galaxies, intracluster medium). Richstone & Malumuth (1983) applied this method to study the evolution of the mass spectrum and the formation of a Cd galaxy in rich clusters. Their work displays all the merits and problems of the Montecarlo approach. Giving initial positions and velocities to a set of particles whose masses are chosen according to a Schechter (1976) mass spectrum , they followed the evolution of positions and mass spectrum. The main uncertainties in the final result seem to come from the input physics, i.e. from the specification of the cross sections and final binding energies of the merging events. They show

that the Schechter spectrum is stable to an evolution including merger events, and that a central Cd galaxy forms only in 30% of the cases. Moreover, they find no evidence for mass segregation between dark and baryonic matter. They also included a dynamical friction term in their equations of motions: contrary to recent claims by Mayoz (1991) their procedure is correct, because the fluctuating component of the gravitational field is not automatically produced in a Monte-carlo simulation, contrary to what happens in N-body simulations.
The most popular algorithm to simulate clsuetr evolution is however the N-body. A full analysis of the major findings of these experiments would require a large review, so here we limit ourselves to summarise the main results.

Density profiles: As for many other topics, N-body simulations seem not to have provided yet an unique answer to the question of the final density profile, and especially of its dependence on the power spectrum. Quinn et al. (1986) find that the density profiles depend strongly on the initial power spectrum: for $n \leq -1$ they get $\rho \approx r^{-2}$, but for $n \geq -1$ the profiles are considerably steeper and in remarkably good agreement with the results of the theoretical infall models by Hoffman & Shaham (1985) (see also Hoffman, 1988, 1989). These findings have been confirmed by the simulations of Efstathiou et al. (1988) but the results of Carlberg & Dubinsky (1991) and Thomas & Couchman (1992) are not consistent with these because they start with CDM spectra which, on the scale of a few Mpcs can be approximated by power-law spectra having indexes $-1 \leq n \leq 0$, and they find profiles decreasing as isothermal spheres ($\rho \approx r^{-2}$) in the outer regions.
On the other hand, West et al. (1987) do not find any evidence of a dependence of the density profile on the power spectrum. The final density profiles in their simulations are well approximated as isothermal. They conclude that clusters are relaxed systems which have already experienced violent relaxation: their conclusions are supported by a comparison with the the optical luminosity profiles for 27 Abell clusters which confirms their numerical results. West (1990) suggests that the discrepancy in the results is only in the interpretation: while Efstathiou et al. (1988) and Thomas & Couchman (1992) use 'friends-of-friends' and minimal spanning tree algorithms, respectively, to extract clusters out of their outputs, West et al. (1987) look 'by eye' at regions having some prescribed overdensity.

As a result, their 'clusters' are in general lesser overdense than those found by former authors. However, they compare their results with luminosity profiles of galaxy distributions, i.e. with data taken in the innermost regions of clusters. Efstathiou et al. (1988) attribute the differences to the different number of particles adopted: their simulations involve many more particles, although West et al. (1987) adopt an Aaarseth direct summation code rather than a P^3M like Efstathiou et al. (1988).

Another feature of the density profiles is the so-called "*secondary maximum*" (Bahcall, 1971; Oemler, 1974; Austin & Peach, 1974; Dressler, 1978a; Kirshner et al., 1979; Yahil et al., 1980; Dekel, 1981). The reality of this feature has been questioned by some of the mentioned authors, and it is not observed in many recent simulations. The reason could be ascribed to the extended dynamical range allowed by these more recent numerical simulations. Farouki et al. (1983) have suggested that this feature could be originated by a large outward gradient of the velocity dispersion profile which produces a local depression at some distance from the core. They also saw in their simulations that the location of the secondary maximum shifts outwards with time, as a consequence of a large outward motion of the outer layers of the cluster. The secondary maximum could then be present only in unrelaxed clusters.

A very important issue addressed often in the N-body simulations is that of substructure. Cavaliere et al. (1986) addressed this question in a series of simulations and showed that substructure, often present in the form of two large lumps, tend to last for quite long times in about 30% of their simulations. As we saw in Chapter 1, observational work (starting from the paper by Geller & Beers (1982)) has tended to confirm this prediction. Moreover, they find a large variance in the outputs of their simulations which could be related to the observed variance in the morphological X-ray properties of clusters. It is clear that this conflicts with the above mentioned claims by West et al. (1987) and West & Richstone (1988). The reason could lie in the proper choice of the scale of the simulations (Richstone, 1990).

Mass and luminosity segregation: Since the original suggestion by Hoffman et al. (1982) many investigations have been devoted to a search for spatial mass and luminosity segregation beteween dark and baryonic matter. The object one looks at is the trend of M/L inside a cluster: i.e. whether dark and luminous

matter are distributed in the same way or not. Hoffman et al. (1982) deduced that the action of dynamical friction should have modified the distribution of galaxies. It can be instructive to review their argument. Suppose for simplicity that matter is distributed in a spherical halo with power law density profile: $\rho(R) = \rho_0 (R/R_0)^{-m}$, with $0 \leq m \leq 3$. If galaxies are on circular orbits their velocity can be written:

$$v^2(R) = \frac{GM_0}{R_0} \left(\frac{R}{R_0}\right)^{2-m} \tag{2.42}$$

where $M_0 = [4\pi/(3-m)]\,\rho_0 R_0^3$. The equation of motion of a single galaxy in presence of dynamical friction is:

$$\frac{dv}{dt} = -\frac{4\pi G^2 M_g \rho (\ln\Lambda + 0.367)}{v^2} g(jv) \tag{2.43}$$

where whe have defined:

$$g(jv) = \frac{4}{\pi^2} \int_0^{\left[\frac{2}{3}\langle v^2\rangle_{DM}\right]^{-1} v} dx x^2 e^{-x^2}$$

Solving eq. 2.43 for the density progile given above, and assuming that the shells inside which galaxies move do not cross, we obtain:

$$\frac{R(t)}{R_0} = \left[1 - \frac{t}{\tau_0}\right]^{\frac{2}{6-m}} \tag{2.44}$$

where one has defined:

$$\tau_0 = \frac{4-m}{2\pi(6-m)(3-m)} \cdot \frac{1}{(\ln\Lambda + 0.367)\, g(jv)} \frac{M_0}{M_g} t_0$$

Now, we can write the M/L ratio as:

$$\frac{M}{L} = \frac{\bar{\rho}(R)}{\bar{n}_g(R)\, l_*} = \left(\frac{M}{L}\right)_\infty \left(\frac{R}{R_0}\right)^{3-m} \tag{2.45}$$

The latter equality comes out because $\bar{n}_g(R) \propto N_g/R^3$ and $\bar{\rho}(R) \propto R^{-m}$. So when the average radius of the farthest shell decreases also the observed M/L will decrease w.r.t. the asymptotic value. This is a consequence of the fact that τ_0 is finite, i.e. that dynamical friction acts on a timescale much lesser than the age of the Universe in the relatively dense interiors of rich Abell clusters. Even larger decreases of the M/L ratios are seen in the opposite case of radially, rather

than circularly, anisotropic distribution functions (Kashlinsky, 1984). Subsequent work by Kashlinsky (1986) showed that the M/L evoluution with time is much reduced when realistic distribution functions and rotational profiles for clusters are considered.

Mass and luminosity segregation is often seen in two component N-body simulations (Roos and Aarseth, 1982; Farouki et al., 1983; Barnes, 1984; West and Richstone, 1988; West, 1990). The amount of segregation depends critically on the amount of dynamical friction, which ultimately depends on the amount of subclustering. West & Richstone (1988) demonstrated this fact in a very elegant way: they compared the mean harmonic radii of dark and baryonic mater particles in two simulations, the first starting from a power-law spectrum and the second from an initial distribution in which all the low-wavelength noise was suppressed (the particle distribution was highly uniform on small scales). While in the first case the harmonic mean of the baryonic particles was 3 times lesser than that of the DM particles, in the second case no appreciable difference could be detected at the end of the simulation.

Finally, the problem of mass segregation has also been studied via solutions of the Fokker-Planck equations (Merritt, 1983, 1985; Inagaki & Saslaw, 1985; Yepes et al., 1991; Yepes & Domínguez-Tenreiro, 1992). The applicability of the Fokker-Planck equation relies on the assumption that a principle of detailed balance applies, an assumption which could not hold over all the extension of a cluster. It could be however valid in the central parts, precisely in those regions where the density is high enough to reduce the typical duration of the stochastic force $T(F)$ below the dynamical time. Whether this applies or not has not yet been completely investigated.

Velocity segregation: The first suggestion that dynamical friction reduces the average relative velocity of galaxies w.r.t. dark matter was put forward by Farouki et al. (1983): they also showed that the amount of velocity segregation could weakly depend on the shape of the mass spectrum. More recent work by Carlberg (1991) and Carlberg& Dubinsky (1991) using a much larger dynamical range has confirmed the previous findings. The main conclusion is that dynamical friction reduces also the velocity dispersion of the galactic population, in addition to the mean average radius (i.e. the M/L). If energy conservation holds

one should expect an increase of the average velocity dispersion of the galactic component as it sinks inside the potential well of the cluster. The fact that a decrease is observed proves that the opposite is true, i.e. that dynamical friction causes energy to be transferred to the dark matter component during the infall. The effect on the mass distribution of the Dark Matter halo due to this transfer is probably very small if $M_{DM} \geq M_{bar}$. This "*velocity bias*" can be quantified by the parameter $b_v = \sigma_{bar}/\sigma_{DM}$: Carlberg & Dubinsky (1991) find: $b_v \approx 0.8$. This number can reconcile the estimates of Ω from the Cosmic Virial Theorem (Peebles, 1980) with the observed values of the galaxies' velocity dispersion which are lower than predicted in a flat $\Omega = 1$ model. The velocity bias could have been recently detected by Biviano et al. (1992).
The only problem with the velocity bias is that the interpretation offered by Carlberg (1991) is unreliable, because it does not correctly take into account the effect of clustering on the dynamical friction coefficient. In chapter 5 we will rederive his results using a N-body code conveniently modified to take into account this effect and we will show the results to be in agreement with the theoretical expectations of chapter 4.

N-body simulations give more definite predictions about the clustering and its temporal evolution. Efstathiou et al. (1988) find that the theoretical predictions of Davis & Peebles (1977) based on a self-similar evolution of the correlation function are reproduced in their N-body simulations only in linear and moderately nonlinear clustering regimes, i.e. for $\xi \leq 50$. In strongly nonlinear regimes the numerical correlation function is steeper than the self-similar one, and the pairwyse velocity in these regimes is much larger than value predicted if clusters were in virial equilibrium. This tends to suggest that virial equilibrium could even never be reached in highly clusterd systems. We will return to this problem in chapter 5.
In conclusion, numerical studies of cluster formation and evolution, when associated with theoretical interpretations, provide useful tests of the dynamical mechanisms of energy transfer among the different components, although the quantitative assessment has to be eventually left to more refined theoretical treatments. N-body simulations outnumber the Montecarlo simulations in the current astrophysical literature. Nonetheless, the Montecarlo method allows to test the

effects of very detailed models of merging, i.e. a better specification of the input physics, while in N-body simulations some more less high degree of simplification is required in order to match present-day computer possibilities. One conceptual difficulty of the Montecarlo method is however the implicit assumption of an underlying Markovian process in the generation of the interaction events: this proves to be false in highly correlated systems like clusters of galaxies, i.e. the probability of having a merger interaction is not only enhanced by the clustering but also dependent on the trajectory of the galaxy inside the cluster. On the other hand, the positions and masses of the galaxies in Richstone & Malumuth (1983) simulations are independent of each other, and this is clearly an oversimplification.

2.2 Bibliography for Chapters 1 and 2.

Abell, G.O., *Ap.J. Supp.*, **3**, 211 (1958)

Abell, G.O., Corwin, H.G. and Olowin, R.P., *Ap.J. Supp.*, **70**, 1 (1989)

Antonuccio–Delogu, *this thesis* and *Ap. J.*, submitted (1992)

Appel, L, and Jones, B.J.T., *M.N.R.A.S.***245**, 522 (1990)

Arnaud, M., Rothenflug, R., Boulade, O., Vigroux, L. and Vangioni-Flam, E. *Astron. Astrophys.* **254**, 49 (1992)

Austin, T.B. and Peach, J.V., *M.N.R.A.S.* **167**, 437 (1974)

Bahcall, N.A., *A.J.* **76**, 995 (1971)

Bahcall, N.A., *Ap. J.* **198**, 249 (1975)

Bahcall, N.A., *Ann. Rev. Astron. Astrophys.* **15**, 505 (1977)

Bahcall, N.A., *Ap. J.* **193**, 529 (1977b)

Bahcall, N.A., *Ap. J.* **232**, 689 (1979)

Bahcall, J.N. and Tremaine, S., *Ap.J.* **244**, 805 (1981)

Baier, F.W., *Astr. Nachr.* **298**, 351 (1977)

Baier, F.W., *Astr. Nachr.* **304**, 211 (1983)

Baier, F.W., *Astr. Nachr.* **305**, 175 (1984)

Baier, F.W., and Oleak, H., *Astr. Nachr.* **304**, 277 (1984)

Bardeen, J.M., Bond, J.R., Kaiser, N. and Szalay, A.S., *Ap. J.* **304**, 15 (1986)

Barnes, J., *M.N.R.A.S.***208**, 873 (1984)

Bechtold, J., Forman, W., Giacconi, R., Jones, C., Schwarz, W., Tucker, L. and Van Speybroeck,L., *Ap. J.* **265**, 26 (1983)

Beers, T.C. and Tonry, J.L., *Ap. J.* **300**, 557 (1986)

Bertschinger, E., *Ap. J. Supp.*, **58**, 39 (1985)

Binggeli, B, Sandage, A. and Tarenghi, M., *A.J.* **90**, 1681 (1984)

Binggeli, B, Sandage, A. and Tarenghi, M., *A.J.* **94**, 251 (1984)

Binggeli, B, Sandage, A. and Tamman, I., *A. J.* **94** 251 (1987)

Binggeli, B, Sandage, A. and Tamman, I., *Astron. Atrophys.* **252**, 27 (1991)

Biviano, A., Girardi, M., Giuricin, G., Mardirossian, F. and Mezzetti, M. preprint (1992)

Bond, J.R., Cole, S., Efstathiou, G. and Kaiser, N., *Ap. J.***379**, 440 (1991)

Bothun, G.D., Geller, M.J., Beers, T.C. and Huchra, J.P., *Ap.J.* **268**, 47 (1983)

Bouchet. F. and Pellat, R., *Astron. Astrophys.***141**, 77 (1984)

Bower, R.G., *M.N.R.A.S.***248**, 332 (1991)

Brainerd, T.G. and Villumsen, J.V., *Ap. J.*(1992)

Briel, U.G., Henry, J.P. and Böhringer, H., *Astron. Astrophys.* **259**, L31 (1992)

Carlberg, R.G., *Ap. J.***367**, 385 (1991)

Carlberg, R.G., and Dubinsky, J., *Ap. J.***369**, 13 (1991)

Cavaliere, A., and Colafrancesco, S., in *Large Scale Structure and Motions in the Universe*, Mezzetti M., Giuricin, G., Mardirossian, F. and Ramella, M., eds., p. 73 (Kluwer eds.), 1989

Cavaliere, A., Colafrancesco, S. and Menci, N., invited lecture at the NATO–ASI Summer School on *Clusters and Superclusters of Galaxies*, Cambridge (1992)

Cavaliere, A., Colafrancesco, S. and Scaramella, R., *Ap. J.***380**, 1 (1991)

Cavaliere, A. and Fusco–Femiano, R., *Astron. Astrophys.***49**, 137 (1976)

Cavaliere, A. and Fusco–Femiano, R., *Astron. Astrophys.***70**, 677 (1978)

Cavaliere, A., Gursky, M. and Tucker, W.H., *Nature* **231**, 437 (1971)

Cavaliere, A., Sanatngelo, P., Tarquini, G., and Vittorio, N., *Ap. J.* **305**, 651 (1986)

Cole, S. and Kaiser, N., *M.N.R.A.S.***237**, 1127 (1989)

Coles, P., *M.N.R.A.S.* **243**, 171 (1990)

Colless, M.M., and Hewitt, P., *M.N.R.A.S.* **224**, 453 (1987)

David, L.P., Arnaud, K.A., Forman, W. and Jones, C. *Ap.J.* **356**, 32 (1990)

David, L.P. and Blumenthal, G.R., *Ap. J.***389**, 510 (1992)

Davis, M. & Peebles, P.J.E.,*Ap. J. Supp* **34**, 425 (1977)

Dekel, A., *Astron. Astrophys.* **101**, 79 (1981)

Doroshkevich, A.G., *Astrophysics* **6**, 320 (1970)

Dressler, A., *Ap.J.* **226**, 55 (1978a)

Dressler, A., *Ap.J.* **231**, 659 (1978b)

Dressler, A. and Schechtman, S., *A.J.* **95**, 284

Efstathiou, G., in "Physics of the early Universe", Peacock, J. ed., Edinburgh (1990)

Efstathiou, G., Frenk, C.S., White, S.D.M. and Davis, M., *M.N.R.A.S.* **235**, 715 (1988)

Eyles, C.J., Well, M.P., Bertram, D., Church, M.J., Pomman, T.J., Skinner, G.K. and Willmore, A.P., *Ap.J.* **376**, 23 (1991)

Fabricant, D., Beers, T.C., Gelller, M.J., Gorenstein, P., Huchra, J.P., and Kurtz, M.J., *Ap. J.* **308**, 530 (1986)

Farouki, R.T., Hoffman, G.L. and Salpeter, E.E., *Ap. J.***271**, 11 (1983)

Felten, J.E., Gould, R.J., Stein, W. and Woolf, N.J., *Ap. J.* **146**, 955 (1966)

Ferguson, P. *A.J.* **98**, 367 (1989)

Fitchett, M., *M.N.R.A.S***230**, 161 (1988)

Fitchett, M., and Merritt, D., *Ap. J.* **335**, 18 (1988)

Fitchett, M., and Webster, R.L., *Ap. J.* **317**, 653 (1987)

Forman, W., Bechtold,J, Blair, W., Giacconi, R., Van Speybroeck, L. and Jones, C., *Ap. J.***243**, L133 (1981)

Forman, W. and Jones, C., *Ann. Rev. Astron. Astrophys.* **20**, 547 (1982)

Fry, J. N., *Ap. J.***279**, 499 (1984)

Geller, M.J., in *Clusters of Galaxies*, Oegerle, W.R., Fitchett, M.J. and Danly, L. eds., p. 25 (Cambridge: Cambridge University Press) (1990)

Gerbal, D., Durret, F., Lima–Neto, G. and Lachièze–Rey, M., *Astron. Astrophys.* **253**, 77 (1992)

Giacconi, R., Murray, S., Gursky, H., Kellogg, E., Schreier, T., and Taanbaum, H., *Ap.J.* **178**, 281 (1972)

Giacconi, R., Murray, S., Gursky, H., Kellogg, E., Schreier, T., Matilsky, T., Koch, D. and Tananbaum, H., *Ap.J. Supp.* **27**, 37 (1974)

Gioia, I.M., Geller, M.J., Huchra, J.P., Maccacaro, T., Steiner, J.E., and Stocke, J., *Ap. J.***255**, 117 (1982)

Godwin, J.C., and Peach, J.V., *M.N.R.A.S.* **181**, 323 (1977)

Gott, J.R. and Turner, E.L., *Ap. J.***209**, 1 (1976)

Gunn, J.E. and Gott, J.R., *Ap.J.*,**176**, 1 (1972)

Hamilton, A.J.S., *Ap. J.***332**, 67 (1988)

Heisler, J., Tremaine, S. and Bahcalll, J.N., *Ap.J.* **298**, 8 (1985)

Henry, J.P., and Arnaud, K.A., *Ap. J.***372**, 410 (1991)

Henry, J.P. and Briel, U. G., *Astron. Astrophys.***259**, L14 (1992)

Hoffman, Y., *Ap. J.***328**, 489 (1988)

Hoffman, Y., *Comm. Astrophys.* **14**, 153 (1989)

Hoffman, Y., and Shaham, J., *Ap. J.***297**, 16 (1985)

Hoffman, Y, Shaham, J. and Shaviv, G., *Ap. J.***262**, 413 (1982)

Hughes, J P., *Ap. J.***337**, 21 (1989)

Inagaki, S. and Saslaw, W.C., *Ap. J.***292**, 339 (1985)

Jones, B.J.T., Martines, V., Saar,E., and Einasto, M., *Ap.J.* **332**, L1 (1988)

Jones, C., and Forman, W., *Ap. J.***276**, 38 (1984)

Juskiewicz, R., *M.N.R.A.S.* **197**, 931 (1981)

Juskiewicz, R., Sonoda, D.H. and Barrow, J.D., *M.N.R.A.S.* **209**, 139 (1984)

Kaiser, N., *Ap. J.* **284**, L9 (1984)

Kashlinsky, A., *M.N.R.A.S.* **202**, 249 (1983)

Kashlinsky, A., *M.N.R.A.S.* **208**, 623 (1984)

Kashlinsky, A., *Ap. J.***306**, 374 (1986)

Kent, S.M. and Gunn, J.E., *A.J.* **87**, 945 (1982)

Kent, S.M., and Sargent, W.L.W., *A. J.* **88**, 697 (1983)

King, I., *A.J.* **67**, 471 (1962)

Kirshner, R.D., Oemler, A., Jr. and Schechter, P.L., *A.J.* **84**, 951 (1989)

Kolb, E. and Turner, M. "*The Early Universe*", Addison–Wesley, (1990)

Koyama, K., Takano, S. and Tawara, Y., *Nature* **350**, (1991)

Lee, K.L., *J. Am. Stat. Ass.* **74**, No. 367, 708 (1979)

Lindgren, W., *Statistical Theory*, Mac Millan, N.Y. (1976)

Lucchin, F., in *Lecture Notes in Physics* **332**, Flin, P. ed., p. 284 (Berlin: Springer Verlag) (1988)

Lucchin, F., and Matarrese, S., *Ap. J.***330**, 535 (1988)

Malumuth, E.M., Kriss, G.A., Van Dyke Dixon, W., Ferguson, M.C. and Ritchie, C., *A.J.* **104**, 495 (1992)

Marinari, E. and Parisi, G., *Europhys. Letters* **19**, 451 (1992)

Mayoz, E., preprint (1991)

Merrifield, M. and Kent, S., *Ap. J.*, , (1990) 101, 783 (1991)

Merritt, D., *Ap. J.***264**, 24 (1983)

Merritt, D., *Ap. J.***289**, 18 (1985)

Mitchell, R.J., Dickens, R.J., Bell Burnell, S.J., and Culhane, J.L., *M.N.R.A.S.* **189**, 329 (1979)

Neymann, J., *A.J.* **66**, 550 (1961)

Oemler, A., *Ap. J.***194**, 1 (1974)

Peacock, J.A. and Heavens, A.F., *M.N.R.A.S.***217**, 805 (1985)

Peebles, P.J.E., *Ap. J.* **153**, 13 (1968)

Peebles, P.J.E., "The Large-Scale Structure of the Universe", Princeton: Princeton University Press (1980)

Pietronero, L., *Physica*, **144A**, 257 (1987)

Press, W.H., and Schechter, P., *Ap. J.***187**, 425 (1974)

Quinn, P.J., Salmon, J.K. and Zurek, W.H., *Nature* **322**, 329 (1986)

Quintana, H., and Melnick, J., *A.J.* **87**, 972 (1982)

Quintana, H., de Souza, R.E. and Arakaki, L.

Rhee, G.F.R.N., van Haarlem, M.P. and Katgert, P., *Astron. Astrophys.* **246**, 301 (1991)

Richstone, D.O., in *Clusters of Galaxies*, Oegerle, W.R., Fitchett, M.J. and Danly, L. eds., p. 231 (Cambridge: Cambridge University Press) (1990)

Richstone, D.O. and Malumuth, E.H., *Ap. J.***268**, 30 (1983)

Roos, N., and Aarseth, S.J., *Astron. Astrophys.***114**, 41 (1982)

Rood, H.J., *Rep. Prog. Phys.* **44**, 1077 (1981)

Rozgacheva, I.K., *Astrophysics* **28**, 368 (1988)

Sarazin, C., *Rev. Mod. Phys.* **58**, 1 (1986)

Sarazin, C., "X–ray emission from Clusters of Galaxies", (cambridge: Cambridge Univ. Press (1988))

Shandarin, S.F. and Zeldovich, Ya.B., *Rev. Mod. Phys.***61**, 185 (1989)

Schechter, P., *Ap. J.***203**, 297 (1976)

Solinger, A.B, and Tucker, W.H., *Ap. J.* **175**, L107 (1974)

Smith, S., *Ap. J*, **83**, 23 (1936)

Smith, H., Jr., Hintzen, P., Holman, G., Oegerle, W. Scott, J. and Sofia, S., *Ap. J.* **234**, L97 (1979)

Takano, S., Awaki, H., Koyama, K., Kurieda, H., TAwara, Y., Yamauchi, S., Makishino, K and Ohashi, T., *Nature* **340**, 289 (1989)

Teague, P.F., Carter, D. and Gray, P.M., *Ap. J. Supp.* **72**, 715 (1990)

Thomas, P.A. and Couchman, H.M.P., *M.N.R.A.S.* **257**, 11 (1992)

Yahil, A., Sandage, A. and Tammann, G.A., *Ap. J.***242**, 448 (1980)

Yepes, G., and Domínguez-Tenreiro, R. *Ap. J.***387**, 27 (1992)

Yepes, G., Domínguez-Tenreiro, R. and del Pozo-Sanz, R., *Ap. J.***373**, 336 (1991)

Vishniac, E., *M.N.R.A.S.* **203**, 345 (1983)

Weinberg, S.W., *Gravitation and Cosmology* (New York: Wiley (1972))

West, M.J., in *Clusters of Galaxies*, Oegerle, W.R., Fitchett, M.J. and Danly, L. eds., p. 65 (Cambridge: Cambridge University Press) (1990)

West, M.J., Dekel, A. and Oemler jr., A., *Ap.J.* **316**, 1 (1987)

West, M.J., Oemler, A., Jr. and Dekel, A., *Ap. J.***327**, 1 (1988)

West, M.J. and Richstone, D.O., *Ap. J.***335**, 532 (1988)

White, S.D.M., *M.N.R.A.S.* **177**, 717 (1976)

Zwicky, F., *Helvetica Physica Acta*, **6**, 110 (1933)

Zwicky, F.E., Herzog, P., Wild, M., Karppowicz, M. and Kowal, C.T., "Catalogues of Galaxies and Clusters of Galaxies" (1961–1968)

Chapter 3

Gravitational Field Fluctuations in Weakly Clustered Systems.

Stochastic fluctuations of the gravitational field in a collisionless, weakly clustered protogalactic system are induced by local fluctuations in the number density of small collapsed peaks. We calculate the probability distribution of the stochastic forces generated by these fluctuations, and we find a generalization of the Holtsmark distribution, previously studied in a stellar dynamical context by Chandrasekhar and Von Neumann (1942) and by Kandrup (1980). We also find the probability distribution of the torques induced by these stochastic forces, introducing the analogue of the Holtsmark law for the torque distribution, and we study different cases corresponding to different power–laws.
We apply these considerations to realistic models of protogalactic and protocluster density perturbations. The force probability distribution is remarkably influenced by the clustering of substructure: the profile is more strongly peaked, and the asymptotic decay $W(F) \rightarrow F^{-5/2}$ is almost suppressed, resulting in an enhanced probability near the average value. The consequences of this fact on the calculation of the dynamical evolution of cosmological density perturbations, which will be developed in a subsequent chapter, are stressed.

3.1 Introduction.

One of the crucial problems in any theory of structure formation in the Universe is the origin and dynamical evolution of density fluctuations. In a hierarchical "bottom–up" scenario high density, nonlinearly collapsed peaks cluster and merge

together to form larger structures. It is often assumed that the density fluctuation field is locally isotropic, the amplitudes are locally gaussian distributed and their phases are uncorrelated (Peebles 1980). Under these assumptions the properties of the density fluctuation field $\delta(r)$ can be entirely expressed in terms of its Fourier transform, the power spectrum $P(k)$. On average, the characteristics of the density field's peaks, e.g. their mass distribution, ellipticity, peculiar velocities etc., are completely determined by the spectrum through its moments of various order, at least during the linear and early nonlinear phases of the collapse (Bardeen et al. 1986; Hoffmann & Shaham 1985; Ryden & Gunn 1987), when the density perturbation detaches from the background expansion and secondary infall of matter gravitationally bound to the peak takes place (Gunn 1977; Bertschinger 1985).

Due to isotropy, the distribution of all physical quantities around density peaks is, on average, spherically symmetric. However, actual realizations of the density and velocity field distributions around peaks which will later form galaxies and clusters, depart both from spherical symmetry and from the average density profile. This produces important consequences to the dynamics of the collapse and formation of protogalactic structures, which have been recently studied by some authors (Hoffman & Shaham 1985; Ryden 1988; Heavens & Peacock 1988). In particular Ryden & Gunn (1987), within the context of an infall model for cluster formation, have considered the tidal coupling between shells of matter which are accreted around a density peak and the inner parts of the forming protostructure. They have shown that the tidal torques and the dragging of Dark Matter due to baryonic infall lead to the formation of haloes with density profiles that well reproduce the general features of the rotation curve of a spiral galaxy. Similar work has been independently carried out by Heavens & Peacock (1988). In both papers, the authors are concerned with the dynamical influence of the substructure of small length scale which is abundantly produced in hierarchical bottom–up scenarios, on the matter gravitationally bound to the density perturbation. However, they consider only those gravitational perturbations generated by the *global* distribution of the substructure, namely by the deviations of this distribution from spherical symmetry. On the other hand, the substructure existing in large wavelength density peaks generates local fluctuations of the gravitational field. Rozgacheva (1988) has recently considered the effect of local fluctuations

on the evolution of the density profile. Our purpose in the present chapter is to start an investigation of these fluctuation fields on the dynamical evolution of cosmological density perturbations.

An analysis of these small scale gravitational field fluctuations can be of interest to understand various aspects of the dynamics of galaxy and cluster formation. They can affect the dynamics of matter infalling onto the cluster, and the redistribution of energy, angular momentum and other dynamical quantities among the dark and baryonic components of a protogalactic structure. This is especially true in the innermost regions, where tidal effects become less important because the density distribution tends to be more spherically symmetric (Ryden 1988).

The study of the small scale "graininess" fluctuations of the gravitational field in a large but discrete gravitating system was pioneered by Chandrasekhar and Von Neumann (1942 a,b): they showed an important fact, namely that the probability distribution of the force experienced by a point particle moving in a region containing other point–like particles randomly distributed with constant density is given by the so called **Holtsmark law**:

$$W(F) = \frac{2}{\pi} F \int_0^\infty dk k \exp\left[-\frac{3}{2} N \left(\frac{G m_*}{r_t^2} k\right)^{\frac{3}{2}}\right] \sin(kF) \qquad (3.1)$$

Here $W(F)dF$ is the probability for a test particle of experiencing a force in the interval $F, F + dF$, N is the total number of particles, m_* a typical mass and r_t a characteristic distance among the particles. A remarkable feature of this distribution is the fact that it has a long tail, decaying at high values as $F^{-\frac{5}{2}}$.

More recently Kandrup (1980a, b)) has performed a detailed analysis of the role of the fluctuations on the relaxation of a self–gravitating system. He verified that the Holtsmark law holds for a system having a density law given by $\rho(r) \sim r^{-p}$, with $0 \leq p \leq 3$. He also found that the largest contribution to the local stochastic force field distribution comes from the statistically more probable interactions with few neighboring particles, rather than from strong perturbations by rare collective effects involving distant particles. This result was already suggested by the numerical simulations of Ahmad and Cohen (1973, 1974) and by Chandrasekhar (1941).

Implicit in the above works is that the gravitational field can be decomposed into the sum of two independent components, namely a mean–field force due to the global density distribution and a stochastic, fluctuating component. As stressed

by Kandrup (1980a), this is rigorously true only for systems with no correlations among the particles. Otherwise it would be difficult even to define a mean–field component. However, if the correlations are weak, as happens when the system is still in the linear regime, the decomposition of the gravitational field mentioned above still applies. All the results we present in this chapter are valid only under this assumption.

It can be useful to compare the relative importance of the mean–field and fluctuating components of the gravitational field in a realistic model of the protogalactic system. To this purpose, we will make use of the results of the Chandrasekhar and Kandrup's investigations. Theoretical work (Ryden 1988) suggests that the density profile inside a protogalactic dark matter halo, before total relaxation and baryonic infall, can be approximated by a power–law:

$$\rho(r) = \frac{\rho_0 r_0^p}{r^p}, \tag{3.2}$$

where: $p \approx 1.6$ on a protogalactic scale. The mean-field gravitational force from this density distribution is thus given by:

$$F_0 = -\frac{GM_{tot}}{R_{sys}^{3-p}} r^{1-p} \tag{3.3}$$

Secondary peaks of the density field inside the spherical region will have a density distribution similar to eq. (2) above: $n(r) = n_0(r/r_0)^{-p}$, and will create small–scale irregularities in the gravitational field. The average value of the force induced by the secondary peaks was found by Kandrup (1980a, eq. (4.32)): however, his formula is valid only for $p \leq 1$. We will assume a conservative point of view and adopt the value of F_{random} for a uniform medium:

$$F_{random} = \int dF FW(F) = 8.879 G m_{peak} n_{av}^{2/3} \tag{3.4}$$

where n_{av} is independent of the position. Here m_{peak} is an average value of the mass of the scatterers. For the innermost regions where $n(r) \geq n_{av}$, this is a lower limit to the actual value (Kandrup, 1980a), and is enough to allow an approximate calculation.

The average force contributed by the secondary peaks of mass dm_{peak} will be given by: $dF_{random} = 8.879 G n_{av}^{2/3} dm_{peak}$, and in order to estimate the total average force contributed by all the peaks in a given mass interval we have to specify n_{av} and

m_{peak}. The average density of the peaks of height $\nu = \delta/\sigma_0$ inside a spherical region is given by (Bardeen*et al.*, 1986):

$$n_{av} = \frac{1}{(2\pi)^2(R_*^3)} e^{-\frac{\nu^2}{2}} G(\gamma, \gamma\nu), \tag{3.5}$$

where R_* is a typical radius of the object forming around a density peak. The function $G(\gamma, \gamma\nu)$ has been given by Bardeen *et al.* (1986) (eq. (A19)). The calculation of the mass associated with a peak of the density field is quite difficult and different authors have given different solutions (Bardeen et al. 1986; Peacock & Heavens 1990; Lucchin & Matarrese 1988; Ryden 1988). Here we will adopt the expression given by Peacock & Heavens (1990):

$$m_{peak} = \frac{2^{3/2}[4\pi/3]\rho_0 \cdot R_*^3}{\gamma^3 + (0.9/\nu)^{1.5}}, \tag{3.6}$$

where ρ_0 is the background density and γ is a parameter which varies in the interval $0.5 - 0.8$ for a cold dark matter (CDM) spectrum. On a galactic scale a CDM spectrum is well approximated by a power–law spectrum of index n=-2, hence we have: $\gamma \approx 0.57, R_* = 2^{1/2} R_f$. By substituting equation (6) in the equation for n_{av} one obtains:

$$n_{av}^{\frac{2}{3}} = \left[\frac{1}{2\pi^2} \cdot 2^{3/2} \cdot \left(\frac{4\pi}{3}\right)\right]^{\frac{2}{3}} \cdot \left[\frac{e^{-\frac{\nu^2}{2}} G(\gamma, \gamma\nu)}{\gamma^3 + (0.9/\nu)^{1.5}}\right]^{\frac{2}{3}} m_{peak}^{-\frac{2}{3}} \rho_0^{\frac{2}{3}}, \tag{3.7}$$

and finally the average force contributed by peaks in the mass range: $0 \leq m_{peak} \leq M_{peak}$ is given by:

$$\bar{F}_{random} = \int_0^{M_{peak}} dF_{random} = 8.879 G c(\gamma, \gamma\nu) \rho_0^{2/3} \cdot 3 M_{peak}^{\frac{1}{3}}, \tag{3.8}$$

where we have defined:

$$c(\gamma, \gamma\nu) = \left[\frac{1}{2\pi^2} \cdot 2^{3/2} \cdot \left(\frac{4\pi}{3}\right)\right]^{\frac{2}{3}} \cdot \left[\frac{e^{-\frac{\nu^2}{2}} G(\gamma, \gamma\nu)}{\gamma^3 + (0.9/\nu)^{1.5}}\right]^{\frac{2}{3}}.$$

We can now compare the relative magnitude of the stochastic and mean–field forces $\bar{F}_{random}$ and F_0, by looking for the region where $\bar{F}_{random} \geq \beta F_0$, being β a parameter which we will vary. From equations (3) and (8) we get:

$$\left(\frac{r}{R_{sys}}\right) \geq \left[\left(\frac{R_{sys}}{R_{f,MAX}}\right) \cdot \frac{4\pi\beta}{3.065 \times 8.879 c(\gamma, \gamma\nu)}\right]^{\frac{1}{p-1}}. \tag{3.9}$$

Here $R_{f,MAX}$ is the value of R_f associated with the value M_{peak}, for a given ν. Choosing the filtering radius sufficiently small w.r.t. R_{sys} will ensure that the peaks generating the stochastic field can be considered point–like objects: in the following we will take a nominal value $R_{f,MAX} = R_{sys}/10$. Moreover, from Fig. 2 of Bardeen et al. 1986, it is evident that n_{av}, and consequently our function $c(\gamma, \gamma\nu)$ has a maximum at $\nu \approx 1$ for $\gamma \approx 0.57$. The most relevant contribution to the stochastic field comes then from the population of 1σ density peaks. Taking $R_{sys} = 1Mpc$ we see that for $p = 1.6$ the region where the average stochastic force of the 1σ peaks is larger that 1/10 of the mean–field force ($\beta = 0.1$) is: $r \geq 0.232 R_{Sys}$, i.e. a large part of the region. If $\beta = 1$, on the other hand, we have: $r \geq 10.75 R_{sys}$, i.e. the stochastic force field does not dominate the dynamics inside a protogalactic region. It can only create a perturbation on the average motion, leading to diffusion effects and dynamical friction.
However, we have still to evaluate the cumulative effect of many stochastic fluctuations over a finite period of time. On average, a typical field fluctuation of magnitude $\bar{F}_{random}$ will last for a time (Kandrup, 1980a, equation (5.29)):

$$T(F_{random}) = \left(\frac{15}{8}\frac{2.603 G m_{peak}}{F_{random}}\right)^{1/2} \frac{1}{(30\pi^3)^{1/6}\sqrt{\langle v^2 \rangle}}. \tag{3.10}$$

At a given distance r from the center the crossing time will be: $T_{cr} = r/\sqrt{\langle v^2 \rangle}$, and during this time a test particle will on average suffer $T_{cr}/T(F_{random})$ random force impulses. Imposing the condition: $[T_{cr}/T(F_{random})] \cdot F_{random} \gg F_0$ we get an estimate of the typical size of the region where the average mean–field force dominates the random one during a characteristic crossing time:

$$r \gg R_{sys}\left[\frac{0.472}{8.879 \times 3c(\gamma, \gamma\nu)}\right]. \tag{3.11}$$

(we have here assumed $\beta = 1$). Adopting the same values as above we get: $r_{lim} \gg 0.082 \times R_{sys}$. Hence we can conclude that, over a large extent of the protogalactic region, the cumulative effect of the "graininess" fluctuations of the gravitational field can significantly affect the local dynamics.

In this chapter we will extend the previous analyses of Chandrasekhar, Von Neumann and Kandrup to a system of *clustered* particles, for which the correlation function is non–negligible: we will see that this fact increases the probability

for it of experiencing a random force and the probability distribution itself. This enhancement has important consequences for the calculation of the average duration of a randomly induced force, but we will discuss these topics in a future chapter (Antonuccio–Delogu, *in preparation*), where we will also study in detail the effect of the stochastic force field on the dynamical evolution of a cosmological density perturbation. In the present chapter we will restrict our attention to the derivation and the main properties of the force and torque probability distribution in a clustered medium.

The plan of the chapter is as follows. In §3.2 we find an exact formula for the probability distribution of the force generated by a random distribution of peaks, inside a gravitationally clustered system, and we comment the different distributions that will arise. The derivation of this formula is quite general and not specific to the cosmological situation: it can be useful in other contexts, for example in stellar dynamics. In §3.3 we derive another formula for the distribution of the torques induced by this population of peaks, and in §3.4 we apply these results to a specific example, namely to perturbations of galactic size inside a cluster. Finally, in §3.5 we summarize our results and comment on their possible implications.

3.2 Force Probability Distribution.

Let us consider the gravitational field generated by point–like sources, randomly embedded in a given spherical region of radius R_{sys}. We will call these objects "subpeaks". We consider two populations of subpeaks, having a correlation function finite or zero. Accordingly, we will characterize the two populations by the subscripts: *cl* (*clustered*) and *uncl* (*unclustered*). This distinction will prove to be useful for the applications we have in mind (§4).
We will assume that *unclustered* peaks have the following number density distribution:

$$\tau_{uncl}(r) = \frac{\alpha_{uncl}}{r^p}, \qquad 0 \leq r \leq R_{sys} \tag{3.12}$$

with $0 \leq p < 3$, while for *clustered* peaks we assume the number density distribution law:

$$\tau_{cl}(r) = \frac{\alpha_{cl}}{r^{p'}} \exp\left(-\frac{r^2}{r_0^2}\right), \qquad 0 \leq r \leq R_{sys} \tag{3.13}$$

with: $p' \geq 0$. The introduction of the exponential cutoff in the latter equation is dictated by mathematical convenience, as will be explained later and in the Appendix. The parameters $\alpha_{cl}, \alpha_{uncl}$ are connected to the total numbers of particles inside the spherical region:

$$N_{uncl} = \frac{4\pi R_{sys}^{3-p}}{3-p}\alpha_{uncl}, \qquad N_{cl} = 4\pi\alpha_{cl}\int_0^{R_{sys}} dr r^{2-p'} \exp\left(-\frac{r^2}{r_0^2}\right) \tag{3.14}$$

We will assume in the following sections that $R_{sys} \geq r_0$, so that we can approximate:

$$\int_0^{R_{sys}} dr r^{2-p'} \exp\left(-\frac{r^2}{r_0^2}\right) \simeq \frac{1}{2} r_0^{3-p'} \Gamma\left(\frac{3-p'}{2}\right)$$

The normalization constant of the clustered density distribution is then:

$$\alpha_{cl} = \frac{N_{cl}}{2\pi r_0^{3-p'}\Gamma\left(\frac{3-p'}{2}\right)} \tag{3.15}$$

If we consider a test particle randomly placed inside the spherical region, we might wonder what is the probability that it experiences a force $\mathbf{F}$ from the population of subpeaks: we denote this probability by $W(\mathbf{F})$. Let $\rho^{(N)}(\mathbf{r}_1, \ldots, \mathbf{r}_N)$ be the N–point probability density function for the subpeaks. In general it will be given by the product of the probability density functions for the clustered and unclustered peaks populations:

$$\rho^{(N)}(\mathbf{r}_1, \ldots, \mathbf{r}_N) = A_{nor} \cdot \rho^{(N_{cl})}(\mathbf{r}_1, \ldots, \mathbf{r}_{N_{cl}})\rho^{(N_{uncl})}(\mathbf{r}_{N_{cl}+1}, \ldots, \mathbf{r}_N), \tag{3.16}$$

where A_{nor} is a normalization constant and: $N_{cl} + N_{uncl} = N$. We will conventionally assign all particles with $1 \leq l \leq N_{cl}$ to the clustered group, and particles with $N_{cl} + 1 \leq l \leq N$ to the unclustered one.
The function $\rho^{(N_{uncl})}$ is given by:

$$\rho^{(N_{uncl})}(\mathbf{r}_{N_{cl}+1}, \ldots, \mathbf{r}_N) = \prod_{j=N_{cl}+1}^{N} \tau_{uncl}(\mathbf{r}_j). \tag{3.17}$$

If the n–point correlations for $n \geq 3$ are negligible, which is a good approximation in the weak correlation limit, the function $\rho^{(N_{cl})}$ can be approximated by:

$$\rho^{(N_{cl})}(\mathbf{r}_1, \ldots, \mathbf{r}_{N_{cl}}) = \prod_{l=1}^{N_{cl}} \tau_{cl}(\mathbf{r}_l) \cdot \left\{1 + \sum_{i=1}^{N_{cl}} \sum_{k<i} \xi(\mid \mathbf{r}_i - \mathbf{r}_k \mid)\right\} \tag{3.18}$$

where $\xi(\mid \mathbf{r}_i - \mathbf{r}_k \mid)$ is the two point correlation function and $\tau(\mathbf{r}_l)$ is the number density distribution. Combining these equations, we get:

$$\rho^{(N)}(\mathbf{r}_1, \ldots, \mathbf{r}_N) = A_{nor} \cdot \prod_{j=N_{cl}+1}^{N} \tau_{uncl}(\mathbf{r}_j) \cdot \prod_{l=1}^{N_{cl}} \tau_{cl}(\mathbf{r}_l) \left\{ 1 + \sum_{i=1}^{N_{cl}} \sum_{k<i} \xi(\mid \mathbf{r}_i - \mathbf{r}_k \mid) \right\} \tag{3.19}$$

To calculate A_{nor} we will assume the normalization:

$$\int \prod_{m=1}^{N} d^3 r_m \rho^{(N)}(\mathbf{r}_1, \ldots, \mathbf{r}_N) = 1 \tag{3.20}$$

Being the two populations of particles independent, the above integral can be decomposed as a product:

$$\int \prod_{m=1}^{N} d^3 r_m \rho^{(N)}(\mathbf{r}_1, \ldots, \mathbf{r}_N) =$$

$$= \int \prod_{m=1}^{N_{cl}} d^3 r_m \rho^{(N_{cl})}(\mathbf{r}_1, \ldots, \mathbf{r}_{N_{cl}}) \cdot \int \prod_{l=N_{cl}+1}^{N} d^3 r_l \rho^{(N_{uncl})}(\mathbf{r}_{N_{cl}+1}, \ldots, \mathbf{r}_N) = N_{cl}^{N_{cl}} \cdot N_{uncl}^{N_{uncl}},$$

so that finally:

$$A_{nor} = \frac{1}{N_{cl}^{N_{cl}} \cdot N_{uncl}^{N_{uncl}}}. \tag{3.21}$$

In order to compute the probability distribution of stochastic forces, we will closely follow the original derivation of Chandrasekhar (1943). More precisely, our starting point will be his equation (52) for the quantity $A_N(\mathbf{k})$, the Fourier transform of the force probability distribution of a N-particle system (see also Padmanabhan, 1990):

$$A_N(\mathbf{k}) = \int \prod_{m=1}^{N} d^3 r_m \cdot \rho^{(N)}(\mathbf{r}_1, \ldots, \mathbf{r}_N) \equiv A_{nor} \cdot A_{N_{uncl}}(\mathbf{k}) \cdot A_{N_{cl}}(\mathbf{k}) \tag{3.22}$$

The expression for $A_{N_{uncl}}(\mathbf{k})$ coincides with eq. (53) of Chandrasekhar (1943):

$$A_{N_{uncl}}(\mathbf{k}) = \left[\frac{1}{N_{uncl}} \int d^3 r e^{i\mathbf{k}\cdot\mathbf{F}(\mathbf{r})} \tau_{uncl}(\mathbf{r}) \right]^{N_{uncl}} \tag{3.23}$$

To obtain $A_{N_{cl}}(\mathbf{k})$ we substitute the probability distribution $\rho^{(N_{cl})}$ in equation (52) of Chandrasekhar (1943):

$$A_{N_{cl}}(\mathbf{k}) = \frac{1}{N_{cl}^{N_{cl}}} \int \prod_{m=1}^{N_{cl}} d^3 r_m e^{i\mathbf{k}\cdot\mathbf{F}(\mathbf{r}_m)} \cdot \prod_{l=1}^{N_{cl}} \tau_{cl}(\mathbf{r}_l) \left\{ 1 + \sum_{i=1}^{N_{cl}} \sum_{k<i} \xi(\mid \mathbf{r}_i - \mathbf{r}_k \mid) \right\} =$$

$$= \left[\frac{1}{N_{cl}} \int d^3 r e^{i\mathbf{k}\cdot\mathbf{F}(\mathbf{r})} \tau_{cl}(\mathbf{r})\right]^{N_{cl}} + \left[\frac{1}{N_{cl}} \int d^3 r e^{i\mathbf{k}\cdot\mathbf{F}(\mathbf{r})} \tau_{cl}(\mathbf{r})\right]^{N_{cl}-2} \cdot$$

$$\frac{N_{cl}(N_{cl}-1)}{2N_{cl}^2} \int d^3 r_1 d^3 r_2 e^{i\mathbf{k}\cdot\mathbf{F}(\mathbf{r}_1)} e^{i\mathbf{k}\cdot\mathbf{F}(\mathbf{r}_2)} \xi\left(\mid \mathbf{r}_1 - \mathbf{r}_2 \mid\right) \tau_{cl}\left(\mathbf{r}_1\right) \tau_{cl}\left(\mathbf{r}_2\right). \qquad (3.24)$$

(We are adopting a different notation from Chandrasekhar (1943) so the vector k here corresponds to his vector $\boldsymbol{\rho}$). Introducing now the definitions:

$$A'_{m,(cl,uncl)}(\mathbf{k}) = \left[\int d^3 r e^{i\mathbf{k}\cdot\mathbf{F}(\mathbf{r})} \tau_{cl,uncl}(\mathbf{r})\right]^m, \qquad (3.25)$$

$$\Sigma_{(cl,uncl)}(\mathbf{k}) = \int d^3 r_1 d^3 r_2 e^{i\mathbf{k}\cdot\mathbf{F}(\mathbf{r}_1)} e^{i\mathbf{k}\cdot\mathbf{F}(\mathbf{r}_2)} \xi\left(\mid \mathbf{r}_1 - \mathbf{r}_2 \mid\right) \tau_{cl,uncl}\left(\mathbf{r}_1\right) \tau_{cl,uncl}\left(\mathbf{r}_2\right), \qquad (3.26)$$

we find:

$$A_{N_{cl}}(\mathbf{k}) = \frac{A'_{N_{cl},(cl)}(\mathbf{k})}{N_{cl}^{N_{cl}}} \cdot \left\{1 + \frac{1}{2}\left(1 - \frac{1}{N_{cl}}\right) \frac{\Sigma_{(cl)}(\mathbf{k})}{A'_{2,(cl)}(\mathbf{k})}\right\}. \qquad (3.27)$$

If the integral in eq. (23) above exists and is finite, also the limit: $\lim_{N_{uncl}\to\infty} A_{N_{uncl}}(\mathbf{k})$ exists, and we have:

$$\lim_{N_{uncl}\to\infty} A_{N_{uncl}}(\mathbf{k}) = \exp\left\{-A_{uncl}(k)\right\} \qquad (3.28)$$

where:

$$A_{uncl}(k) = \alpha_{uncl} \cdot \frac{\left(G\langle m\rangle_{av} k\right)^{\frac{3-p}{2}}}{2} \int_{G\langle m\rangle_{av} k/R_{sys}^2}^{\infty} dz z^{\frac{p-5}{2}} \cdot \left[1 - \frac{\sin z}{z}\right], \qquad (3.29)$$

We have denoted by: N and $\langle m\rangle_{av}$ the total number and average mass of the subpeaks, respectively, and by R_{sys} the radius of the system. Observe that, due to the isotropy of the density distribution, all the preceding quantities depend only on $k \equiv \mid \mathbf{k} \mid$.

Similarly we obtain:

$$\lim_{N_{cl}\to\infty} A'_{N_{cl}}(\mathbf{k}) = \exp\left[-A_{cl}(k) \cdot \left\{1 + \frac{1}{2}\frac{\Sigma_{(cl)}(\mathbf{k})}{A'_{2,(cl)}(\mathbf{k})}\right\}\right], \qquad (3.30)$$

and A_{cl} is given by:

$$A_{cl}(k) = \alpha_{cl} \cdot \frac{\left(G\langle m\rangle_{av} k\right)^{\frac{3-p'}{2}}}{2} \int_{G\langle m\rangle_{av} k/R_{sys}^2}^{\infty} dz z^{\frac{p'-7}{2}} \exp\left(-\frac{G\langle m\rangle_{av} k}{r_0^2} \cdot \frac{1}{z}\right) \cdot [z - \sin z], \qquad (3.31)$$

We now proceed to compute some quantities appearing in equation (27). From equation (25) we obtain: $A'_{2,(cl)}(\mathbf{k}) = [A'_{1,(cl)}(\mathbf{k})]^2$, and because of the isotropy this last quantity does also depend on $\mid \mathbf{k} \mid$:

$$A'_{1,(cl)}(\mathbf{k}) =$$

$$= \frac{N_{cl}}{2\pi r_0^{3-p'}\Gamma\left(\frac{3-p'}{2}\right)} \int_0^{R_{sys}} dr \exp\left(-\frac{r^2}{r_0^2}\right) r^{2-p'} \cdot 2\pi \int_0^{\pi} d\theta \sin\theta \exp\left(ikr\cos\theta \frac{G\langle m\rangle_{av}}{r^3}\right) =$$

$$= -\frac{N_{cl}}{r_0^{3-p'}\Gamma\left(\frac{3-p'}{2}\right)} \int_0^{R_{sys}} dr \exp\left(-\frac{r^2}{r_0^2}\right) r^{2-p'} \cdot \int_{-1}^{1} dz \exp\left(ikz \frac{G\langle m\rangle_{av}}{r^2}\right) =$$

$$= \frac{2N_{cl}}{r_0^{3-p'}\Gamma\left(\frac{3-p'}{2}\right)} \cdot \frac{(G\langle m\rangle_{av})^{\frac{3-p'}{2}}}{k} \int_{G\langle m\rangle_{av}/R_{sys}^2}^{\infty} d\phi \exp\left(-\frac{G\langle m\rangle_{av}}{r_0^2\phi}\right) \frac{\sin(k\phi)}{\phi^{(7-p')/2}} =$$

$$= \frac{2N_{cl}}{r_0^{3-p'}\Gamma\left(\frac{3-p'}{2}\right)} \cdot k^{\frac{3-p'}{2}} (G\langle m\rangle_{av})^{\frac{3-p'}{2}} B\left(7-p', \frac{kG\langle m\rangle_{av}}{R_{sys}^2}\right), \qquad (3.32)$$

where we have defined:

$$B\left(7-p', \frac{kG\langle m\rangle_{av}}{R_{sys}^2}\right) = \int_{kG\langle m\rangle_{av}/R_{sys}^2}^{\infty} dz \exp\left(-\frac{kG\langle m\rangle_{av}}{r_0^2 z}\right) \frac{\sin z}{z^{(7-p')/2}}. \qquad (3.33)$$

The calculation of $\Sigma_{cl}(\mathbf{k})$ is rather lengthy and requires some care: we refer the interested reader to Appendix A. In short, we perform an asymptotic evaluation of the integral in the last term of (24) for large $G\langle m\rangle_{av}$; the result is:

$$\Sigma_{(cl)}(\mathbf{k}) =$$

$$= \alpha_{cl}^2 \cdot 4\pi^2 k^{3-p'} \cdot \frac{17}{52}\xi(0)\,(GM_\odot)^{3-p'} \int_0^{\infty} dv v^{-(5-p')} \exp\left(-\frac{2k}{r_0^2 v}\right) \cos\left(2\langle m\rangle_{av} v\right) =$$

$$= \alpha_{cl}^2 \cdot 4\pi^2 k^{3-p'} \cdot \frac{17}{52} \left(\frac{2\langle m\rangle_{av}}{M_\odot}\right)^{4-p'} (GM_\odot)^{3-p'}\, \xi(0) a(k), \qquad (3.34)$$

where we have defined:

$$a(k) = \int_0^{\infty} dz z^{-(5-p')} \exp\left(-\frac{4G\langle m\rangle_{av}}{r_0^2}\frac{k}{z}\right) \cos(z). \qquad (3.35)$$

In the above formulas, distance is measured in Mpcs, mass in units of solar mass and k' in units of $Mpc^2/GM_\odot$. In order to obtain the probability distribution $W(\mid \mathbf{F} \mid)$ of the force induced by the subpeaks, we now consider the limit:

$\lim_{N\to\infty} A_N(\mathrm{k})$, in the case: $N_{cl}, N_{uncl} \to \infty$,$N_{uncl}/N_{cl} = constant$. From what has been previously stated, it is evident that:

$$A_f(k) = \lim_{N\to\infty} A_N(\mathrm{k}) =$$

$$= A_{nor} \exp\left(-\left[A_{uncl}(k) + A_{cl}(k)\right]\right) \cdot \left\{1 + \frac{1}{2}\frac{\Sigma_{(cl)}(k)}{A'_{2,(cl)}}\right\} \qquad (3.36)$$

and $A_{uncl}(k)$, $A_{cl}(k)$, $\Sigma_{cl}(k)$ are given by equations (29), (31) and (26), respectively[1]. The final step to obtain $W(\mid \mathbf{F} \mid)$ consists in substituting this last equation for $A_f(k)$ in equation (4.16) of Kandrup (1980a):

$$W(\mid \mathbf{F} \mid) = \frac{1}{2\pi^2 \mid \mathbf{F} \mid} \int_0^\infty dk k \sin(k \mid \mathbf{F} \mid) A_f(k). \qquad (3.37)$$

We will plot the function: $W(F) = 4\pi \mid \mathbf{F} \mid^2 W(\mid \mathbf{F} \mid)$ in §4, whit a discussion of some particular cases. For the moment we will make some remarks to justify some of the assumptions we made during the derivation of equation (37).
Apparently, the introduction of two populations of subpeaks, with different clustering properties, seems rather artificial. However, some of the integrals entering into the definition of the function $A_f(k)$ are divergent if the density profile is not properly chosen. For example, the integral in equation (29) converges only for $p < 3$, if $R_{sys} \to \infty$ (Kandrup, 1980a), hence for power–law density profiles the force probability distribution is defined only for these values. Considering the number density distribution (13), the integral $A_{cl}(k)$ and the asymptotic expansion of $\Sigma_{cl}(\mathrm{k})$ exist for arbitrary values of the power–law exponent. However, if we had chosen only one population of subpeaks with the number density law (13), we would have noticed that the integral in equation (37) exists only if the function $kA_f(k)$ decays rapidly enough for $k \to \infty$, and this does not always occur for the cases of physical interest considered in §4. The introduction of a second population of unclustered peaks remedies this situation, and guarantees the convergence of the integrals for arbitrary values of the power index p' (provided, of course, that the unclustered peaks distribution has a power–law index $p < 3$). From a physical point of view, one can think of the clustered peaks as associated with shells of matter just infalling onto a protostructure which has

[1]Note the difference with the analogous equation published in Antonuccio–Delogu & Atrio–Barandela (1992) due to a journal's misprint

already collapsed and violently relaxed, so that the correlations have been destroyed and the substructure contained inside it is predominantly non clustered. We will show in §4 that, in a clustered medium, the force probability distribution has a marked enhancement about the average values, and decreases much faster at high values of F. This behaviour can be explained on the basis of Kandrup's (1980a) analysis, which shows that the most probable contributions to $W(F)$ come from the nearest particles. The correlation function causes an enhancement of the probability of finding a particle in the neighborhood of a given one. Following Kandrup (1980a), one expects that the resulting probability force distribution will be modified at about the maximum, which is of the order of the average force produced by particularly proximate particles.
In the next section we will consider the probability distribution of the torques generated by the subpeaks.

3.3 Torque Probability Distribution.

Let the torques be measured w.r.t. the center of the system: denoting by $\boldsymbol{R}$ the distance vector from the center, the torque will be: $\boldsymbol{T} = \boldsymbol{R} \times \boldsymbol{F}$. The torque depends linearly on the force, so it is possible to derive the probability distribution of the torques applying a reasoning similar to the one already followed in the previous section. In fact, the force $\mathbf{F}$ enters into the derivation of the force probability distribution (equation (37)) only through equations (20)-(21), so only through terms of the form: $e^{i\mathbf{k}\cdot\mathbf{F}}$. Substituting $\boldsymbol{T}$ for $\boldsymbol{F}$ we have: $\boldsymbol{k} \cdot \boldsymbol{T} = \boldsymbol{k} \cdot \boldsymbol{R} \times \boldsymbol{F} = \boldsymbol{k} \times \boldsymbol{R} \cdot \boldsymbol{F}$. For a fixed k we will denote by Θ the angle between k and $\boldsymbol{R}$, and assume a spherical coordinate system having the axis $\theta = 0$ lying along the direction of: $\hat{z} = \boldsymbol{k} \times \boldsymbol{R} / \mid \boldsymbol{k} \times \boldsymbol{R} \mid$ we easily obtain: $\boldsymbol{k} \cdot \boldsymbol{T} = kR \sin\Theta \cdot \cos\theta \mid \mathbf{F} \mid$. Hence, in order to get the Fourier transforms: $A_{T|uncl}, A_{T|cl}$, which are the analogous of equations (29), (31), it is enough to make the substitution: $k \rightarrow kR\sin\Theta$ in those equations, and so we obtain:

$$A_{T|uncl} \equiv A_{uncl}(kR\sin\Theta), \qquad A_{T|cl} \equiv A_{cl}(kR\sin\Theta). \tag{3.38}$$

The torque probability distribution will finally be:

$$W(\boldsymbol{T}) = \frac{1}{(2\pi)^3} \int d^3\mathrm{k} A_{T|f}(\mathrm{k}) e^{-i\mathrm{k}\cdot\boldsymbol{T}}, \tag{3.39}$$

where:

$$A_{T|f}(\mathrm{k}) \equiv a_{nor} \exp\left(-\left[A_{T|uncl}(kR\sin\Theta)+\right.\right.$$
$$\left.\left. A_{T|cl}(kR\sin\Theta)\cdot\left\{1+\frac{1}{2}\frac{\Sigma_{T|cl}(kR\sin\Theta)}{A'_{T|2,(cl)}(kR\sin\Theta)}\right\}\right]\right).$$

In order to compute the integral in equation (39) we consider a new spherical coordinate system having as $\theta = 0$ axis a direction coinciding with the vector $\boldsymbol{R}$. From a simple application of spherical trigonometry we obtain: $\mathrm{k}\cdot\boldsymbol{T} = k \mid \boldsymbol{T} \mid \sin\Theta\cos\Phi$, where Φ denotes the angle between the planes defined by the vectors $\boldsymbol{R}-\boldsymbol{T}$ and $\boldsymbol{R}-\mathrm{k}$. The integral in equation (39) then becomes:

$$W(\boldsymbol{T}) = \frac{1}{(2\pi)^3}\int_0^{\pi} d\Theta\sin\Theta\int_0^{2\pi} d\Phi\int_0^{\infty} dk k^2 A_{T|f}(kR\sin\Theta)\cdot\exp\left[-ik\mid\boldsymbol{T}\mid\sin\Theta\cos\Phi\right].$$

The integral w.r.t. Φ can be performed with the help of equation 3.715(18) from Gradshteyn and Ryzhik (1968):

$$\int_0^{2\pi} d\Phi\exp\left[-ik\mid\boldsymbol{T}\mid\sin\Theta\cos\Phi\right] = 2\pi J_0\left(k\mid\boldsymbol{T}\mid\sin\Theta\right),$$

where J_0 denotes the Bessel function of first kind. Finally we get:

$$W(\boldsymbol{T}) \equiv W(T) =$$
$$\frac{2}{(2\pi)^2}\int_0^{\pi/2} d\Theta\sin\Theta\int_0^{\infty} dk k^2 A_{T|f}(kR\sin\Theta)\cdot J_0(kT\sin\Theta). \qquad (3.40)$$

The integration of the latter is possible under conditions similar to those already introduced in the previous section for the integral $W(\mid \mathbf{F} \mid)$: the presence in the integrand of the Bessel function, which has a damped oscillatory behaviour for high values of the argument does not substantially modify the conclusions we have already reached in the previous section. Moreover, being the torque a linear function of the force, one might expect that the dominating contribution to the stochastic torques experienced by a given particle comes from a few very close particles, as it was the case with the force distribution.

The knowledge of the distributions $W(F)$ and $W(T)$ allows one to calculate various important quantities, such as, for example, the coefficients of the higher order terms in a Fokker–Planck expansion of the kinetic equations for a given system, the average friction force, and so on (Kandrup, 1980a). In the rest of this chapter, however, we will only be concerned with the distribution themselves and in the next section we will show how clustering affects their shape.

3.4 Probability Distributions in Protogalactic Structures.

In the Cold Dark Matter scenario galaxies and clusters form by the gravitational clustering, merging and eventually violent relaxation of small–scale substructure accreted onto the local peaks of the density field. We might expect that the matter inside a given region that will later collapse to form galaxies and/or a cluster will be clumped in an hierarchy of "objects" having a wide range of dimensions. In this section, we will restrict our attention to the force probability distribution generated by "objects" of "small" size ($0 \leq M_{obj} \leq 10^9 M_\odot$), which we call "*subpeaks*", contained inside a perturbation having the typical mass and size of a galaxy ($M_{Gal} \approx 10^{11} M_\odot$), called protogalaxy. The protogalaxy is contained inside a density perturbation having the size and mass of a cluster ($M_{Clu} \approx 10^{14} M_\odot$), which we call protocluster. The subpeaks inside M_{Gal} come either from the protogalaxy or from the protocluster: the two groups, however, will have different density profiles and clustering properties. Following Ryden (1988), the density profile inside the galactic perturbation can be described by equation (12) with an index: $p = 1.6$, while for the peaks coming from the cluster we will assume a truncated density profile given by equation (13) with $r_0 \approx R_{sys}$ and $p = p'$. By assuming these values the density profile in the interval $r \leq R_{Gal} \ll R_{sys}$is accurately described by a power–law.

In an hierarchical scenario a protogalaxy forms and becomes nonlinear before the protocluster inside which it is contained. All the considerations of the preceding section apply under the hypothesis that the higher order correlations ($n \geq 3$) are negligible, i.e. during an early phase of the collapse, while the density perturbation itself is still in the linear phase of growth. The Universe today is non–linear on a scale $8 - 10 h^{-1} Mpc$ (Peebles 1974), while on larger scales (roughly corresponding to clusters of galaxies), it is still in a linear phase. Many clusters of galaxies are turning around at about the present epoch, so until recently they were probably in a linear phase.

As concerns galaxies, we can obtain an upper limit of the duration of the linear phase of evolution, and consequently of the regime within which our considerations are valid. It is often assumed that after recombination Gaussian density fluctuations were present in the Universe, whose spectrum can be described by

a power-law: $P(k) = Ak^n$ (Peebles 1980). The constant A can be obtained from present-day galaxy number counts (Davis & Peebles, 1983), and the two-point correlation function will be given by the Fourier transform of $P(k)$, which initially will be very small. Fall and Saslaw (1976) and Kandrup (1983) have computed the growth of $\xi(r,t)$ in the case: $\xi(r,0) = 0$: if this condition is not satisfied the time scale to reach non-linearity will be shorter. We will then use their calculations to get an upper limit for this time scale. They find that the linear approximation applies as long as: $\tau = \Delta t/t_0 = (t - t_0)/t_0 \leq 1$, where t_0 is an epoch at which clustering inside the given perturbation begins. In a $\Omega = 1$, Cold Dark Matter scenario we have: $t = T/(1+z)^{3/2}$, where: $T = 2/(3H_0)$ is the age of the Universe. Assuming now an epoch of galaxy formation of $z_0 \approx 2.5$ (Kashlinsky and Jones, 1990) the condition $\tau \leq 1$ translates into: $z \geq 1.2$. A protogalaxy becomes nonlinear at $\tau = 1$, i.e. $t = 2t_0$; a protocluster becomes nonlinear at an epoch given by (Efstathiou, 1990):

$$t = 2t_0 \left(\frac{M_{NL,Cl}}{M_{NL,Gal}} \right)^{\frac{n+3}{4}},$$

that in our case corresponds to a redshift: $z = 0.02$. Hence, in the redshift interval $1.2 \leq z \leq 2.5$ the protocluster is essentially in a linear phase of evolution and with a much smaller clustering, and our approximations apply.

Following Ryden (1988), if we take into account secondary infall the density profile will be well approximated by a power law with index $p = 1.6$. The two-point correlation function inside a protogalactic region will be the Fourier transform of the power spectrum. In the following, we will first consider the case of a power-law spectrum $P(k) = Ak^n$, for some values of the index n, and then the Cold Dark Matter spectrum.

In order to apply the results of the preceding section we still have to specify N_{cl}, N_{uncl}, the number densities of subpeaks originating inside the protogalaxy and the protocluster, respectively. If we identify the subpeaks with regions of small size surrounding local density maxima, our problem consists in specifying the mass spectrum of structures forming in an hierarchical clustering scenario, a problem tightly connected with the so called *cloud-in-cloud* problem (Bardeen et al. 1986). This problem has been recently deeply investigated by many authors, mostly because its solution allows to determine the mass function of cosmic structures (see Heavens & Peacock (1988) for a recent discussion). Bower (1991)

found a formula for the total mass fraction contained inside collapsed regions of mass M_{SG} around subpeaks of height δ_{SG} inside a larger region of typical mass M_{typ} around a subpeak of height δ_{typ}:

$$\tilde{f}\,(M_{SG}, \delta_{SG} \mid M_{typ}, \delta_{typ})\, dM_{SG} = \frac{1}{(2\pi)^{1/2}} \frac{n+3}{3} \left[\frac{M_{SG}}{M_*(z)}\right]^{\frac{n+3}{6}} \times \exp\left\{-\frac{1}{2}\left[\frac{M_{SG}}{M_*(z)}\right]^{\frac{n+3}{3}}\right\} \frac{dM_{SG}}{M_{SG}}, \qquad (3.41)$$

where $M_*(z)$ is the typical mass (averaged over the whole Universe) which has collapsed by the epoch z. Substituting in this equation M_G and M_{Clu} in place of M_{typ} and dividing $\tilde{f}$ by M_{SG} we can compute N_{cl} and N_{uncl}, respectively, after multiplying the resulting value by the volumes of the region.
We are now ready to show the results of the calculations, beginning with the power–law cases.

3.4.1 Power–law Spectra.

In Figure 1 we plot $W(F)$ for various values of the index n, ranging from $n = -2$ up to $+1$. We have assumed $2r_0 = R_{sys} = 1Mpc$, $M_{SG} = 1.2 \cdot 10^6 M_\odot$, $M_G = 10^{11} M_\odot$, $M_{Clu} = 10^{13} M_\odot$. A clear enhancement of the maximum probability occurs, together with a rapid decrease of the distribution after an average value. The enhancement is even more pronounced when we vary N_{cl}: in Figure 2 we keep $n = -1$ fixed and change N_{cl}/N_{uncl} in the range: $0 \leq N_{cl}/N_{uncl} \leq 3 \times 10^{-7}$. The distribution is even more concentrated toward the maximum values.
In Figure 3 we plot $W(T)$ for the same power spectrum of the preceding Figure, for $N_{cl}/N_{uncl} = 2 \times 10^{-7}$ and for different distances from the center. The steepening of the distribution as one approaches the center suggests that stochastic effects will influence energy and angular momentum transport especially in the central regions of the protogalaxy. However, this can be intuitively understood: the effect of the clustering will be to increase the average number of the nearby particles, which are precisely those which mostly contribute to the average values of the field.

3.4.2 Cold Dark Matter Spectrum.

The CDM spectrum is given by (Bond and Efstathiou, 1984):

$$P(k) \propto \frac{k}{[1+(ak+(bk)^{3/2}+(ck)^2)^{1.13}]^{2/1.13}} \tag{3.42}$$

with: $a = 6.4(\Omega h^2)^{-1} Mpc, b = 3.0(\Omega h^2)^{-1} Mpc, c = 1.7(\Omega h^2)^{-1} Mpc$. On galactic and subgalactic scales this spectrum resembles a power–law with index between -1.5 and -2.

In Figure 4a) we show different distributions corresponding to different values of M_{SG}. Observe that also the unperturbed distribution, corresponding to a system in which there are only unclustered peaks, has a maximum value of about 0.3, slightly higher than the pure power–law case. Moreover, the decrease after the maximum is very pronounced when clustering is present, together with a more pronounced steepening of the function near the maximum values. This is also evident from Figure 4b), which is the same as the preceding Figure but with a different R_{sys}. As R_{sys} increases, the relative fraction of clustered over unclustered peaks decreases, and this explains why on average the distributions for the clustered cases show less pronounced variations. Finally in Figure 4c) we can see the effect of the decrease of R_{sys} and of the increase of M_{SG}. This plot is relevant to ubderstand galaxy formation inside a group rather than a cluster. The effect of clustering is the same as the preceding cases.

In Figure 5a) we plot $W(T)$ for the same range of parameters as in Figure 4b) and at a distance $R = 50Kpc$ from the center of the protogalaxy. The sharp decrease of the distribution is quite evident also for the torque distribution. From Figure 5b) we can see how the torques' distribution evolves with time: the two curves correspond to $z = 1$ and $z = 0.5$. As clustering proceeds the distribution becomes more and more peaked around the central, maximum value, in agreement with the expectations from a near–neighbour theory for the complexion of stochastic forces (Kandrup, 1980b).

3.5 Conclusions.

Our task in the present chapter was to start an analysis of the gravitational field fluctuations in a weakly clustered system. We derived an exact formula for the

force and angular momentum distributions induced by "graininess" fluctuations in weakly clustered systems and we showed explicitly their dependence on the correlation function. The integrations were performed through asymptotic expansions, but, as is shown in Appendix A, they are valid for a wide range of realistic cases. We will shortly consider some of the possible applications of these results, which are still under development (Antonuccio–Delogu, 1991).

Various authors have stressed the importance of dynamical friction in determining the observed properties of clusters of galaxies (White 1976; Kashlinsky 1986, 1987). However, many authors have adopted the classical Chandrasekhar's (1943) formula which was derived under the hypothesis of an infinite homogeneous, unclustered system having a Maxwellian distribution. It is evident that an analysis of the dynamical friction taking explicitly into account the clustering property of the system (with all the limitations already noticed) can provide a more realistic representation of cluster evolution. Generally speaking, the effect of clustering on dynamical friction must be taken into account in any calculation, either numerical or analytical, of the evolution of a collisionless system. These considerations can be applied to high density systems, because these systems can contain a significant fraction of their mass, gravitational and correlational energy in small collapsed regions. The formalism we have developed will allow us to investigate the effect of substructure on the dynamical evolution of a density perturbation. Other authors have already pointed out the role of neighbouring density peaks on the temporal evolution of the density profile of a cosmological perturbation (Rozgacheva, 1988). In both cases, the purpose is to go over the standard scheme of an isolated density perturbation made up of spherically distributed, gravitationally interacting shells.

The main limitation of the present work is that, as we have already stressed, it is valid only as far as the correlations are weak; otherwise the spatial correlations make it impossible to decompose the gravitational field into an average and a stochastic component (Kandrup, 1980a). Many clusters and groups of galaxies presumably verify this condition, and actually many authors have adopted a mean–field approach to describe their dynamics (e.g. Fitchett and Merritt, 1988). Our next goal will be to apply these considerations to the study of the dynamical evolution of galaxies in clusters, and in particular to the motions within the Local Group (Antonuccio–Delogu, 1991).

3.6 Appendix A. Asymptotic evaluation of $\Sigma_{cl}(\mathrm{k})$.

Our goal is to compute the six–dimensional integral $\Sigma_{cl}(\mathrm{k})$:

$$\Sigma_{cl}(\mathrm{k}) = \int_{\Re^3} d^3\mathrm{r}_1 \int_{\Re^3} d^3\mathrm{r}_2 \exp\left(i\frac{Gm_{av}\mathrm{k}\cdot\hat{\mathrm{r}}_1}{r_1^2}\right)\exp\left(i\frac{Gm_{av}\mathrm{k}\cdot\hat{\mathrm{r}}_2}{r_2^2}\right)\tau_{cl}(\mathrm{r}_1)\tau_{cl}(\mathrm{r}_2)\xi\left(\mid \mathrm{r}_1-\mathrm{r}_2\mid\right) \tag{3.43}$$

As we already mentioned, mass is measured in units of solar mass $M_\odot$ and distances in Mpc, so that k will be measured in units of $(Mpc)^2/GM_\odot$. For arbitrary $\tau_{cl}(\mathrm{r}_1), \tau_{cl}(\mathrm{r}_2)$, the integral (A.1) is not necessarily finite neither ought to be expressed in closed form. For the density profiles we are interested in (equation (13)) it is possible to obtain an accurate asymptotic expansion. We will also estimate the error.

Let us define a new vector: $\boldsymbol{\rho} = \mathrm{r}_2 - \mathrm{r}_1$ and choose a spherical coordinate system having the vector k as reference axis for the calculation of the angles. Let $(\theta_1, \phi_1), (\theta, \phi)$ be the coordinate angles for the vectors r_1,$\boldsymbol{\rho}$. Performing a change of variables: $d^3\mathrm{r}_1 d^3\mathrm{r}_2 \to d^3\mathrm{r}_1 d^3\boldsymbol{\rho}$, where:

$$r_2^2 = r_1^2 + \rho^2 + 2r_1\rho\left\{\cos\theta\cos\theta_1 + \sin\theta\sin\theta_1\cos(\phi_1-\phi)\right\},$$

substituting equation (13) for $\tau_{cl}(r)$, introducing two new variables: $\boldsymbol{\sigma}_{1,2} = \mathrm{r}_{1,2}/\sqrt{k}$ and performing the integrations w.r.t. the angular coordinates, we arrive at:

$$\Sigma_{cl}(\mathrm{k}) = A\cdot 4\pi^2 k^{3-p}\left\{\left[\mathbf{H}_{1+}(k;\xi)+\mathbf{H}_{1-}(k;\xi)\right]-\left[\mathbf{H}_{2+}(k;\xi)+\mathbf{H}_{2-}(k;\xi)\right]\right\}, \tag{3.44}$$

where we have defined:

$$\mathbf{H}_{(1,2)\pm}(k;\xi) =$$

$$= \int_0^\infty d\sigma_1\sigma_1^{2-p}\int_0^\infty d\sigma \mid \sigma_1-\sigma\mid^{2-p}\exp\left(\pm im_{av}k\phi_{(1,2)}(\sigma_1,\sigma) - 2\frac{\sigma^2}{r_0^2}k\right)\xi(\sqrt{k}\sigma), \tag{3.45}$$

and the functions appearing in this equation are given by:

$$\phi_1(\sigma,\sigma_1) = \frac{1}{\sigma_1^2} + \frac{\sigma_1+\sigma}{\mid\sigma_1-\sigma\mid^3}, \quad \phi_2(\sigma,\sigma_1) = \frac{1}{\sigma_1^2} + \frac{\sigma_1-\sigma}{\mid\sigma_1+\sigma\mid^3}. \tag{3.46}$$

We will look for asymptotic expansions of the functions $\mathbf{H}_{1\pm}, \mathbf{H}_{2\pm}$ in the limit $GM_1 \to \infty$. For all the cases we consider in this chapter one has: $m_{av} \geq 10^6 M_\odot \gg 1$, so we are justified in adopting this approximation. The expansions

for the integrals containing $\phi_1(\sigma,\sigma_1)$ and $\phi_2(\sigma,\sigma_1)$ are different, so we will consider them separately. Many techniques of asymptotic expansions for Fourier–type integrals assume that the region of integration is bounded (see, e.g. Bleistein and Handelsman, 1986), so we will first choose a bounded region of the plane and we will later study the behaviour of our expansion when the region is extended to infinity.

Let us begin with $\mathbf{H}_{1\pm}(k;\xi)$. The function $\phi_1(\sigma,\sigma_1)$ has no extremum point in any bounded region of the first quadrant of the real plane, and is singular on the straight line: $\sigma_1-\sigma=0$. We will consider the following region of integration: $\Gamma\equiv(0,\sigma_1^*)\times(0,\sigma_1^*)$, and divide it into three regions: $\Gamma=\Gamma_1^*\cup\Gamma_2^*\cup\Gamma_3^*$ (see Figure 6), where we have defined:

$$\Gamma_1^*\equiv\{(\sigma,\sigma_1):\epsilon\leq\sigma\leq\sigma_1^*,\sigma+\epsilon\leq\sigma_1\leq\sigma_1^*\},$$

$$\Gamma_2^*\equiv\{(\sigma,\sigma_1):2\epsilon\leq\sigma\leq\sigma_1^*,\epsilon\leq\sigma_1\leq\sigma_1^*-\epsilon\},$$

$$\Gamma_3^*\equiv\{(\sigma,\sigma_1):\mid\sigma-\sigma_1\mid\leq\epsilon\}.$$

In the limits: $\epsilon\rightarrow 0,\sigma_1^*\rightarrow\infty$, Γ_1^* fills asymptotically $\Re^{2+}$. We will first consider the integration over Γ_3^*.

If $1\leq p\leq 5$ the integral over the region Γ_3^* exists and is bounded. Using $\mathbf{H}_{1\pm}^{(3)}$ to denote the part of the integral $\mathbf{H}_{1\pm}$ restricted to the region Γ_3^*, we obtain:

$$\mathbf{H}_{1\pm}^{(3)}=$$

$$=\int_0^\infty d\sigma_1\int_0^\infty d\sigma\,[\sigma_1\mid\sigma_1-\sigma\mid]^{2-p}\exp\left[im_{av}\left(\frac{1}{\sigma_1^2}+\frac{\sigma+\sigma_1}{\mid\sigma-\sigma_1\mid^3}\right)-2\frac{\sigma^2}{\sigma_0^2}\right]\xi(\sqrt{k}\sigma)\leq$$

$$\leq\epsilon^{2-p}\max(\xi)\int_0^\infty d\sigma_1\sigma_1^{2-p}\exp\left[i\frac{m_{av}}{\sigma_1^2}\right]\leq$$

$$\leq\epsilon^{2-p}\max(\xi)\int_0^\infty dv v^{-\frac{2-p}{2}-\frac{3}{2}}\exp[im_{av}v]$$

Then:

$$\mid\mathbf{H}_{1+}^{(3)}+\mathbf{H}_{1-}^{(3)}\mid\leq\epsilon^{2-p}\max(\xi)\int_0^\infty v^{\frac{p-5}{2}}\sin(m_{av}v),$$

and this integral converges if and only if: $-2\leq(p-5)/2\leq 0$, which implies: $1\leq p\leq 5$. We assume that the value $\max(\xi)$ is bounded, which is true for the correlation functions we consider in this chapter. In what follows, we will be interested in the limit $\epsilon\rightarrow 0$. Clearly: $\lim_{\epsilon\rightarrow 0}\left[\mathbf{H}_{1+}^{(3)}+\mathbf{H}_{1-}^{(3)}\right]=0$.

Let us denote by $\mathbf{H}_1'$ the remaining part of the integral having as integration domain the region $\Gamma_1^* \cup \Gamma_2^*$. The asymptotic expansions of the integral over this region can be computed through equation (8.4.49) from Bleistein and Handelsman (1986), because the function $\phi_1(\sigma, \sigma_1)$ is of class C^1 and $\nabla\phi_1 \mid_{x \in \partial\Gamma_{1,2}^*} > 0$ on the boundaries of these regions :

$$\mathbf{H}_{1\pm}'(m_{av}) = -\sum_{j=0}^{\infty} \left(-\frac{1}{im_{av}}\right)^{j+1} \int_{\partial\Gamma_1^* \cup \partial\Gamma_2^*} (\mathbf{L}_j \cdot \mathbf{n}) W \exp\{im_{av}\phi_{1\pm}\}, \qquad (3.47)$$

where we have defined:

$$\mathbf{L}_j = g_j \frac{\nabla\phi_1}{|\nabla\phi_1|^2} \qquad \text{j=0,1,...}$$
$$g_{j+1} = \nabla \cdot \mathbf{L}_j$$

By definition: $g_0(\sigma, \sigma_1) = [\sigma_1 \mid \sigma_1 - \sigma \mid]^{2-p} e^{-2\frac{\sigma^2}{\sigma_0^2}} \xi\left(\sqrt{k}\sigma\right)$, and W denotes the elements of arc along $\partial\Gamma_1^* \cup \partial\Gamma_2^*$.

We will stop our expansion at the first ($j = 0$) term. The boundary $\partial\Gamma_1^* \cup \partial\Gamma_2^*$ is composed of six arcs, each of which contributes an integral. Five of these integrals are finite and go to zero when $\sigma_1^* \to \infty, \epsilon \to 0$, and only one is different from zero. In the limit $\epsilon \to 0$ one obtains:

$$\mathbf{I}_{1\pm} = \frac{4\xi(0)}{52} \int_0^{\infty} dv v^{7-2p} \exp\left[\pm im_{av}\frac{2}{v^2}\right] \cdot \exp\left[-2\frac{v^2}{r_0^2}k\right] \qquad (3.48)$$

Moreover, the condition for the existence of the limits $\epsilon \to 0$ for some of the six line integrals mentioned above imposes the constraint: $0 \leq p \leq 3$, which results to be the most severe upper bound on this quantity.

In conclusion, we have obtained the asymptotic expansion of $\mathbf{H}_1(k;\xi) = \mathbf{H}_{1+}(k;\xi) + \mathbf{H}_{1-}(k;\xi)$:

$$\lim_{m_{av}\to\infty} \mathbf{H}_1 \approx \mathbf{I}_{1+} + \mathbf{I}_{1-} = \frac{8\xi(0)}{52} \int_0^{\infty} dv v^{7-2p} \cos\left(m_{av}\frac{2}{v^2}\right) \cdot \exp\left[-2\frac{v^2}{r_0^2}k\right].$$

Finally we will estimate the magnitude of the error we made by restricting our expansion to the first term $j = 0$. From equation (8.4.2) by Bleistein and Handelsman (1986) we see that for $j = 0$ the higher order terms in the expansion are given simply by:

$$I = -\frac{2}{m_{av}} \int_{\Gamma} dx g_1 \left(\sin(m_{av}\phi_1) + \sin(m_{av}\phi_2)\right) = -\frac{2}{m_{av}} \int_{\partial\Gamma} dn \cdot \mathbf{L}_0.$$

After some algebra, the main contribution to this integral turns out to come from the arc element $\sigma = 0, \sigma_1 > 0$, and is:

$$I = \frac{\xi_0}{4} \int_0^\infty d\sigma_1 \sigma_1^{7-2p} \exp\left(-\frac{\sigma_1^2}{r_0^2} k\right) = \frac{\xi(0)}{8} \frac{\Gamma(4-p)}{\left(\frac{k}{r_0^2}\right)^{4-p}}.$$

The integral is very small if:

$$k \gg \left[\frac{\xi(0)}{8}\Gamma(4-p)\right]^{\frac{1}{4-p}} r_0^2,$$

Our choice $p = 1.6, r_0 = 0.8$ is sufficient to ensure the validity of this relation over a large range of k.

Let us now turn our attention to the other integral, namely: $\mathbf{H}_2(k;\xi) = \mathbf{H}_{2+}(k;\xi) + \mathbf{H}_{2-}(k;\xi)$. The function $\phi_2(\sigma, \sigma_1)$ does not have a stationary point in the first quadrant of $\Re^2$; at variance with the preceding case it is completely regular in every bounded region of $\Re_+^2$. We will then choose as region of integration the square:

$$\Gamma_4^* = \{(\sigma, \sigma_1) : 0 \leq \sigma \leq \sigma_1^*, \epsilon \leq \sigma_1^* \leq \sigma_1^* + \epsilon\}.$$

(see Figure 7). Also in this case we will adopt the expansion (8.4.49) by Bleistein and Handelsman (1986) and once again we find that the only term which is non–zero in the limits: $\sigma_1^* \to \infty, \epsilon \to 0$ is precisely the one computed along the arc lying on the axis $\sigma = 0$. The result is:

$$\lim_{m_{av}\to\infty} \mathbf{H}_{2\pm} = -\frac{4\xi(0)}{32} \int_0^\infty dv v^{7-2p} \exp\left[\pm i m_{av} \frac{2}{v^2}\right] \cdot \exp\left[-2\frac{v^2}{r_0^2} k\right]. \qquad (3.49)$$

The total contribution comes from the summation of $\mathbf{H}_{2+}$ and $\mathbf{H}_{2-}$, and we obtain:

$$\mathbf{H}_2 = -2\frac{\xi(0)}{32} \cdot 4 \int_0^\infty dv v^{7-2p} \cos\left(m_{av}\frac{2}{v^2}\right) \exp\left[-\frac{2v^2}{r_0^2} k\right]. \qquad (3.50)$$

Finally, combining together the various integrals we obtain:

$$\mathbf{H}_1 - \mathbf{H}_2 = [\mathbf{H}_{1+} - \mathbf{H}_{1-}] - [\mathbf{H}_{2+} - \mathbf{H}_{2-}] \approx$$

$$\frac{17}{52}\xi(0) \int_0^\infty dw w^{p-5} \exp\left[-\frac{2k}{r_0^2 v}\right] \cos(2m_{av}v). \qquad (3.51)$$

Figure Caption.

Figure 1.–Force probability distribution for a clustered system having a power–law spectrum of fluctuations, for different values of the index: no correlations (*solid line*), n=–2 (*long–dashed line*), n=–1 (*short–dashed line*), n=+1 (*dot–dashed line*).

Figure 2.–Same as Fig. 1, but for $M_{SG} = 1.2 \times 10^7 M_\odot$ and different values of N_{cl}/N_{uncl}: $N_{cl}/N_{uncl} = 0$ (*solid line*), $N_{cl}/N_{uncl} = 10^{-7}$ (*dotted line*), $N_{cl}/N_{uncl} = 3 \times 10^{-7}$ (*dashed line*).

Figure 3.–Torque probability distribution for power–law spectrum with n=–2, and different distances from the center: r=0.1 (*solid line*), r=0.2 R_{sys} (*dotted line*), r=0.5 R_{sys} (*dashed line*). The torque is measured in units of $GM_{typ}r_0^{-1}$.

Figure 4.–a) Force probability distribution for CDM spectrum, and different values of M_{SG}: $M_{SG} = 10^4 M_\odot$ (*solid line*), $M_{SG} = 10^6 M_\odot$(*dashedline*), $M_{SG} = 10^7 M_\odot$ (*dotted line*).
b) Same as 4a), but for $M_{SG} = 10^4 M_\odot$ and different values of R_{sys}: $R_{sys} = 1 Mpc$ (*dashed line*), $R_{sys} = 1.5 Mpc$ (*dotted line*), $R_{sys} = 2.5 Mpc$ (*solid line*).
c) Same as 4a), but for $M_G = 10^{13} M_\odot$, $R_{sys} = 0.7 Mpc$.

Figure 5.–a) Torque probability distribution inside a galaxy–size perturbation ($M_G = 10^{11} M_\odot$) at a distance r=50 Kpc for different values of R_{sys} as given in Figure 4b).
b)Same as 5a), but for $R_{sys} = 1 Mpc$, z=1 (*dotted line*) and z=2 (*dashed line*).

Figure 6.–Path of integration for $\mathbf{H}_{1\pm}$.

Figure 7.–Path of integration for $\mathbf{H}_{2\pm}$.

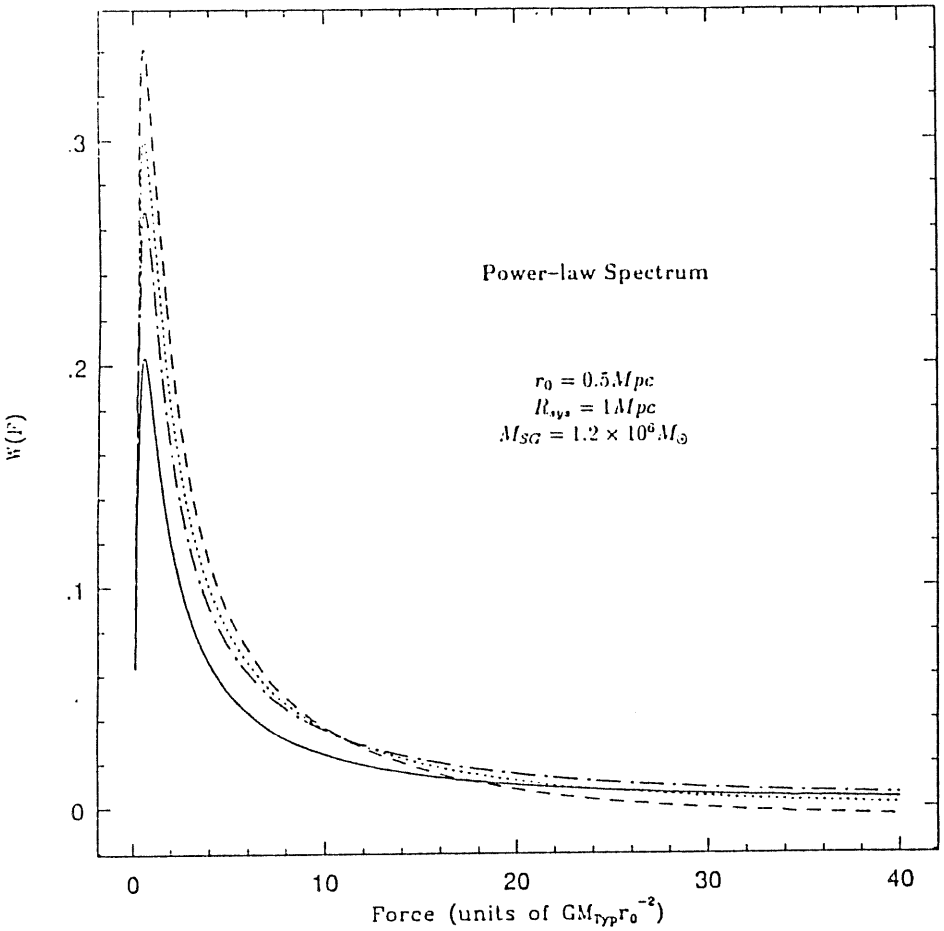
Power-law Spectrum
$r_0 = 0.5Mpc$
$R_{sys} = 1Mpc$
$M_{SG} = 1.2 \times 10^6 M_\odot$
W(P)
0
.1
.2
.3
0
10
20
30
40
Force (units of $GM_{Typ}r_0^{-2}$)

Fig.1

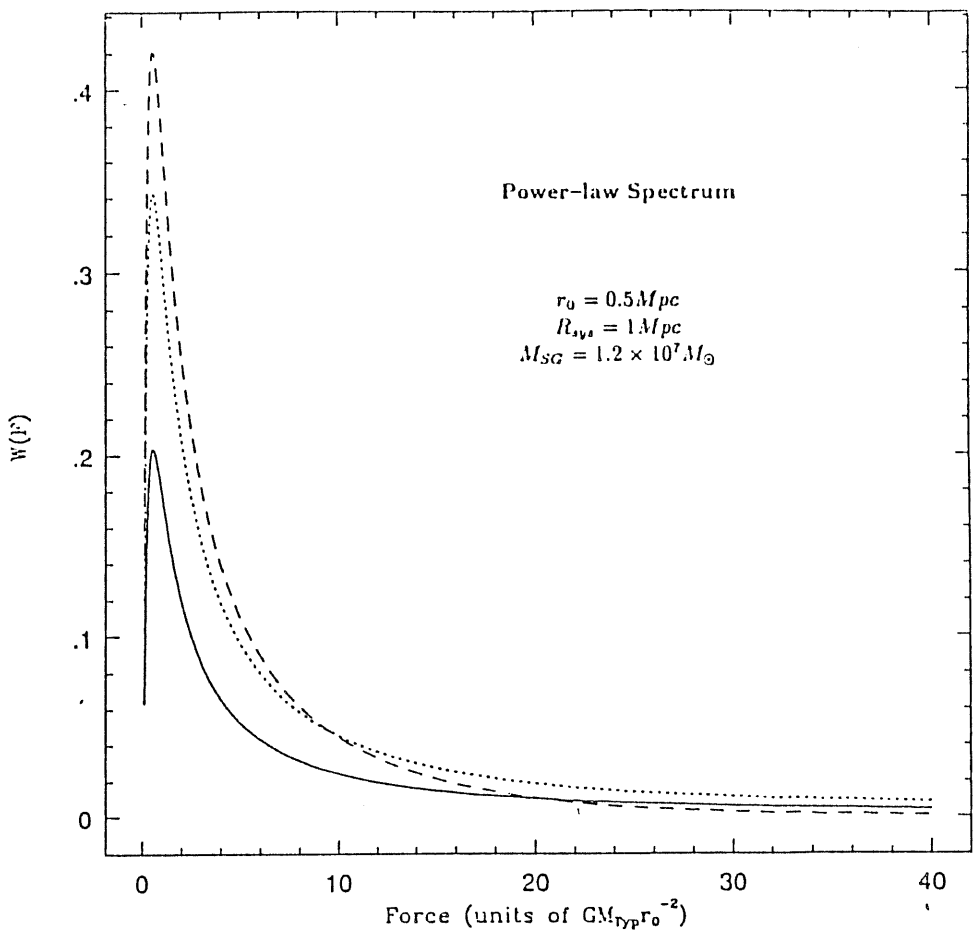
Power-law Spectrum
$r_0 = 0.5Mpc$
$R_{sys} = 1Mpc$
$M_{SG} = 1.2 \times 10^7 M_\odot$
W(P)
0
.1
.2
.3
.4
0
10
20
30
40
Force (units of $GM_{Typ}r_0^{-2}$)

Fig.2

Figure 3

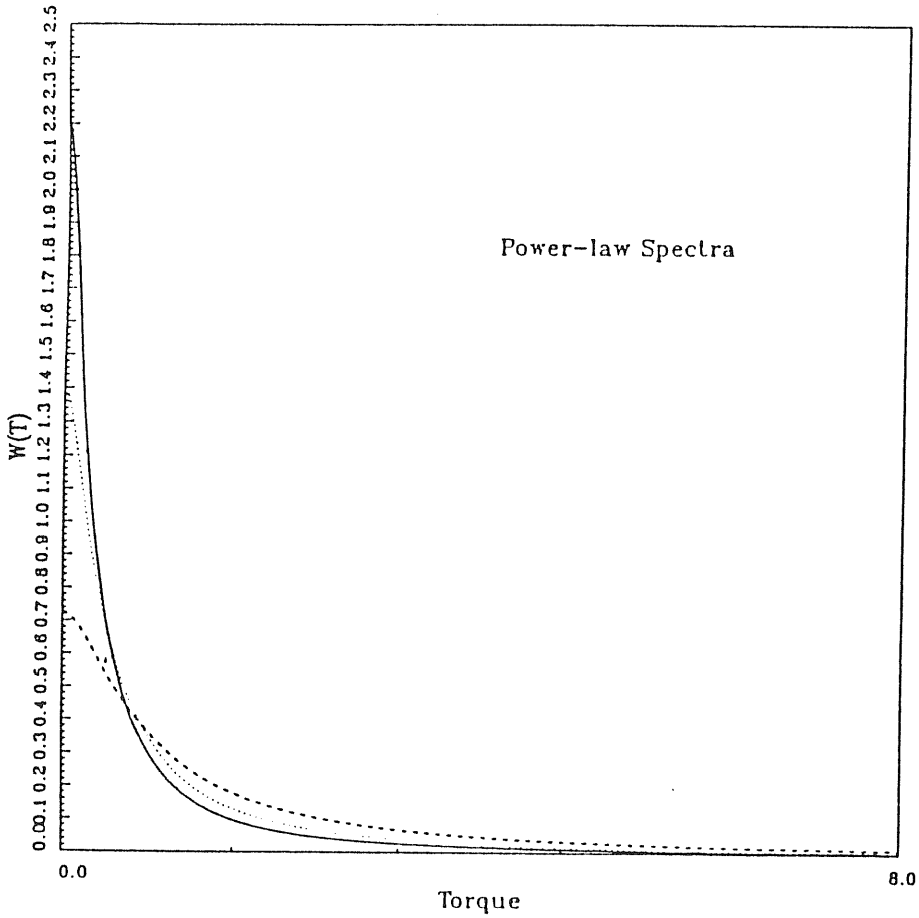

Figure 4a)

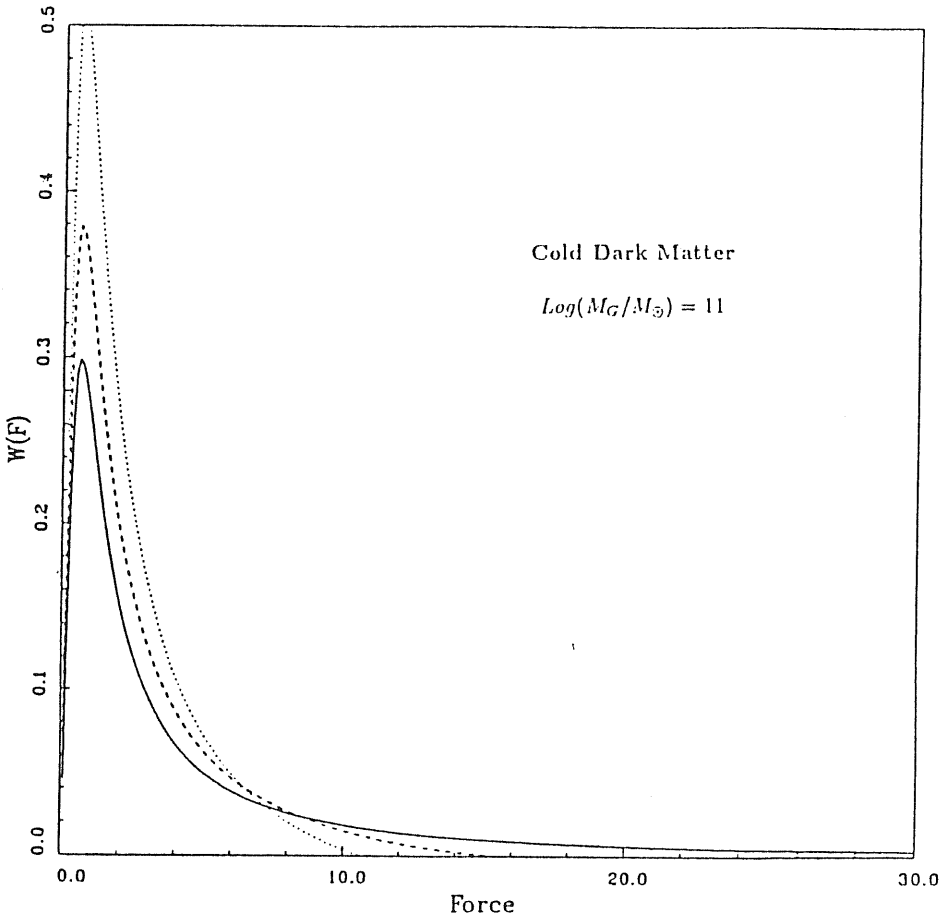

Figure 4b)

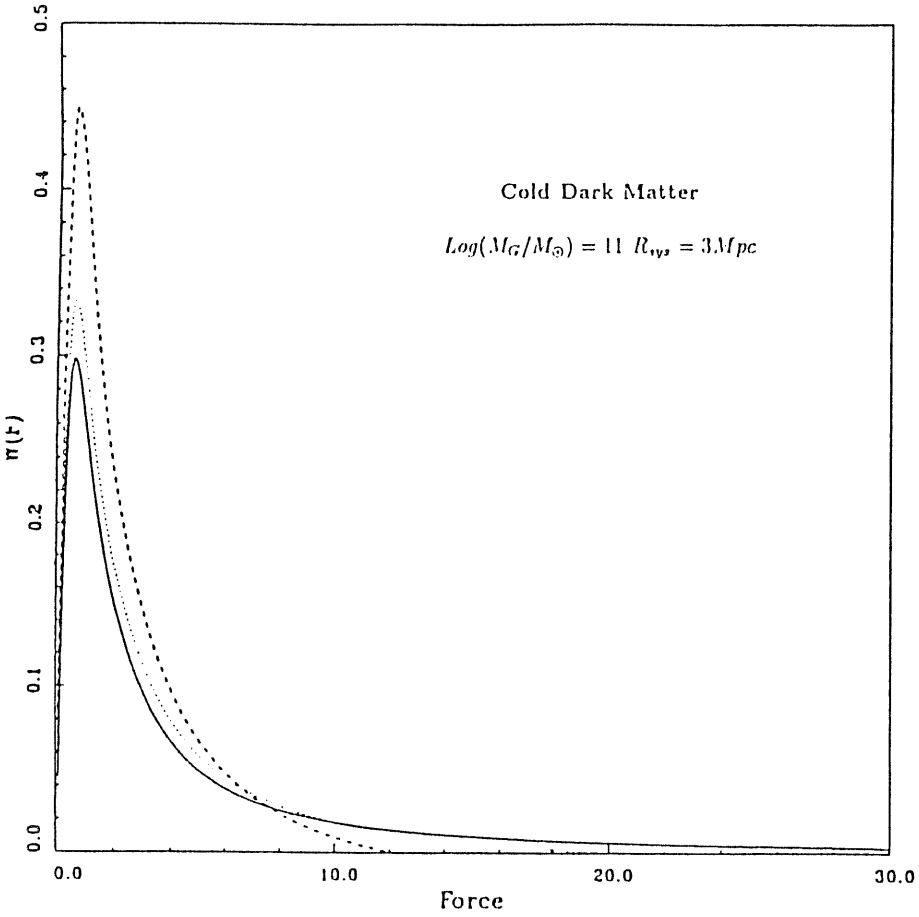

Figure 4c)

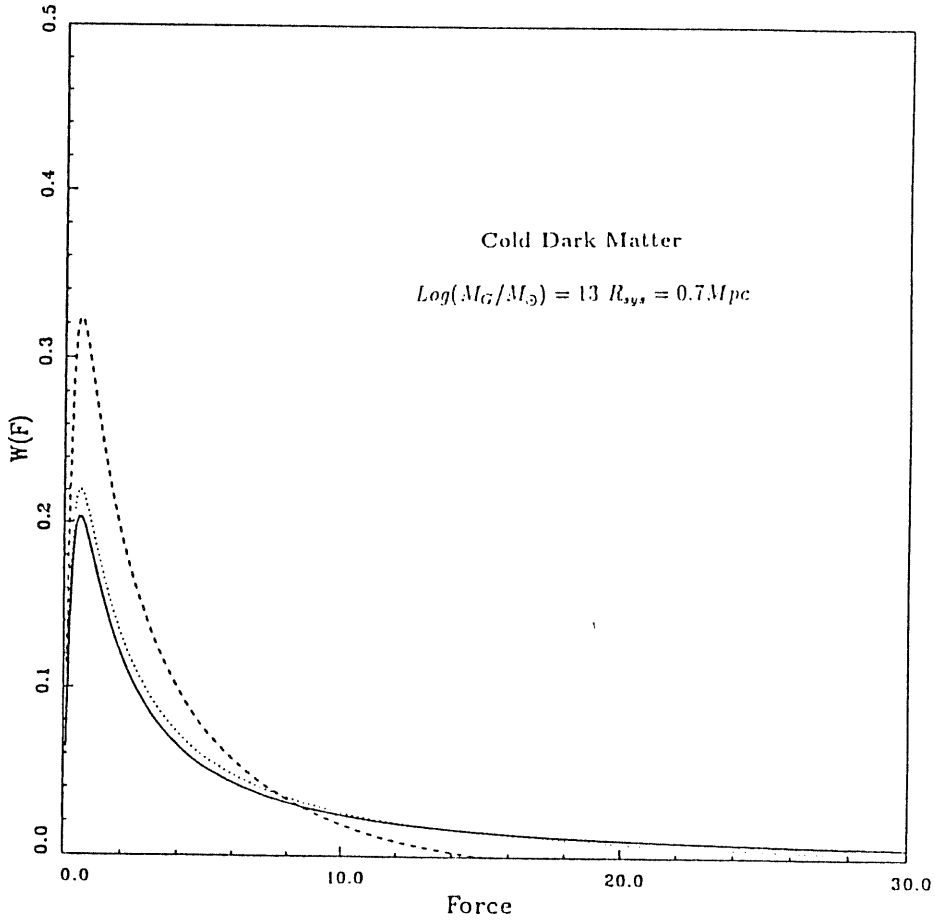

Figure 5a)

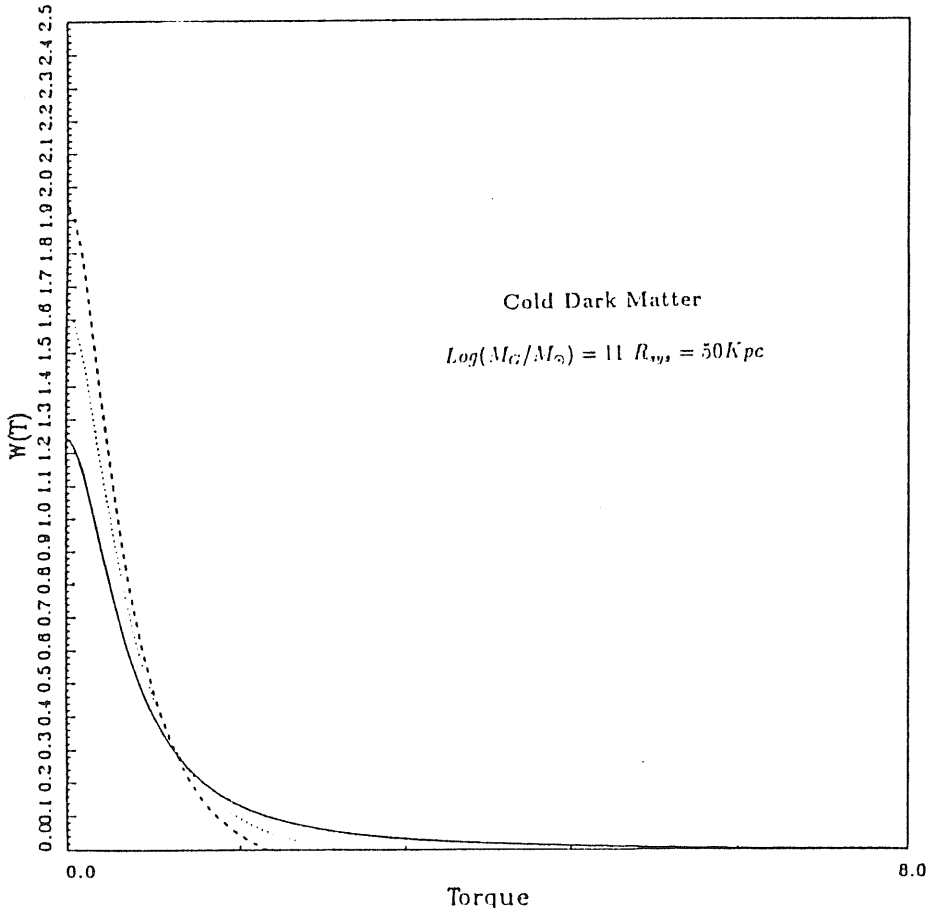

Figure 5b)

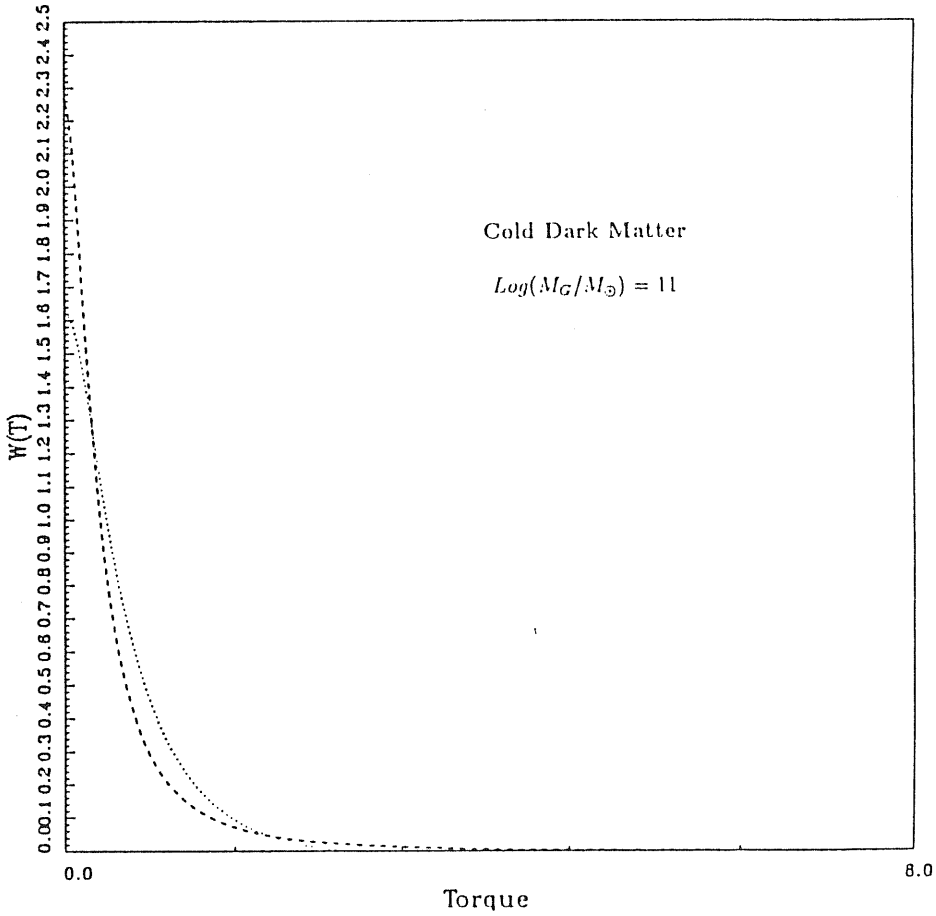

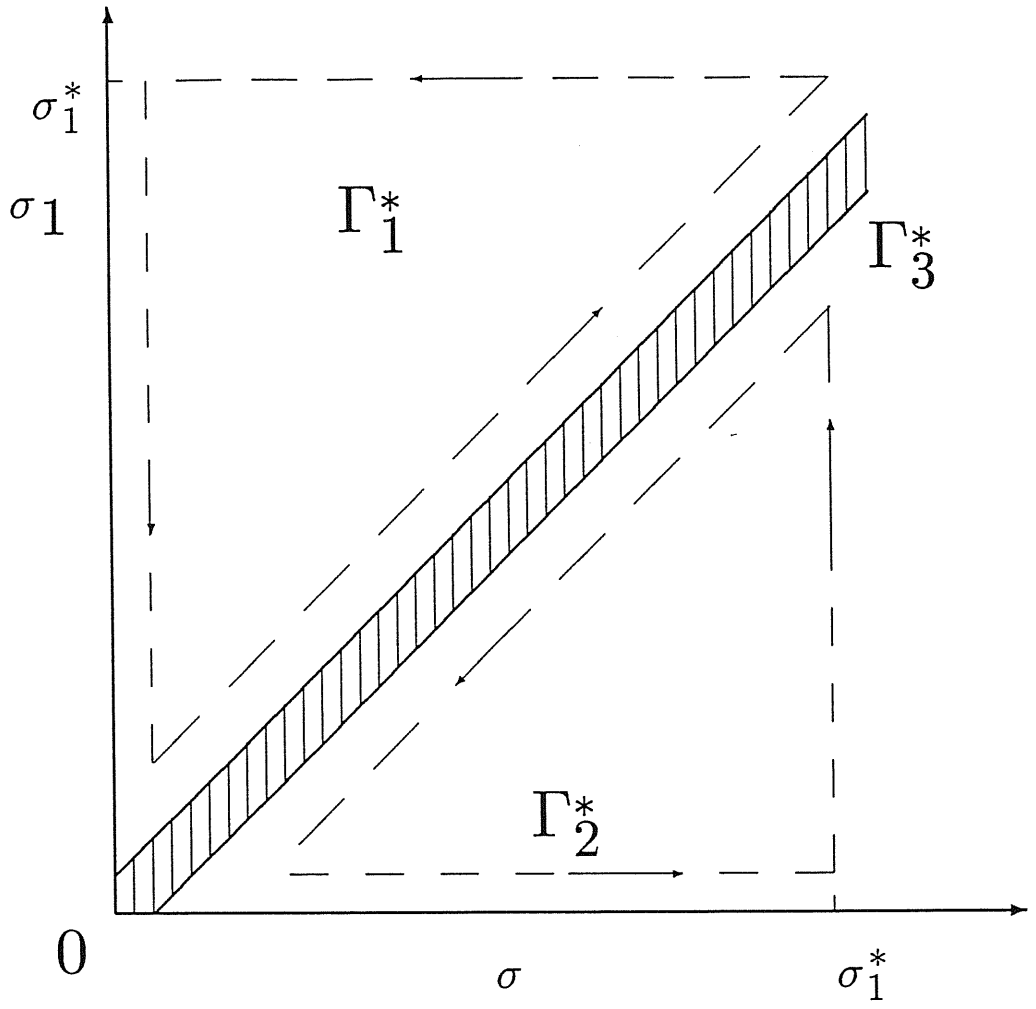

Figure 6: Integration path for the integral $\mathbf{H}_{1\pm}$. The dashed region is Γ_3^*.

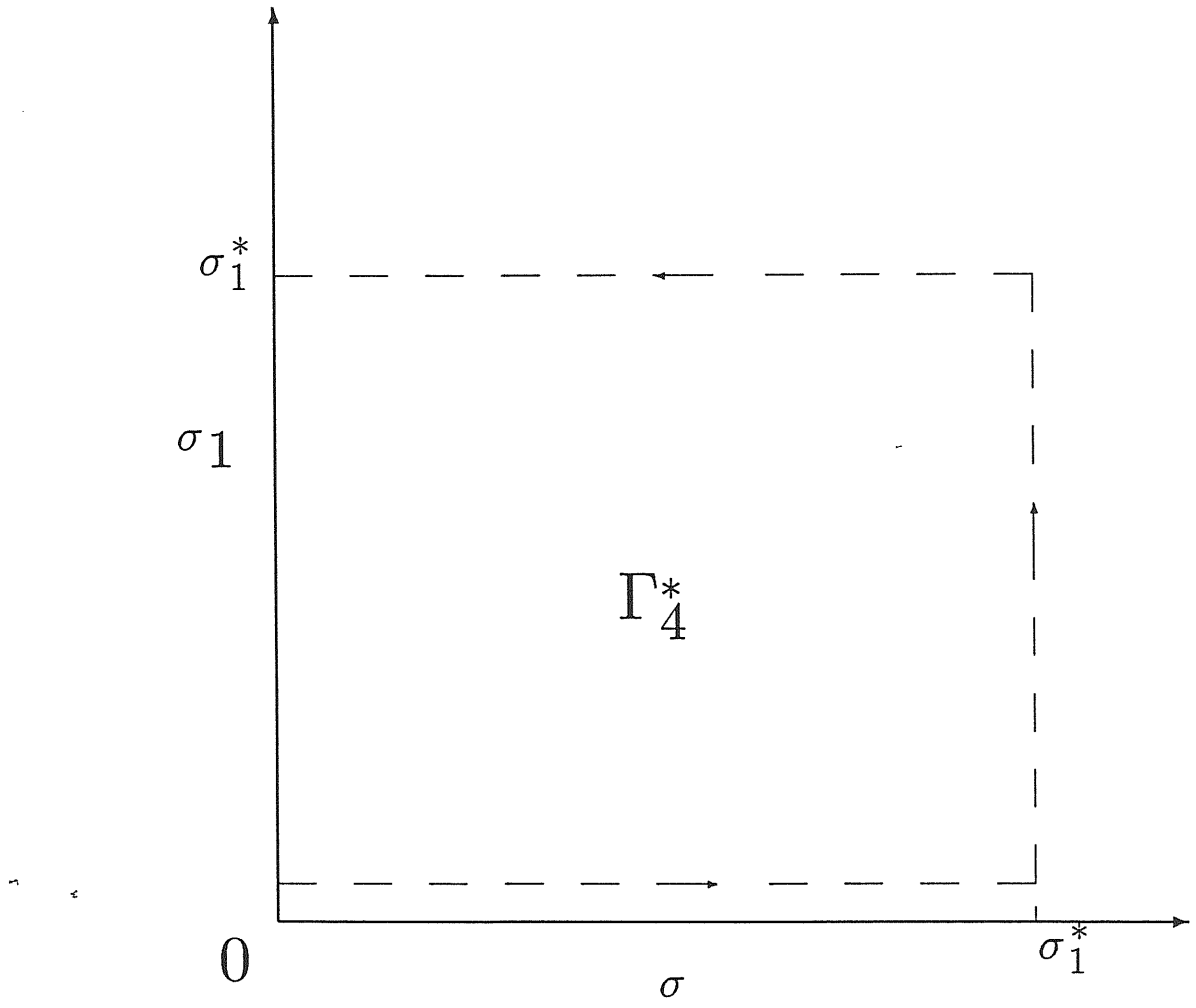

Figure 7: Integration path for the integral $\mathbf{H}_{2\pm}$.

Chapter 4

The effect of Dynamical Friction on the Secondary Infall of Matter on Protoclusters.

4.1 Introduction.

The accretion of matter by protocluster and protogalaxies before turnaround and (eventually) full virialization, called secondary infall, has often been recognized as an important feature to understand the formation of cosmological structures. Starting with the seminal paper by Gunn & Gott (1972), many authors have investigated the consequences of secondary infall on the features of the final collapsed objects, like density profiles and collapse times (Gunn, 1977; Fillmore & Goldreich, 1984; Bertschinger, 1985; Hoffmann & Shaham, 1985; Ryden & Gunn, 1987; Bertschinger & Watts, 1988; Hoffmann, 1988; Ryden, 1988a; Hoffmann, 1989). Evidence for ongoing accretion and secondary infall comes from the peculiar velocity field in the outer regions of clusters of galaxies (Regös & Geller, 1989), as well as from recent X–ray surveys (Briel et al., 1991). In fact, the effects of secondary infall are conjectured to be more easily observable in the profiles of clusters, because these latter have a very long formation time scale, comparable to the age of the Universe (in hierarchical clustering models), and have probably not suffered violent relaxation in their outer regions (Geller, 1990). For example, West et al. 1988 (see also West, 1990) from the results of numerical simulations conjecture that subclustering should be more easily observable in the outer regions of the clusters, outside the central virialized core, where the accreted material has not yet relaxed. It is however very difficult to verify pre-

dictions like these directly from the observations: as we saw in chapter 1, the evidence for subclustering mostly comes from data near the center of the cluster, simply because the number of galaxies decreases very fast with distance from the center. The statistics then becomes very poor.

The mass function of cosmic structures could however also be strongly affected by secondary infall. In a recent paper Cavaliere, et al. (1991) investigated the effect of secondary infall on the mass spectrum of cosmic structures. They found that relaxing the hypothesis of "istantaneous collapse", which is implicit into the original treatment of Press & Schechter (1974), in favour of a "time–resolved approach", i.e. by taking into account the fact that actual halos accrete on a finite time scale, the mass spectrum of the resulting structures is modified from the original Press & Schechter form. One of the main ingredients in their paper was an equation for the total mass accreted up to a given time t from Gunn & Gott (1972) (eq. 27):

$$M(t) = M_i \left\{ 1 + \frac{\Delta M}{M_i} \frac{(t/t_i)^{2/3} - 1}{\Delta M/M_i + (t/t_i)^{2/3}} \right\} \tag{4.1}$$

where $\Delta M = M_{max} - M_i$ and M_{max}, M_i are the final total accreted mass and the initial mass, respectively. This equation however was derived without taking into account the effect of dynamical friction on the secondary infall. Our purpose in this chapter will be to repeat the calculations of Cavaliere et al. (1991) making use of an equation for $M(t)$ which explicitly takes into account this effect. As we suggested alreay in the introduction to chapter 3, in CDM models one expects a significant dragging due to the enhancement of dynamical friction inside clustered environnment. Because we are interested only into the effects of dynamical friction in the outer parts of a typical cluster, where linear theory can probably still apply, the theory developed in the last chapter can be safely applied. In §4.2 we will compute the dynamical friction coefficient η starting from the probablity distribution $W(F)$ introduced in the last chapter. Then we will study the dynamics of a density perturbation when frictional forces produced by dynamical friction are taken into account, and we will derive an approximate solution for the expansion factor, the final collapse time and the total accreted mass (§4.3). Finally, in §4.4 we will repeat the calculation of Cavaliere et al. (1991) starting with this modified accreted mass equation, and we will study the modification this produces on the final mass spectrum. Comments and a short summary of

the results are provided in §4.5.

4.2 Dynamical Friction Coefficient.

Dynamical friction in a gravitating collisionless medium arises as a consequence of the discrete nature of the phase space structure. The actual gravitational field felt by an average particle will be the superposition of the mean field resulting from the global mass distribution, and of a second flucuating component generated by the interactions of the particle with the nearest particles, which occur randomly as the particle travels through the system. In an ideal continuous system this latter component would be zero in the absence of dissipational effects, in actual self–gravitating systems this fluctuating component modifies gently the average motion of a particle, introducing a frictional force $-\eta\mathbf{v}$; the average displacement of a particle from its initial position $\mathbf{v}$ then verifies an equation:

$$\frac{d\mathbf{v}}{dt} = \nabla\Phi(\mathbf{r}) - \eta\mathbf{v} \tag{4.2}$$

The connection between η and $W(F)$ was studied by Chandrasekhar (1943) and further clarified by Kandrup (1980a). Under the rather restricting assumption that there are no correlations among forces $\mathbf{F}$ and force derivatives $d\mathbf{F}/dt$, which amounts to assume that the random process generating the force probablity distribution is a Markoff process, one obtains (Kandrup, 1980a, eqs. 5.2 and 5.22):

$$\eta = \frac{\langle F^2 T(F)\rangle}{2\langle v^2\rangle}, \tag{4.3}$$

where we have defined:

$$\langle F^2 T(F)\rangle = \int d^3\mathbf{F} W(F) F^2 T(F) \tag{4.4}$$

The outer regions of a cluster which are still infalling are also in the linear phase of evolution, and the formalism developed in the preceding chapter (see also Antonuccio–Delogu & Atrio–Barandela, 1992) allows a calculation of η taking explicitly into account the effects of clustering (eq. 3.36). Observe that, according to eq. (336), $W(F)$ depends linearly on the correlation function, and from eq. 4.3-4.4 we see that η depends linearly on $W(F)$, so that we can write: $\eta = \eta_0 + \eta_{cl}$. In order to evaluate η_0 we will closely follow Kandrup (1980a). We represent the cluster environment as a collisionles medium, composed of a hierarchy of

local density fluctuations characterized by some mass spectrum, consistently with a hierarchical clustering scenario as it could arise in a CDM cosmology. The precise shape of the mass spectrum will not be relevant for the calculation of the dynamical friction coefficient: it can only introduce some factors of order unity, but anyhow the calculation of η_0 is only approximated and exploits many other approximations which introduce comparable factors (Kandrup, 1980a). The most difficult initial step is the calculation of the time scale for large individual deflections in a collisionless system, $T(F)$. Many arguments suggest that in a realistic collisionless system the contributions to this quantity coming from rare scatterings with far and massive density fluctuations are statistically lesser important than those originating from more numerous interactions with small and nearby fluctuations. Then one can adopt eq. (5.48) from Kandrup (1980a) and write:

$$\langle F^2 T(F) \rangle \approx 8.88 \frac{G^2 \langle m \rangle_{av}^2 n_{av}}{\langle v^2 \rangle^{1/2}} \log \left\{ 1.12 \frac{\langle v^2 \rangle}{G \langle m \rangle_{av} \langle n \rangle_{av}^{1/3}} \right\} \tag{4.5}$$

Here $\langle m \rangle_{av}$ and n_{av} are the average mass and number density,respectively, of the generators of the fluctuating field. The average squared velocity for a system in approximate virial equilibrium can be estimated as:

$$\langle v^2 \rangle \approx G \langle m \rangle_{av} N^{2/3} n_{av}^{1/3}, \tag{4.6}$$

where we have introduced the total number of objects N which generate the fluctuation field. We identify the latters with the peaks in our density field having an average size up to a given fraction f of the radius of the system, and we will arbitrarily put: $f = 0.1$ The reason is that all the statistics in chapter 3 were derived under the assumption that the fundamental interaction is newtonian: if the generators of the stochastic field were distributed objects, one should also take into account dipolar and eventually higher order terms. So we will cosnider only that part of dynamical friction which is generated by "point–like" irregularities of the gravitational field. It this way *we are providing only a lower limit to a more realistic situation*: yet we will see that significant changes in the standard dynamics of spherical density perturbations arise.

As a further approximation we will assume that density perturbations are gaussian distributed. As we already stressed, many pieces of theoretical evidence suggest that deviations from a pure gaussian behaviour develop early during the

evolution and clustering of cosmological structures (Bernardeau, 1992; Fry, 1982, 1984, 1985, 1986; Grinstein & Wyse, 1986; Hamilton, 1988; Lucchin & Matarrese, 1988; Scherrer et al., 1991). Our choice is dictated by mathematical convenience: as is well known, in the case of gaussian statistics many calculations involving the density distribution of peaks can be performed exactly or with the help of well known approximations (Bardeen et al, 1986, hereafter BBKS), and this allows a significant simplification. With all these premises, the density $\langle n \rangle_{av}$ can now be estimated with the help of eqs. (4.5) and (4.11b) from BBKS:

$$\langle n \rangle_{av} = 1.6 \times 10^{-2} \left(\frac{n+5}{6} \right)^{3/2} \frac{1}{a^3(t) R_f^3}, \tag{4.7}$$

where R_f is the filtering radius and $a(t)$ is the cosmological expansion factor (density here is measured in proper units). This equation gives the total number density of peaks of any overdensity and mass. Given the radius of the cluster, R_{cl}, from what we said above we have: $R_F = f R_{cl}$. Inside a cluster of average overdensity δ_{typ}, only a fraction of the total mass will be contained in regions of average overdensity δ_0. This fraction can be computed from eq. (11) of Bower (1991), and is given by:

$$c_p = erf \left[\left(1 + z - \frac{\delta_{typ}}{\delta_0} \right) \frac{\delta_0}{\sigma(\langle m \rangle_{av})} \right] \tag{4.8}$$

In this equation $\sigma(\langle m \rangle_{av}) = A \langle m \rangle_{av}^{-\frac{n+3}{6}}$ is the mass variance. After having introduced eqs. (4.7- 4.8) into eqs. (4.3) and (4.5) and having performed some algebra one finally finds:

$$\eta_0 = 4.44 \left(\frac{6}{n+5} \right)^{3/4} \left(\frac{3}{4\pi} \right) \frac{f^3}{a^{3/2} (1.6 \times 10^{-2})^{1/2}} \left(\frac{G \langle m \rangle_{av}}{R_f^3} \right)^{1/2} c_p \tag{4.9}$$

The coefficient η_{cl} can be computed in a similar way. We obtain:

$$\eta_{cl} = \eta_0 \cdot \mu_\xi, \tag{4.10}$$

where the factor μ_ξ does depend on the correlation function only, and for a pure power–law spectrum it is a product of a function of the spectral index n and of the central value ξ_0. We compute this latter function numerically with the help of the equations and the asymptotic expansion for $\Sigma_{cl}(\mathrm{k})$ of the preceding chapter for each value of the index.

As we said already in chapter 3, the friction coefficient is expected to be quite small. However, as we will see in the next section, the dimensionless quantity $\eta T_c^{(0)}$, where $T_c^{(0)}$ is a time scale for gravitational collapse is not negligible.

4.3 Dynamics.

The introduction of a drag term modifies the equation of motion of a shell of matter embedded within a cosmological background. Adopting the same notation as in Gunn & Gott (1972) we can write the proper radius of a shell:

$$r(r_i, t) = r_i a(r_i, t), \tag{4.11}$$

where r_i is the initial radius and $a(r_i, t)$ is the expansion factor (the initial condition is then: $a(r_i, t_i) = 1$). The equation of motion of the shell is (Peebles, 1980, eq. 19.9):

$$\frac{d^2 r}{dt^2} = -\frac{GM}{r^2(t)} - \eta \frac{dr}{dt} \tag{4.12}$$

Assuming no shell crossing the total mass inside the shell can be considered constant. The average density inside the shell is given by:

$$\bar{\rho}(r_i, t) = \frac{3M}{4\pi a^3(r_i, t) r_i^3} \tag{4.13}$$

Mass conservation requires:

$$\bar{\rho}(r_i, t) = \frac{\bar{\rho}_i(r_i, t_i)}{a^3(r_i, t)} \tag{4.14}$$

and inserting eqs. (4.11), (4.13- 4.14) into eq. (4.12) we finally get:

$$\frac{d^2 a}{dt^2} = -\frac{4\pi G}{3} \frac{\bar{\rho}_i}{a^2} - \eta \frac{da}{dt} \tag{4.15}$$

The coefficient η is also a function of $a(t)$: from eqs. (4.9- 4.10) we can write:

$$\eta = \epsilon_0 a^{-3/2},$$

where:

$$\epsilon_0 = 4.44 \left(\frac{6}{n+5}\right)^{3/4} \left(\frac{3}{4\pi}\right) \frac{f^3}{(1.6 \times 10^{-2})^{1/2}} c_p \left(\frac{G\langle m \rangle_{av}}{R_f^3}\right)^{1/2} \tag{4.16}$$

It will prove more convenient to rewrite eq. (4.15) in terms of a dimensionless time variable: $\tau = t/T_{c0}$, where:

$$T_{c0} = \frac{\pi \rho_{ci}^{3/2}}{H_i (\rho_i - \rho_{ci})} \tag{4.17}$$

is the collapse time of the shell in the unperturbed case, i.e. for $\eta \equiv 0$ (Gunn & Gott, 1972), and ρ_{ci} is the critical density. Introducing the notation: $\lambda_0 = \epsilon_0 T_{c0}$ we find:

$$\frac{d^2 a}{d\tau^2} + \lambda_0 a^{-3/2} \frac{da}{d\tau} = -\frac{4\pi G}{3} \frac{\bar{\rho}_i T_{c0}^2}{a^2} \tag{4.18}$$

We will be interested in the following into solution of this equation for small values of the parameter λ_0; in Appendix 1 we derive an asymptotic expansion in power of λ_0 to the solution. However, we will not really make use of this solution in the present context, but of a related quantity, namely the correction to the collapse time T_{c0}. The drag forces determines a diminution of this quantity w.r.t the unperturbed case; it is shown in Appendix 1 that the first order corrected collapse time will be given by:

$$T_c = T_{ci} \left\{ 1 + \lambda_0 \left[1 - \frac{\sqrt{2}\pi}{3c} \frac{\left(1 + \bar{\delta}\right)^{3/2}}{\bar{\delta}^{3/2}} \right]^{-1} \right\} \tag{4.19}$$

where the quantity c is a constant depending on the initial conditions a_{min} and $\bar{\delta} = \mid 1 - \bar{\rho}_i/\rho_c \mid$ is the average overdensity.

Plots of the solutions of equation (4.18) are presented in Figure 8, for a power-law spectrum with $n = -1.6$, which, on the scale of clusters, approximates very well the standard CDM spectrum (Ryden, 1988a). We solved eq. 4.18 also numerically, using a standard Runge-Kutta fifth-order integrator. The differences between the numerical solution and the first-order asymptotic expansion are negligible, and we plot only the aymptotic expansions in Figure 8. The small difference is a consequence of the smallness of the parameter λ_0. From this Figure it clear that an average shell spends most of its time near its maximum radius, and the later collapse is enough rapid. Because we are inetersted into the behaviour of outer infalling regions of cluster, we will predominantly consider values of the parameters and initial conditions appropriate to these low density regions near the maximum of their turnaround.

In Figure 9 we show the variation of T_c/T_{ci} with the overdensity $\bar{\delta}$. Observe that

even in the limit of large $\bar{\delta}$, the collapse time is always larger than in the unperturbed case: the magnitude of the deviation is simply proportional to λ_0 and, as we see, is never lesser than about 1.1, even for low, very conservative estimates of the total mass contained inside the peaks. The changes are even more noticeable for lower $\bar{\delta}$. In Figure 10 we show the variation of T_c/T_{ci} with $\langle m \rangle_{av}$ for different $\bar{\delta}$.

We must also observe that during the calculation we have kept fixed the value of ξ_0 at the initial value, i.e. we have not taken into account any mildly nonlinear evolution of the clustering, which would then have increased the dynamical friction coefficient. In all respects, the estimates of λ_0 and T_c/T_{ci} presented in this chapter must be considered as lower limits: the real effects are probably larger. These calculations show that the effect of dynamical friction is small but detectable: one can then wonder about how this change in the characteristic time scale for cluster evolution reflects on the time evolution of other quantities, like the total mass accreted by secondary infall. We assume that no shell crossing occurs , so the total mass inside the radius $r(t) = r_i a(r_i, t)$ will be given by the cumulative mass distribution of all the shells. We consider the same density model as in Gunn & Gott (1972, eq. 8):

$$\rho_i = \begin{cases} \rho_{ei} + (\rho_{ci} + \rho_+ - \rho_{ei}) \frac{R_i^3}{r^3} & r > R_i \\ \\ \rho_{ci} + \rho_+ & r \leq R_i \end{cases} \tag{4.20}$$

Here ρ_{ci}, ρ_{ei} are the critical and external densities (i.e. outer to the region of given initial radius R_i), ρ_+ measures the deviation of the inner part from the critical state and R_i is the radius of the inner collapsed reagion. It is easy to verify that for this profile the inner collapse time becomes:

$$T_{ci} = \frac{\pi}{H_i} \frac{(\rho_{ci} + \rho_+)\, \rho_{ci}^{1/2}}{\rho_+^{3/2}}$$

The time for collapse of the outer region can then be obtained from the following equation:

$$\left(\frac{T_c}{T_{ci}}\right)^{2/3} = \frac{\rho_+}{(\rho_{ei} - \rho_{ci}) + \left(\frac{R_i}{r}\right)^3 (\rho_{ci} + \rho_+ - \rho_{ei})} \left\{1 + \lambda_0 \frac{2}{3} \lambda_0 \mu\right\} \tag{4.21}$$

where we have defined:

$$\mu = \frac{\sqrt{2}\pi}{3c} \left(\frac{1}{\bar{\delta}} + 1\right)^{3/2}$$

The overdensity is usually quite small, so we can approximate the total mass inside R_i as: $M(t) \approx (4\pi/3)\,\rho_{ci} R_i^3\,(r/R_i)^3$. Inverting eq. 4.21 to find (r/R_i) and substituting in this later equation we finally find:

$$M(t) = \frac{4\pi}{3} R_i^3 \cdot \frac{\rho_{ci}\left(\rho_{ci} + \rho_+ - \rho_{ei}\right)\left(\frac{t}{T_{ci}}\right)^{2/3}}{\rho_+\left[1 + \frac{2\lambda_0}{3}(1-\mu)\right] + \left(\rho_{ci} - \rho_{ei}\right)\left(\frac{t}{T_{ci}}\right)^{2/3}} \tag{4.22}$$

Eq. (4.22) can be rewritten in terms of the cluster mass at the epoch T_c of core collapse:

$$M(t) = M\left(T_c\right)\left\{1 + \rho_+ \frac{\left(\frac{t}{T_c}\right)^{2/3} - \left[1 + \lambda_0 + \frac{2\lambda_0}{3}(1-\mu)\right]}{\rho_+\left[1 + \lambda_0 + \frac{2\lambda_0}{3}(1-\mu)\right] + \left(\rho_{ci} - \rho_{ei}\right)\left(\frac{t}{T_c}\right)^{2/3}}\right\} \tag{4.23}$$

This equation reduces to the Gunn & Gott's (1972) eq. (20) in the limits of $\lambda_0 \to 0$. Introducing a new time:

$$T_c' = \left[1 + \lambda_0 + \frac{2\lambda_0}{3}(1-\mu)\right]^{3/2} T_c$$

one can rewrite eq. (4.23) in a a form more similar to that of eq. (4.1):

$$M(t) = M\left(T_c'\right)\left\{1 + \frac{\left(\frac{t}{T_c'}\right)^{2/3} - \left[1 + \lambda_0 + \frac{2\lambda_0}{3}(1-\mu)\right]}{\rho_+\left[1 + \lambda_0 + \frac{2\lambda_0}{3}(1-\mu)\right] + \frac{\left(\rho_{ci} - \rho_{ei}\right)}{\rho_+}\left(\frac{t}{T_c'}\right)^{2/3}}\right\} \tag{4.24}$$

In Figure 11 we show how dynamical friction affects mass accretion: the three different curves correspond to different asymptotic masses M_{max}. Larger M_{max} are produced by larger initial overdensities, so the largest effects are seeen for the smaller initial masses, as was already evident from Figure 9.

Finally we investigate another aspect of the dynamics of the collapse of a shell, namely the dependence of the collapse time on the initial position of the shell. In all the preceding figures we have considered the dynamics of those shells having as initial conditions $a_{0,min} = 10^{-3}$, and then fixing the parameter c. We will now look at the dependence of the evolution on the initial position of the shell. At variance with the pure Gunn & Gott (1972) self-similar solution, we expect that dynamical friction modifies in a different way the behaviour of different shells. From Appendix 1, eq.(??) defining: $\alpha_{min} = a_{0min}\lambda/\nu$ and noticing that

$a_{0max}\lambda/\nu = 1 - a_{0min}\lambda/\nu$ one can write the coefficient c as:

$$c(\alpha_{min}) = \frac{(1-\alpha_{min})^{1/2}}{\alpha_{min}} - \frac{{\alpha_{min}}^{1/2}}{(1-\alpha_{min})} + \frac{1}{2}\ln\left\{\frac{1-(1-\alpha_{min})^{1/2}}{1-{\alpha_{min}}^{1/2}}\cdot\frac{1+{\alpha_{min}}^{1/2}}{1+(1-\alpha_{min})^{1/2}}\right\} \tag{4.25}$$

Let us now put $T_c = 2t_0$ in eq.(4.19). In a flat $\Omega = 1$ Universe, if time is measured in units of the the value of t_0 corresponding to an Hubble constant of 100 $Km/sec/Mpc$ the age of the Universe will be given by $t_0 = 2/(3h)$, and the collapse time in the no-friction case T_{ci} will be given by $T_{ci} = t_0 \cdot (3\pi h/2)\left(1+\bar{\delta}\right)/\bar{\delta}^{3/2}$ so one can write:

$$\frac{T_c}{T_{ci}} = \frac{4}{3h\pi}\frac{\bar{\delta}^{3/2}}{1+\bar{\delta}}$$

From eq.(4.19) we obtain an implicit equation for the initial value of a of the shell whose collapse time is twice the age of the Universe:

$$c(\alpha_{min}) = \frac{\frac{\sqrt{2\pi}}{3}\left(\frac{1}{\bar{\delta}}+1\right)^{3/2}}{1-\frac{\lambda_0}{[(T_c/T_{ci}-1)]}} \tag{4.26}$$

In Figure 13 we plot α_{min} as a function of the initial overdensity for two values of the total mass contained inside the peaks. The interesting feature to observe is that for small overdensities a large part of the region has a very large collapse time, while for larger overdensities, as those expected for the core of clusters at turnaround, the critical radius is quite large. This shows that the effect of dynamical friction is large for small density perturbations, where the binding action of gravity is comparable to or smaller than the resistance produced by dynamical friction. This supports our preceding conclusion that the effects of dynamical friction could be more evident in the outer regions of clusters.

4.4 Mass Spectrum.

The results of the preceding sections can be applied to the determination of the evolution of the mass spectrum of cosmic structure, at least within those regimes in which structure formation can be reasonably thought to proceed mainly by collisionless gravitational hierarchical clustering. In CDM models this range probably extends from groups of galaxies upward in total mass. On smaller scales the formation of structure has been probably strongly afffected by the interaction with gas. On the larger scales, dynamical friction produced by substructure is

the only dissipative effect, and, although very weak, it can significantly affect the formation of those structure whose characteristic formation time scales are very long, e.g. clusters of galaxies, as we have already shown in the introduction to chapter 3.

A very successfull approach to the description of the mass spectrum has been the Press & Schechter (1974) approach. Although based on some oversimplifying assumptions on the statistics and the dynamics of structure evolution, its prediction are remarkably close to the observations over a wide mass (luminosity) range (Bahcall, 1979). One of the main weak points of the PS approach lies in the lack of "temporal resolution" (Cavaliere et al., 1991), i.e. on the consideration that structures on different scales evolve on different time scales. in a recent paper, Cavaliere, Colafrancesco & Scaramella (1991) (hereafter CCS) have remedied this situation introducing and solving an evolutionary equation which takes explicitly into account the dynamics into the evolution of the mass spectrum (CCS, eq. 5.5):

$$\frac{\partial N}{\partial t} + \frac{\partial \left(\dot{M} N\right)}{\partial M} = \frac{N}{\tau_+} - \frac{N}{\tau_-} \tag{4.27}$$

The quantity $N(M,t)$ is such that $N(M,t)dM$ is the total number of "objects" in the mass range $M, M+dM$, and τ_+, τ_- are the timescales for formation and destruction of the objects. These are specified by the following equations:

$$\tau_+ = 2t_c m^{-\Theta}/\Theta, \qquad \tau_- = 2t_c/\Theta, \tag{4.28}$$

where $m \equiv (M/M_c)$, M_c is a critical mass and $t_c = M_c/\dot{M}_c$ is an infall time scale for the critical mass. The production time scale τ_+ is explicitly dependent on mass, while the destruction time scale τ_- is constant. The balance is then determined by the second term on the left-hand side, which describes the inertial shiift of the mass spectrum as mass is produced. The only uncertainty left is in the definition of the "objects" to which an equation like eq. 4.27 applies: ultimately to a conversion from mass to luminosity which allows a direct comparison of the theoretical predictions with the observed luminosity function.

CCS adopted the Gunn & Gott (1972) formula for the accretion rate $M(t)$:

$$M(t) = M_i \left\{ 1 + \frac{M_{max} - M_i}{M_i} \cdot \frac{(t/t_i)^{2/3} - 1}{(M_{max}/M_i - 1) + (t/t_i)^{2/3}} \right\} \tag{4.29}$$

We will repeat their calculations using the modified accretion rate (4.23). Eq. (4.27) with the source terms (4.28) can be solved exactly (Appendix 2), and the solution reads:

$$N\left(t, t_1(t,M)\right) = N\left(0, t_1(t,M)\right) \exp\left\{ a_{sp} \left(\int_0^{t/t_c} d\sigma \left[\frac{M(\sigma) + t_1(t,M)}{M_c} \right]^{2a_c} \right) \right\} \tag{4.30}$$

where we have defined:

$$t_1(t,M) = M - M\left(T_c'\right) \left\{ 1 + \frac{\left(t/T_c'\right)^{2/3} - 1}{1 + \frac{\rho_{ci} - \rho_{ei}}{\rho_+} \left(t/T_c'\right)^{2/3}} \right\} \tag{4.31}$$

and the coefficient a_{sp} is connected to the index of power spectrum: $a_{sp} = (n+3)/6$. As initial distribution we take a modified Press-Schechter distribution (CCS, eq. 3.3):

$$N(0,M) = N_0 \frac{1}{M_c^2(z_i)} \left[\frac{M}{M_c(z_i)} \right]^{-\Gamma} \exp\left[-\frac{b^2}{2} \left(\frac{M}{M_c(z_i)} \right)^{\Theta} \right] \tag{4.32}$$

where: $\Theta = 2a_{sp} = (n+3)/2$, $\Gamma = 2 - a_c(1+p)$ and the coefficient $p \approx 1.5$ comes from a polynomial approximation to the number density of peaks (CCS, eq. 3.1). A slight difference in the way we count peaks in this equation and in the theory formulated above to calculate the coefficient of dynamical friction λ_0 does not affect substantially our results, because the peaks which give rise to the observed structure have typical sizes much larger than those producing the substructure which originates the dynamical friction.

Given a mass spectrum $N(M,t)$ one can obtain a luminosity function $N(L,t)$ provided one specifies a relation between M/L and total mass. In order to ease the comparison with the results of CCS we will adopt the same relations they adopted, namely: $M/L \propto M^{1/4}$. The results are shown in Figure 12. The two curves have the same normalization, but the mass is shifted toward higher values as a consequence of the variation in the accretion timescale (the shift term $\dot{M}$ in eq. (4.27). The lower accretion rate connected to the revised accretion formula of eq. (4.23) reflects in a larger shift from smaller to larger masses: the modification of the mass spectrum is however not very large.

4.5 Conclusions.

We have discussed the effects of dynamical friction on the dynamics of isolated cosmological density perturbations and on the mass spectrum. The calculation of the dynamical friction coefficient made use of the theory developed in a recent work (Antonuccio–Delogu & Atrio–Barandela, 1992) and takes into account the dependance on clustering. The efficiency of secondary infall increasing the total nonbaryonic mass in the outer regions of the protostructures is significantly decreased, becuse dynamical friction introduces a drag which slows the accretion. The effect is more prominent in regions with low overdensities, and tends to vary very fast with $\bar{\delta}$. The effect on the mass spectrum is to produce deviations from the original spectrum lesser prominent than those found when the Gunn & Gott (1972) dissipationles model is adopted, and we have shown this by comparing our results with those obtained by Cavaliere et al. (1991).

Our treatment however has exploited a few simplifying asumptions. First, our equations for the dynamical friction coefficient applies only in the linear and early-nonlinear stages of clustering, because of a theoretical limitation in the underlying theory (chapter 3). Second, we had to model the amount of substructure present, and we assumed that this substructure does not evolve, i.e. that the number density and mass spectrum of the subpeaks' population producing the stochastic component of the gravitaional field, which originates the dynamical friction, do not vary in time. We did neither consider the temporal evolution of the correlation function.

However, all these assumptions tend to *underestimate* the importance of dynamical friction. For example, during the evolution clustering increases and consequently also the coefficient of dynamical friction η_{cl} raises. All the effects quoted above, if included, tend to slow the accretion and secondary infall of matter. The results presented here can be seen as a sort of "low order" approximation to a more realistic calculation, in which all the effects seen here should be larger. Ultimately, the combination of mean-field gravitational field, dynamical friction (weakly dissipative, first-order effect) and clustering should bring a given initial system toward a quasi-relaxed, slowly evolving configuration. Dynamical friction tends to slow the infall, to diminish the average separation of peaks, and as a consequence to increase the clustering. But a higher clustering tends to raise the dynamical friction coefficient: in the linear phase one has $\eta_{cl}/\eta_0 \propto \xi_0 \propto t^{4/3}$, and

this backup effects acts as a secular relaxation mechanism.

One of the main effects of dynamical friction should be a transfer of momentum and angular momentum from the subpeaks to the larger-scale structure: this induces a secular variation of the density profile of the subpeaks' w.r.t. the higher peaks of the density field inside which galaxies form, a process often called "segregation" (Hoffmann et al., 1982; Farouki et al. 1983; Yepes et al., 1991). Another effect observed in numerical simulations is the "velocity segregation" (Carlberg, 1991; Carlberg & Dubinsky, 1991), i.e. a tendency for larger mass particles to have a smaller average pairwise velocity and velocity dispersions than the field particles. Both these effects are a byproduct of dynamical friction exerted on rare, high-density by the population of more numerous, low-density peaks. In the next chapter we will mostly focus on these effects and we will compare the predictions of a simplified exact theory for the evolution of clustering with the results of these numerical simulations.

4.6 Appendix 1.

An asymptotic expansion for the solutions of eq. (4.18) can be found using the methods developed by Bourland & Habermann (1988, 1990) (hereafter BH88 and BH90, respectively.). Let us write again eq. (4.18):

$$\frac{d^2a}{d\tau^2} + \lambda_0 a^{-3/2}\frac{da}{d\tau} = -\frac{4\pi G}{3}\frac{\bar{\rho}_i T_{ci}^2}{a^2}$$

If we consider the term containing the coefficient λ_0 as a perturbation, and we look for an asymptotic solution for small values of the parameter λ_0, we can exploit the fact that we know in closed the form the solution of the "unperturbed" problem ($\lambda_0 = 0$).

We now introduce a "*slow time scale*": $T = \lambda_0\tau$ and a *phase* (BH88, after eq. 2.1):

$$\psi = \frac{\Theta(T)}{\lambda_0} + \phi(T) \tag{4.33}$$

The precise functional form of $\Theta(T)$ and $\phi(T)$ depends on the problem: we will define it later.

The solutions of the "unperturbed" problem can be given in parametric form (§2.2.1):

$$a_0(\theta) = \begin{cases} \left(\frac{\beta}{2\gamma} + a_{0,min}\right)\cos\left([-\gamma]^{1/2}\,\theta\right) - \frac{\beta}{2\gamma} & \gamma < 0 \\ \left(\frac{\beta}{2\gamma} + a_{0,min}\right)\cosh\left(\gamma^{1/2}\theta\right) - \frac{\beta}{2\gamma} & \gamma \geq 0 \end{cases}$$

$$H_i\tau - H_i\tau_0 = \frac{1}{\mid\gamma\mid^{1/2}} \begin{cases} \left(\frac{\beta}{2\gamma} + a_{0,min}\right)\sin\left([-\gamma]^{1/2}\,\theta\right) - \frac{\beta}{2\gamma}\theta & \gamma < 0 \\ \left(\frac{\beta}{2\gamma} + a_{0,min}\right)\sinh\left(\gamma^{1/2}\theta\right) - \frac{\beta}{2\gamma}\theta & \gamma \geq 0 \end{cases} \tag{4.34}$$

where we have defined:

$$\beta = \frac{\bar{\rho}_i}{\rho_{ci}}, \quad \gamma = \frac{\rho_{ci} - \bar{\rho}_i}{\rho_{ci}}, \quad H_i = \frac{8\pi G}{3}\rho_{ci}$$

In the following we will also need an "angular velocity": $\omega(T) = \Theta'(T)$, where the apex means here derivation w.r.t. the slow time scale and $E(T)$ is a slowly varyin phase averaged energy:

$$E(T) = \frac{\omega^2(T)}{2}\left(\frac{da_0}{d\psi}\right) - V(a_0, T) \tag{4.35}$$

and we have defined:

$$V(a_0,T)=\left[-\frac{4\pi G\bar{\rho}_i T_c^2}{3a_0}+\frac{4\pi G}{3}\left(\bar{\rho}_i-\rho_{ci}\right)T_{c0}^2\right] \tag{4.36}$$

We will look for asymptotic expansions of positions and velocities in terms of λ_0:

$$a\left(r_i,T\right)=a_0\left(r_i,T\right)+\lambda_0 a_1\left(r_i,T\right)+\ldots$$

$$\frac{da}{dt}=b_0\left(r_i,T\right)+\lambda_0 b_1\left(r_i,T\right)+..., \tag{4.37}$$

The dependence of E on T can be obtained solving an equation for an "action", as shown in BH90:

$$\frac{dI}{dT}=-D(E,T) \tag{4.38}$$

where the *dissipation* $D(E,T)$ is defined as (Bourland & Habermann, 1988, eq. 2.11):

$$D(E,T)=\int_{a_{0,min}}^{a_{0,max}} dy_0 \frac{\sqrt{2}\left[E-V(y_0,T]^{1/2}\right.}{y_0^{3/2}} \tag{4.39}$$

The "action" $I(E,T)$ is defined by:

$$I(E,T)=2\int_{a_{0,min}}^{a_{0,max}} d\alpha\sqrt{2}\left[E(T)-V(\alpha,T)\right] \tag{4.40}$$

The integral in equation (4.39) for the $V(a_0,T)$ given in eq. (??) can be reduced to:

$$D(E,T)=2\sqrt{2}\frac{\nu}{\lambda^{1/2}}\int_{(\lambda/(a_{0,min}\nu)^{1/2}}^{(\lambda/(a_{0,max}\nu)^{1/2}} d\sigma_0\left(\sigma_0^2-1\right)^{1/2},$$

where we have introduced the dimensionless quantities:

$$\lambda=\frac{4\pi G\bar{\rho}_i}{3}T_{c0}^2,\quad \nu=\frac{4\pi G\left(\bar{\rho}_i-\rho_{ci}\right)}{3}T_{c0}^2-E \tag{4.41}$$

The latter integral can be calculated with the help of eq. (2.225.(2)) from Gradshteyn & Ryzhik (1968), and finally we find:

$$D(E,T)=2\sqrt{2}\frac{\nu}{\lambda^{1/2}}\cdot\left\{\frac{\left[1-(a_{0,min}\nu/\lambda)^{1/2}\right]}{(a_{0,min}\nu/\lambda)}-\frac{\left[1-(a_{0,max}\nu/\lambda)^{1/2}\right]}{(a_{0,max}\nu/\lambda)}+\right.$$

$$\left.\frac{1}{2}\ln\left[\frac{\sqrt{1-(a_{0,min}\nu/\lambda)}-1}{\sqrt{1-(a_{0,max}\nu/\lambda)}-1}\cdot\frac{\sqrt{1-(a_{0,max}\nu/\lambda)}+1}{\sqrt{1-(a_{0,min}\nu/\lambda)}+1}\right]\right\} \tag{4.42}$$

We denote this latter function of $a_{0,max}, a_{0,min}$ as c. Putting equations (4.40-4.39) into eq. (4.38) one gets an equation for $E(T)$:

$$\frac{dE}{dT} + \frac{4c}{\pi\lambda^{3/2}}\left[-\gamma\frac{H_i^2 T_{c0}^2}{2} - E\right]^{5/2} = 0 \tag{4.43}$$

Following BH90 we now solve this equation with the initial condition $E(0) = 0$ (bound case), substitute the solution into eq. (4.34) and find $\omega(T)$. This then allows us to find the phase $\Theta(T)$ defined above from eq. (4.32). Proceeding this way we obtain

$$\frac{\Theta(T)}{\lambda_0} = \frac{\sqrt{2}}{\pi\lambda}\left(-\frac{\gamma H_i^2 T_{c0}^2}{2}\right)^{3/2}\tau + \lambda_0\frac{\sqrt{2}}{\pi\lambda}\left(\frac{4c}{\pi\lambda^{3/2}}\right)\left(-\frac{\gamma H_i^2 T_{c0}^2}{2}\right)^3\frac{3}{2}\tau^2 + O({\lambda_0}^2). \tag{4.44}$$

Now, the zeroth-order solution a_0 verifies the equation (BH88, eq. 2.3):

$$\frac{\partial^2 a_0}{\partial\psi^2} + \frac{4\pi G}{3}\cdot\frac{\overline{\rho_i}}{a_0^2\omega^2(T)} = 0, \tag{4.45}$$

which can be solved exactly w.r.t. the variable ψ. This is the standard equation for the expansion factor (Gunn & Gott (1972)), but for a modified, slowly varying coefficient. The solution then reads:

$$a_0(\psi, T, r_i) = \left(\frac{\beta}{2\gamma} + a_{0,min}\right)\cos\left(\left[-\gamma^{1/2}\right]\theta\right) - \frac{\beta}{2\gamma} \tag{4.46}$$

(for $\gamma < 0$) and $\theta(\psi)$ is determined inverting the equation:

$$\psi = \omega(T)\cdot\frac{\beta}{2\gamma^{3/2}H_i T_{c0}}\left[\gamma^{1/2}\theta - \sin\left([-\gamma]^{1/2}\,\theta\right)\right] + \psi_+, \tag{4.47}$$

where:

$$\beta = \frac{\overline{\rho_i}}{\rho_{ci}}, \quad \gamma = 1 - \beta.$$

The condition of full collapse is $a_0 = a_{0,min}, \mid\gamma\mid^{1/2}\theta = 2\pi$. Equating eqs. (4.33) and eq. (4.47) one obtains, for $\theta = 2\pi$ (the initial value ψ_+ is neglibly small, see e.g. Gunn & Gott (1972)):

$$\frac{\Theta(T_*)}{\lambda_0} + \phi(T_*) = \omega(T_*)\cdot\frac{\pi\beta}{\mid\gamma\mid^{3/2} H_i T_{c0}}, \tag{4.48}$$

where T_* is the final collapse time. One now expands this time in terms of $\lambda_0 : \tau_* = \tau_0 + \lambda_0\tau_1 + ..., T_* = \lambda_0\tau_* = \lambda_0\tau_0 + {\lambda_0}^2\tau_1 + ...$The zeroth order contribution

from the latter equation is:

$$\phi(\tau_0) + \frac{\sqrt{2}}{\pi\lambda}\left(-\gamma\frac{H_i^2 T_c^2}{2}\right)^{3/2}\tau_0 = \omega(\tau_0)\cdot\frac{\pi\beta}{\mid\gamma\mid^{3/2} H_i T_c} \tag{4.49}$$

At zero order in λ_0 one has $\phi(\tau_0) = 0$ and:

$$\omega(\tau_0) = \frac{\sqrt{2}}{\pi\lambda}\left(-\gamma\frac{H_i^2 T_{c0}^2}{2}\right)^{3/2}$$

so finally one has:

$$\tau_0 = \frac{\pi\beta}{\mid\gamma\mid^{3/2} H_i T_c} \tag{4.50}$$

in agreement with Gunn & Gott (1972).
At first order in λ_0 one has:

$$\phi'(\tau_0)\,\tau_1 + \frac{\sqrt{2}}{\pi\lambda}\left(-\gamma\frac{H_i^2 T_{c0}^2}{2}\right)^{3/2} + \frac{\sqrt{2}}{\pi\lambda}\left(\frac{4c}{\pi\lambda^{3/2}}\right)\left(-\gamma\frac{H_i^2 T_{c0}^2}{2}\right)^{3}\frac{3}{2}\tau_0^2 = \omega'(\tau_0)\cdot\frac{\pi\beta}{\mid\gamma\mid^{3/2} H_i T_{c0}}\tau_1. \tag{4.51}$$

Now, from BH88 one has $\phi'(\tau) = A\omega'(\tau)$ and, if $a_1(0) = 0$ one obtains: $A = 0, \phi'(\tau_0) = 0$. After some manipulations one obtains:

$$\tau_1 = -\tau_0\frac{1}{\frac{\sqrt{2}\pi}{3c}\left(-\frac{\beta}{\gamma}\right)^{3/2}\frac{1}{\tau_0} - 1}. \tag{4.52}$$

This is the dimensionless first order correction to the collapse time.

4.7 Appendix 2.

We will solve eq. 4.27 by the standard method of characteristics (see, e.g. Zwillinger (1989), §88). This can be applied to any linear partial differential equation whose solution is known to be unambigously determined by the initial data and the boundary conditions (i.e. if caustics do not arise) in the in the domain of interest . It consists in reducing the problem for the original PDE to a set of coupled ordinary differential equations. In our case we obtain:

$$\frac{dx_1}{ds} = 1, \frac{dx_2}{ds} = \dot{m}(x_1(s)),$$

$$\frac{du}{ds} = \frac{a_{sp}}{t_c}x_2^{2a_{sp}}u - \frac{a_{sp}}{t_c}u, \tag{4.53}$$

with the initial conditions:

$$x_1(0) = 0, \quad x_2(0) = t_1, \quad u(0) = f(t_1) \tag{4.54}$$

Where we have introduced a new variable: $m = M/M_c$, because the coefficient τ_+ in the original eq. (4.27) depends on this variable. The form of the equations for $N(m,t)$ is the same as the original one, provided one substitutes $\dot{m} = \dot{M}/M_c$ in place of $\dot{M}$. In eq. (4.54) we adopted some new definition for old variables: $x_1 \equiv t$, $x_2 \equiv m$, $u \equiv N$ and $a_{sp} = \Theta/2$. It is easy to verify that $x_1 = s$, so s is actually the time. The equation for x_2 can then be solved:

$$x_2(t) = \int_0^t d\sigma \dot{m}(\sigma) + t_1 \tag{4.55}$$

so that now the last of eqs 4.53 becomes:

$$\frac{du}{dt} = \frac{a_{sp}}{t_c}\left[m(t) + t_1\right]^{2a_{sp}} u - \frac{a_{sp}}{t_c} u \tag{4.56}$$

The quantity t_1 coincides with the mass variable at $t = 0$, and, using the identification $x_2 \equiv m$ we then write $t_1 = m - m(t) + m(0)$. We will adopt the expression for $m(t)$ given in the text, eq. (4.24), so $m(0) = 0$. Let us now introduce the variable:

$$w(t,t_1) = u(t,t_1)\exp\left(\frac{a_{sp}t}{t_c}\right)$$

our eq. 4.56 then reduces to:

$$\frac{dw}{dt} = \frac{a_{sp}}{t_c}\left[m(t) + t_1\right]^{2a_{sp}} w \tag{4.57}$$

whose solution can be written:

$$w(t,t_1) = w(0,t_1)\exp\left\{\frac{a_{sp}}{t_c}\int_0^t d\sigma\left[m(\sigma) + \frac{t_1(\sigma,m)}{t_c}\right]\right\}$$

so that the solution for $u \equiv N$ will be:

$$N(m,t) = f(0,t_1(m,t))\exp\left(\frac{a_{sp}}{t_c}\int_0^t [m(\sigma)t_1(\sigma,m)] - \frac{t}{t_c}\right), \tag{4.58}$$

with:

$$t_1(t,m) = m - m'\left\{1 + \frac{(t/T_c')^{2/3} - 1}{1 + (\beta/\rho_+)(t/T_c')^{2/3}}\right\} \tag{4.59}$$

and $m' = M(T_c')/M_c$, $\beta = \rho_{ci} - \rho_{ei}$.

Figure Caption.

Figure 8.–Modified expansion due to the introduction of dynamical friction effects. The scale of the vertical axis is arbitrary, and $\bar{\delta} = 2 \times 10^{-2}$. The unperturbed solution (*solid line*) and two perturbed solutions for $\langle m \rangle_{av} = 10^{11} M_{\odot}$ (*dashed line*) and $\langle m \rangle_{av} = 5 \times 10^{12} M_{\odot}$ (*dotted line*), respectively, are displayed.

Figure 9.–Variation of the collapse time with peaks' overdensity, for different $\langle m \rangle_{av}$. The value od δ_{typ} chosen is proper to the outer regions of a cluster computed from the models of Ryden (1988b), assuming a central value of the overdensity $\bar{\delta}_0 = 1.68/(1 + z_f) \approx 1.29$, corresponding to a formation eppoch $z_f \approx .3$ (Gioia et al., 1990; Hnery & Arnaud, 1991). *solid line*: $\langle m \rangle_{av} = 5 \times 10^{10} M_{\odot}$, *dotted line*: $\langle m \rangle_{av} = 2 \times 10^{11} M_{\odot}$, *dashed line*: $\langle m \rangle_{av} = 5 \times 10^{11} M_{\odot}$.

Figure 10.–Variation of the collapse time with peaks' mass, for different $\bar{\delta}$. *solid line*: $\bar{\delta} = 3 \times 10^{-2}$, *dotted line*: $\bar{\delta} = 2 \times 10^{-1}$, *dashed line*: $\bar{\delta} = 10^{-1}$.

Figure 11.–The relative ratio of the accreted mass with friction effects included to the accreted mass in the dissipantionless scenario of Gunn & Gott (1972). *solid line*: $M_{max} = 2M_i$; *short dashed line*: $M_{max} = 4M_i$, *dashed line*: $M_{max} = 19M_i$. The value of δ_{typ} are as in Figure 9.

Figure 12.–Luminosity functions. We plot the variation of the modified Press-Schechter luminosity function *solid line* after accretion the lowest mass peaks have accreted a mass comparable to the initial mass *dashed line.*

Figure 13.–Radius of the shell whose total collapse time is twice the age of the Universe t_0. *Solid line*: $\langle m \rangle_{av} = 5 \times 10^{10} M_{\odot}$; *dashed line*: $\langle m \rangle_{av} = 5 \times 10^{12} M_{\odot}$.

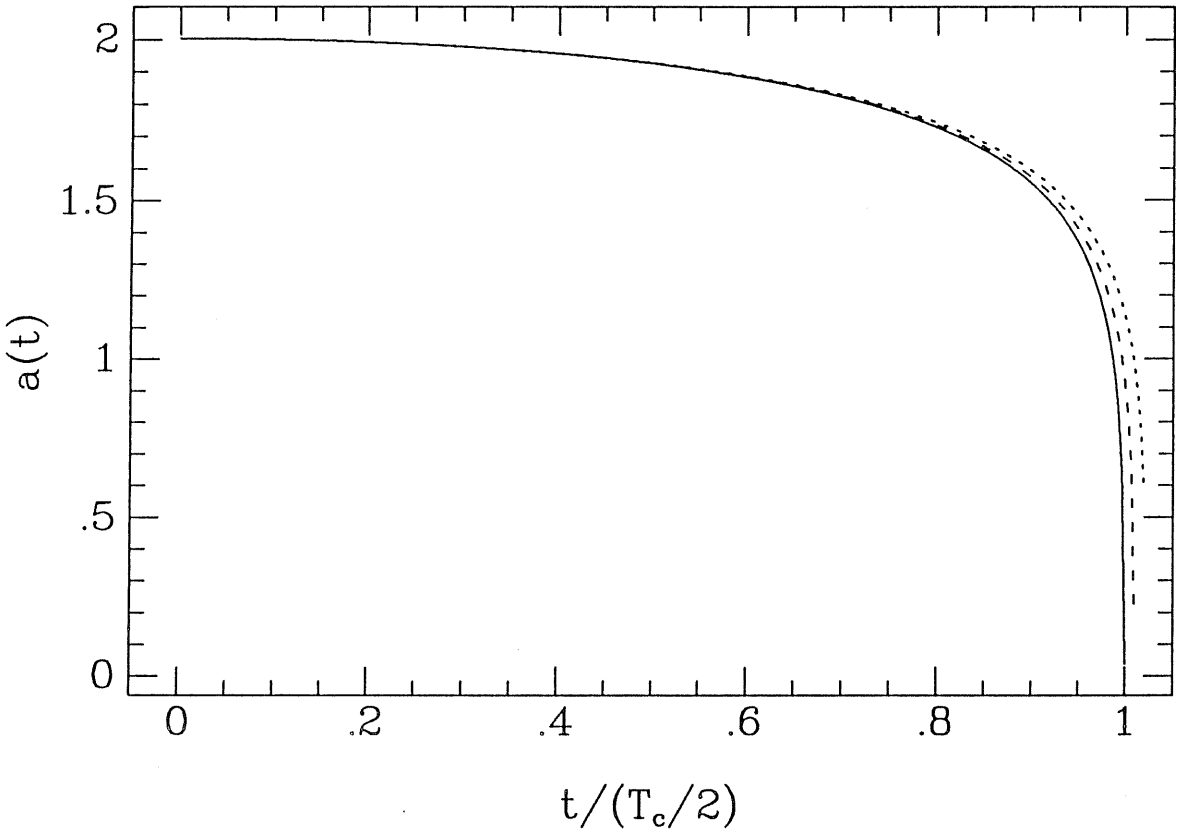

Fig. 8

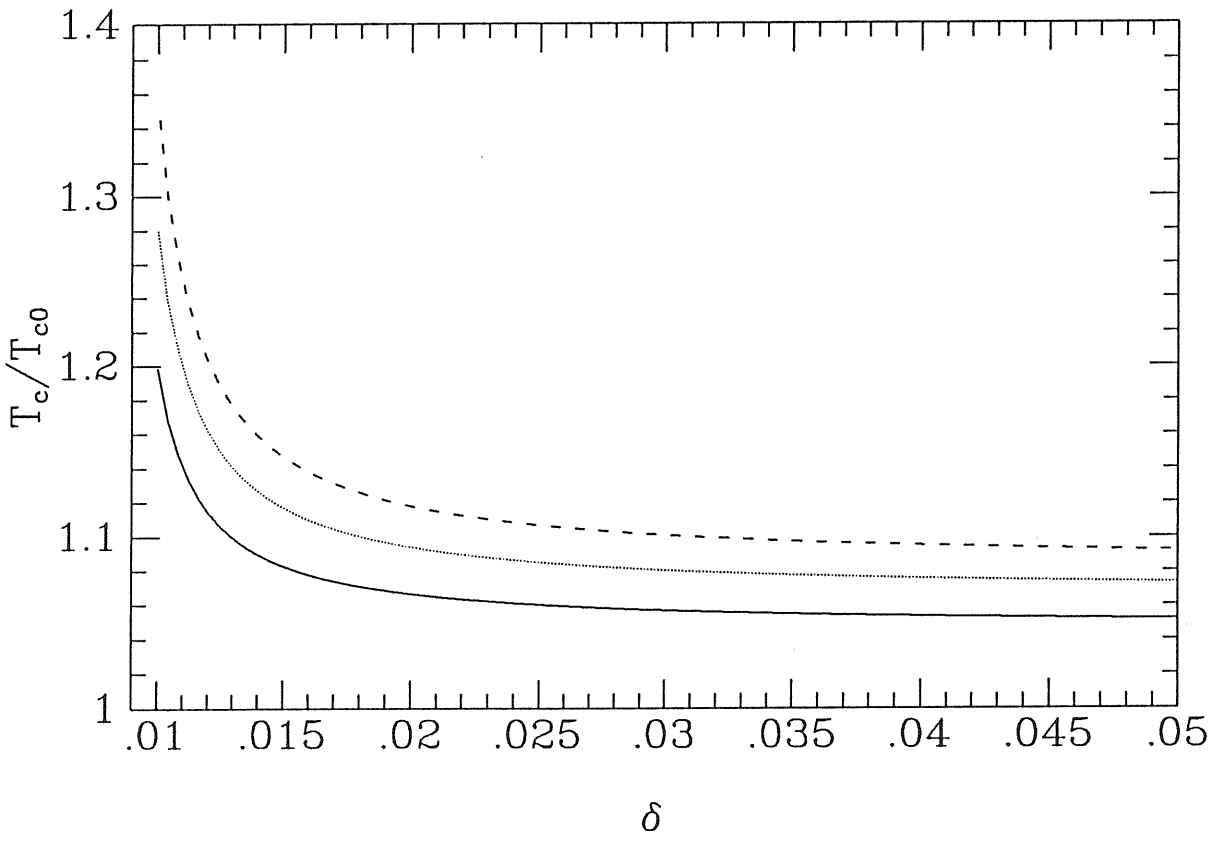

Fig. 9

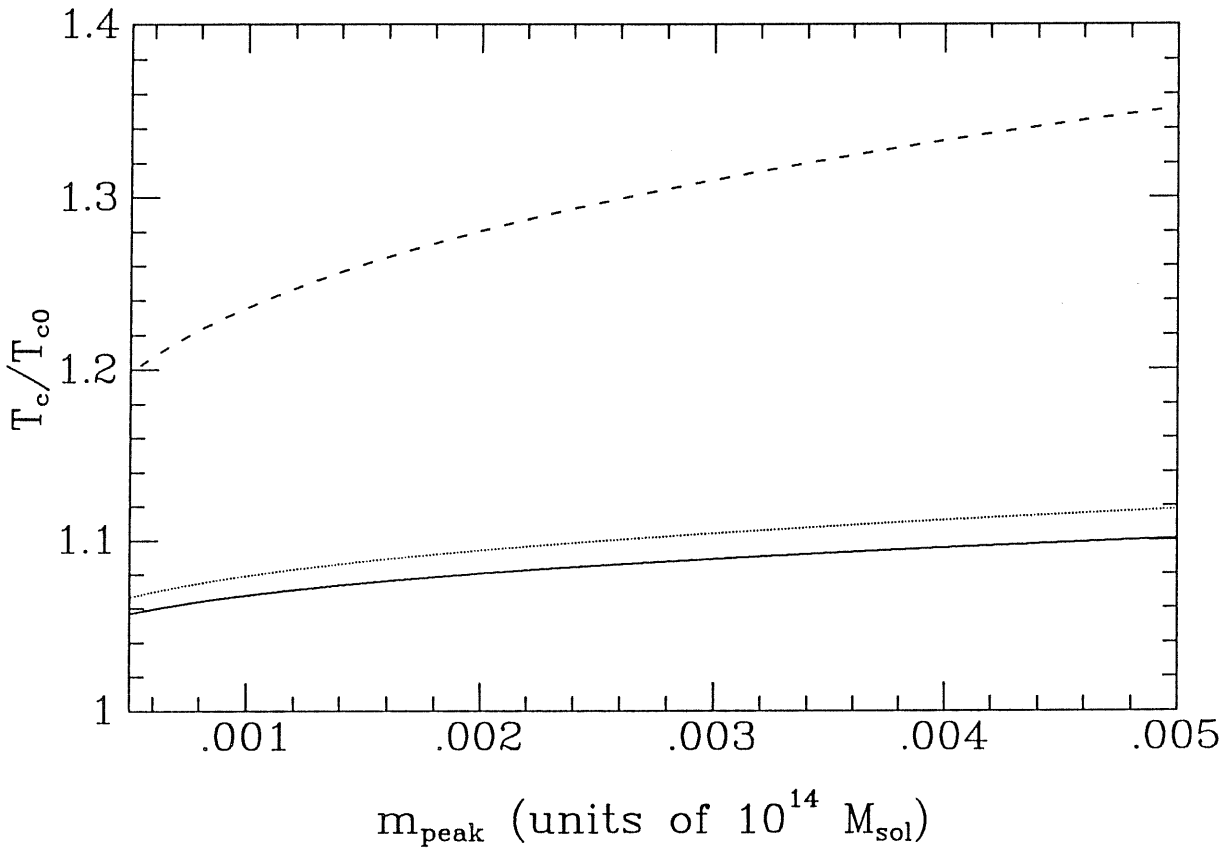

Fig. 10

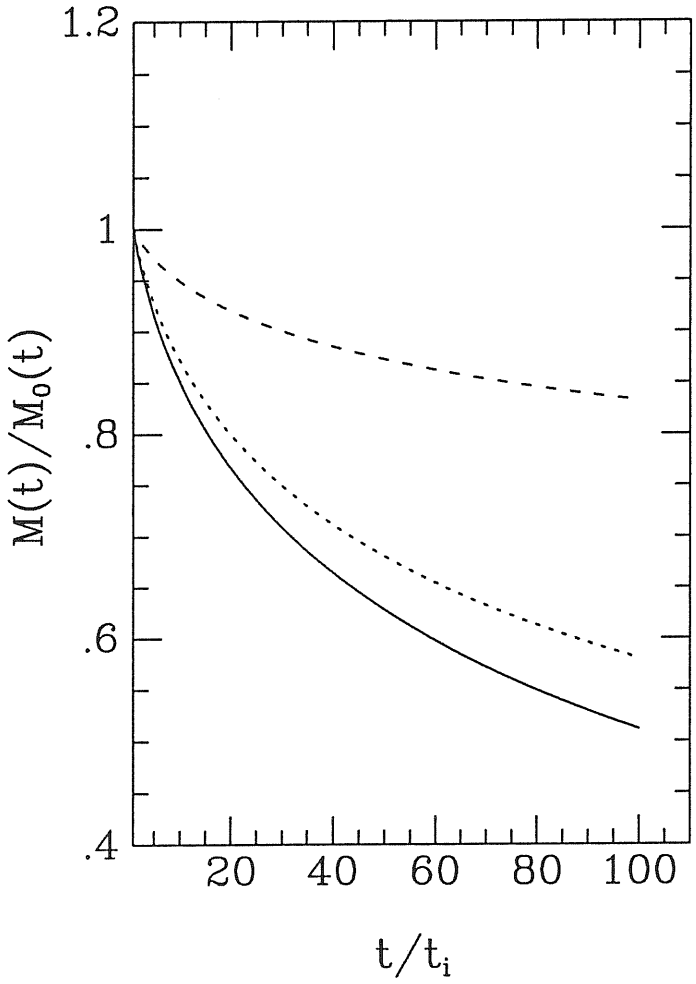
1.2
1
.8
.6
.4
20
40
60
80
100
M(t)/M₀(t)
t/tᵢ

Fig. 11

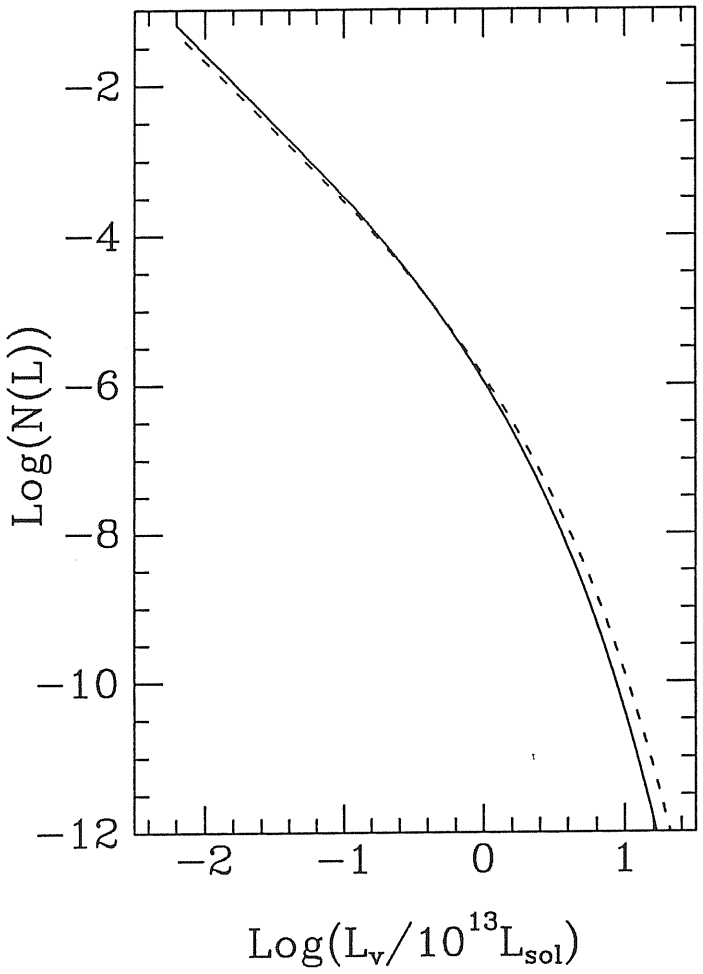
−2
−4
−6
−8
−10
−12
−2
−1
0
1
Log(N(L))
Log(Lᵥ/10¹³L_sol)

Fig. 12

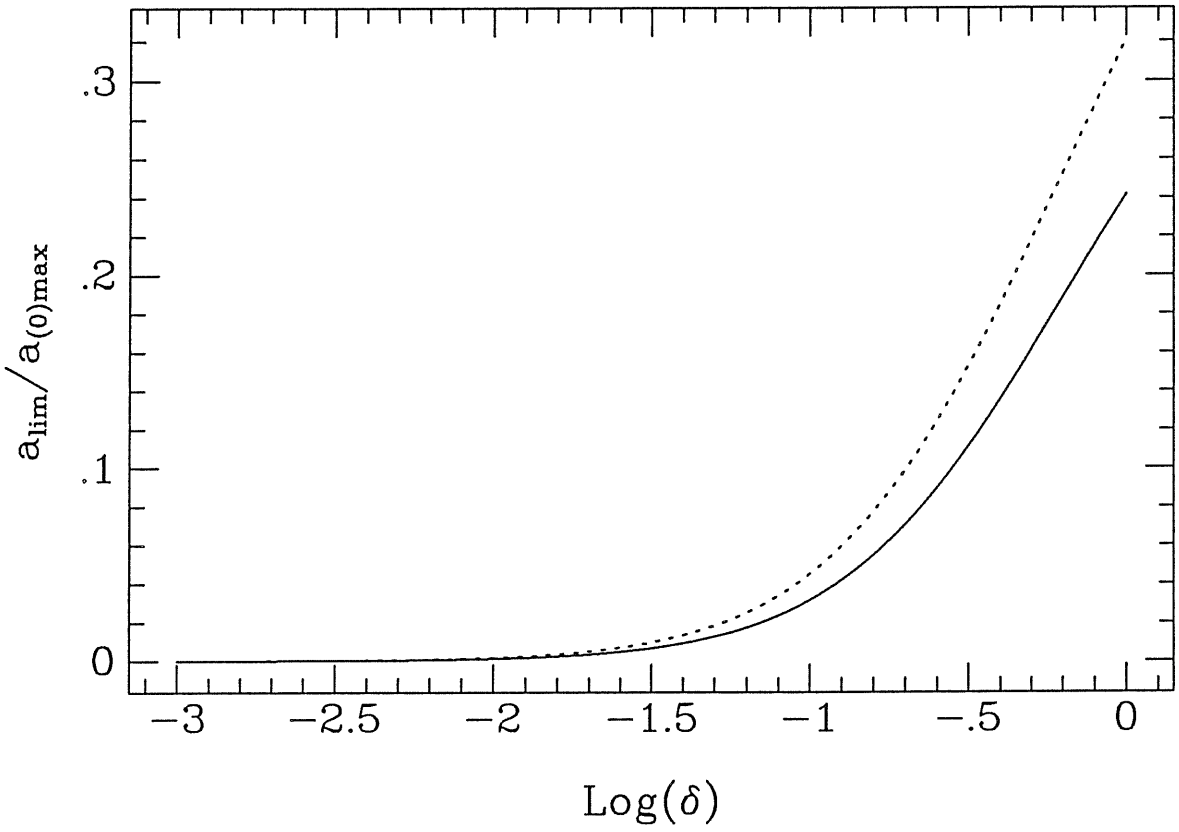

Fig. 13

Chapter 5

Evolution of Clustering in CDM Models.

5.1 Introduction.

One of the distinctive feature of the CDM models for the formation of structure in the Universe is the fact that objects form mainly through a dissipationless aggregation mechanism, commonly referred as *hierarchical clustering.* Structures on larger scales form via the clustering, collapse and eventually relaxation of substructure on smaller scales. This process should produce at least two distinctive features of present-day observed structures: a luminosity function very near (but not necessarily) coincident with a Press-Schechter form (Bahcall, 1979; Binggeli et al., 1988) and a two-point correlation function of the form $\xi \approx r^{-1.8}$ on scales between $10^{-2} - 10$ Mpc (Peebles, 1980). In the preceding chapter we have considered the first aspect and we saw that when the dynamics of the collapse is taken into account the mass spectrum does not evolves self similarly, as predicted in "istantaneous collapse" models. However, we found that dynamical friction in the outer low density regions of a forming cluster can slow this process.
In this chpater we will consider the effect of dynamical friction on the evolution of the dynamical properties of hierachical clustering models. In chapters 3 and 4 we have sen that a linear connection exists between an integral quantity involving the correlation function and the coefficient of dynamical friction; this suggests that this sligthly dissipative effect could influence some average properties of structures forming on long time scales, like the outer infalling parts of clusters of galaxies. A confirmation of this comes from recent numerical simula-

tions which showed an effect denoted *velocity bias* (Carlberg, 1991; Carlberg & Dubinsky, 1991): structures forming inside peaks of relatively high density (called galaxies) tend to have a relative pairwise velocity dispersion lower than that of the background structure. Carlberg (1991) attributed this effect to the action of dynamical friction, and showed that his results are in *qualitative* agreement with a model in which the relative pairwise peculiar velocity changes as:

$$\frac{dv_p}{dt} = -4\pi G\rho_0 \frac{\int_0^r \xi(x)x^2dx}{r^2} - 4\pi\rho_0\xi(r)G^2 \ln\Lambda M_s(r) \left[erf(X) - \frac{2}{\sqrt{\pi}} X e^{-X^2}\right] \frac{\mathbf{v}_p}{v_p^3} \tag{5.1}$$

where $X = v_p/\left[2^{1/2}\sigma_1\right]$, σ_1 is the velocity dispersion of the background particles (halo), and Λ is the usual logarithmic Coulomb factor which takes into account the probability of having rare, large scattering events. This equation can be derived from the classical theory of Chandrasekhar (1943), so it can only provide an approximation to the treatment of dynamical friction in an inhomogeneous system. Kandrup (1980a) has shown that, for power-law density profiles, the left-hand side of eq. (5.1) should be multiplied by a factor up to about 3 in order to get the proper dynamical friction coefficient. However, eq. (5.1) has the merit of showing an explicit dependence of the dynamical friction on the correlation function. The implicit assumption underlying the derivation of eq. (5.1) is that the statistics of the gravitational field fluctuations is *unaffected* by the clustering, so one can apply all the mathematical formalism of Chandrasekhar (1943) assuming that clustering increases the local average density ($\rho(r) \rightarrow \rho(r)\left[1 + \xi(r)\right]$). However, we have shown in chapter 3 that clustering *modifies* the force probability distribution function, and in chapter 4 we have computed the dynamical friction coefficient (eq. 4.9) and we have found that it has a value different from the one given in eq. (5.1). It is interesting to attempt an analysis of the origin of the velocity bias based on our new equations.

An equation like eq. (5.1) alone, however, does not allow a complete analysis, because it is not self-consistent. Rather, it would be desirable to investigate how the introduction of a secular weakly dissipative term of dynamical friction into a complete set of moments of kinetic equations like the BBGKY hierarchy (Davis & Peebles, 1977) affects the evolution of the clustering. This poses a formidable mathematical problem, however. A possibly equivalent way could be to perform N-body simulations, although present-day computers do not yet allow to perform simulations on a very large dynamical range in a reasonable time.

In this chapter we will attempt to follow both these strategies, i.e. we will look for solutions of the BBGKY hierarchy and we will compare the results with the outputs of numerical simulations. In §5.2 we will discuss the BBGKY hierarchy and the modifications to take into account dynamical friction effects. In §5.3 we will look for *self-similar* solutions of the equations introduced in §5.2: the system of partial differential equations introduced in §2 will be shown to be equivalent to a system of ordinary differential equations, and we will solve the boundary value problem associated to this system. We then compare our solutions to those of Davis & Peebles (1977), and, in §5.4, to numerical simulations performed according to an algorithm which explicitly takes into account the frictional effects introduced by small-scale structure on the evolution of large-scale structure.

5.2 BBGKY Hierarchy.

A complete description of the clustering of matter in the Universe can be given by the knowledge of the $n-point$ probability distributions in configuration space $\rho^{(n)}$, defined in such a way that: $dP = \rho^{(n)}(\mathbf{x}_1, \mathbf{p}_1, ..., \mathbf{x}_n, \mathbf{p}_n, t) \cdot \Pi_1^n d\mathbf{x}_i d\mathbf{p}_i$ is the probability of finding particle i at a point $\mathbf{x}_i, \mathbf{p}_i$ at a given time t. In general, the BBGKY hierarchy of equations can be written (Fry, 1982):

$$\frac{\partial \rho^{(k)}}{\partial t} + \sum_{i=1}^{k} \frac{\mathbf{p}_k}{ma^2} \frac{\partial \rho^{(k)}}{\partial \mathbf{x}_i} + \sum_{i=1}^{k} \sum_{j \neq i}^{k} \frac{Gm^2}{a} \left[\frac{\partial}{\partial \mathbf{x}_i} \frac{1}{\mid \mathbf{x}_j - \mathbf{x}_i \mid} \right] \frac{\partial \rho^{(k)}}{\partial \mathbf{p}_i} +$$

$$\int d\mathbf{x}_{k+1} d\mathbf{p}_{k+1} \sum_{i=1}^{k} \frac{Gm^2}{a} \left[\frac{\partial}{\partial \mathbf{x}_i} \frac{1}{\mid \mathbf{x}_{k+1} - \mathbf{x}_i \mid} \right] \frac{\partial \rho_{k+1}}{\partial \mathbf{p}_i} = 0 \qquad (5.2)$$

It proves however more convenient to introduced the "reduced" correlation functions $c(1, .., k)$ defined as (Davis & Peebles, 1977; Peebles, 1980; Fry, 1982):

$$c(1) \equiv \rho^{(1)}(\mathbf{x}_1, \mathbf{p}_1, t),$$

$$c(1,2) \equiv \rho^{(2)}(\mathbf{x}_1, \mathbf{p}_1; \mathbf{x}_2, \mathbf{p}_2, t)) - \rho^{(1)}\mathbf{x}_1; \mathbf{p}_1, t)\rho^{(2)}(\mathbf{x}_2, \mathbf{p}_2, t),$$

$$c(1,2,3) \equiv \rho^{(3)}(\mathbf{x}_1, \mathbf{p}_1; \mathbf{x}_2, \mathbf{p}_2; \mathbf{x}_3, \mathbf{p}_3, t) - \rho^{(1)}(\mathbf{x}_1, \mathbf{p}_1, t)c(2,3) -$$

$$\rho^{(2)}(\mathbf{x}_2, \mathbf{p}_2, t)c(1,3) - \rho^{(3)}(\mathbf{x}_3, \mathbf{p}_3, t)c(1,2), \qquad (5.3)$$

and so on. In the following we will consider moments (and reduced moments) of these quantities. One of the most useful defines the two-point spatial correlation function:

$$\int d^3\mathbf{p}_1 d^3\mathbf{p}_2 c(1,2) = \left(na^3\right)^2 \xi\left(\mid \mathbf{x}_2 - \mathbf{x}_1 \mid, t\right), \tag{5.4}$$

and analogously one can define the three-point spatial correlation function $\zeta(1,2,3)$:

$$\int d^3\mathbf{p}_1 d^3\mathbf{p}_2 d^3\mathbf{p}_1 c(1,2,3) = \left(na^3\right)^2 \zeta\left(\mid \mathbf{x}_2 - \mathbf{x}_1 \mid, \mid \mathbf{x}_2 - \mathbf{x}_3 \mid, \mid \mathbf{x}_3 - \mathbf{x}_1 \mid, t\right) \tag{5.5}$$

We will not derive here all the set of moments of the BBGKY hierarchy, and in the following we will look for solutions of a system of equations derived from some of these moments. We mostly based our work on the [a[er by Davis & Peebles (1977), where a full account of the derivation can be found. We will only derive in full extent an equation for the average pairwise velocity:

$$\langle \mathbf{v}_{12} \rangle = \frac{1}{\left(na^3\right)^2} \int d^3\mathbf{p}_1 d^3\mathbf{p}_2 c(1,2) \left(\mathbf{v}_2 - \mathbf{v}_1\right)$$

Here an in the following, $\mathbf{v}$ denotes the proper velocity. As we already saw in the introduction to chapter 3, an approximate description of the motion of a particle in the gravitational field of an highly structured system (like the environment of a protogalactic distribution in a hierarchical clustering model) can be obtained by summing to the mean-field contribution $\nabla\Phi(\mathbf{r})$ a stochastic component with a given probablity distribution $W(F)$. However, this latter component is usually much smaller than the mean-field one (Kandrup, 1980b), and it changes on a very rapid time scale, so the average effect on a particle will be that of introducing a small drag force $-\eta\mathbf{v}$. The pairwise velocity $\mathbf{v}_{21}$ between two particles at position vectors $\mathbf{r}_1, \mathbf{r}_2$ will then obey the equation:

$$\frac{d\mathbf{v}_{21}}{dt} = -\left[\left(\frac{\dot{a}}{a}\right)\mathbf{v}_{21} + \eta(\xi)\mathbf{v}_{21}\right] - \left(\nabla_{\mathbf{r}_1}\Phi - \nabla_{\mathbf{r}_2}\Phi\right). \tag{5.6}$$

We must observe that this equation is valid only in an average sense, i.e. when one averages over a time scale longer than the typical scale $T(F)$ of duration of the stochastic force and smaller than a typical macroscopic time scale for the system. These two extreme time scales are usually well separated in realistic systems (Kandrup, 1980b), and eq. (5.6) gives an appropriate description of the motion. In this sense, this is only a *phenomenological* equation: the real equation of motion for a particle contains a first-order term which is a random variable of

time: $\mathbf{F}_{random}(t)$.

Multiplying eq. 5.6 by $c(1,2)$, integrating over momentum space and making use of eq. (72.1) from Peebles (1980) one obtains:

$$\frac{\partial \langle v_{21}\rangle^{\alpha}}{\partial t} + \langle v_{21}\rangle^{\alpha}\frac{\partial}{\partial t}\ln\left[\left(na^3\right)^2(1+\xi)\right] -$$

$$\frac{1}{1+\xi}\left\{\frac{1}{a}\frac{\partial}{\partial r^{\beta}}\left[(1+\xi)\left\langle v_{21}^{\alpha}v_{21}^{\beta}\right\rangle\right] + \frac{2Gm}{a^2}\frac{r^{\alpha}}{r^3}(1+\xi) + 2G\rho_b a\frac{r^{\alpha}}{r^3}\int_0^r d^3r\xi(r) -\right.$$

$$\left. 2G\rho_b a\int d^3r\zeta(1,2,3)\frac{r_{31}^{\alpha}}{r_{31}^3}\right\} = -\left[\left(\frac{\dot{a}}{a}+\eta\right)\right]\langle v_{21}\rangle\frac{r^{\alpha}}{r} + \frac{1}{1+\xi}\frac{\partial\phi}{\partial r^{\alpha}} \qquad (5.7)$$

In order to derive this equation we adopted the assumption of spatial homogeneity of the Universe, which is appropriate for the applications we have in mind which are restricted to Friedmann-Robertson-Walker models. Under this assumption all average quantities have components depending only on the radius, and this allows one to write $\mathrm{v}_{21} \equiv \langle v_{21}\rangle r^{\alpha}/r$. Finally, ρ_b in the latter equation denotes the background density.

In principle the BBGKY hierarchy provides an infinite system of equations for all the correlation functions. Under the hypothesis that the reduced correlation functions are separable in momentum and physical space, an exact solution of the hierarchy has been found (Davis & Peebles, 1977). However, this hypothesis restricts greatly the possible mathematical form of the three-pont spatial correlation function. Hansel et al. (1986) showed that this solution can reasonably be applied only in the highly nonlinear regime.

In this chapter we will follow a more physical approach and we will introduce a reasonable truncation scheme based on some plausible assumptions. In order to make easier the comparison with previous results, we will adopt the truncation scheme introduced by Davis & Peebles (1977), with some slight differences in the notation. Before writing the full system of moment equations we recall some of the notations adopted by Davis & Peebles (1977) and in this chapter. The second order moment $\langle v_{21}^{\alpha}v_{21}^{\beta}\rangle$ can be decomposed in radial (i.e. directed along the radius vector) and tangential components:

$$(1+\xi)\left\langle v_{21}^{\alpha}v_{21}^{\beta}\right\rangle = \left[\frac{\Sigma}{(ma)^2} + \frac{2}{3}\langle v_1\rangle^2\right]\delta^{\alpha\beta} + \frac{\Pi-\Sigma}{(ma)^2}\cdot\frac{r^{\alpha}r^{\beta}}{r^2} \qquad (5.8)$$

This quantity obeys an equation (Davis & Peebles, 1977, eqs. (48), (56)):

$$\frac{\partial}{\partial t}\left[(ma)^2\left(na^3\right)^2(1+\xi)\left\langle v_{21}^{\alpha}v_{21}^{\beta}\right\rangle\right] +$$

$$\frac{1}{ma^2}\frac{\partial}{\partial r^\alpha}\left[(ma)^3\left(na^3\right)^2(1+\xi)\left\langle v_{21}^\alpha v_{21}^\beta v_{21}^\gamma\right\rangle\right]+4Gm^3\left(na^3\right)^2(1+\xi)\left\langle v_{21}\right\rangle\frac{r^\alpha r^\beta}{r^4}+$$

$$2Gm^3\left(na^3\right)^3\int d^3r_3\frac{r_{31}^\alpha r_{31}^\beta}{r_{31}^3}\left\langle v_{23}\right\rangle\left[1+\xi\left(r_{23}\right)\right]+\frac{4Gm^2}{a}\left(na^3\right)^3\int d^3r_3\frac{\left\langle v_{21}\right\rangle}{r_{31}}\frac{r^\beta}{r}\frac{\partial}{\partial r_3^\alpha}\lambda\left(r_{12},r_{23},r_{31}\right)=0 \tag{5.9}$$

In this equation appears an important term, namely the skew third order moment $\langle v_{21}^\alpha v_{21}^\beta v_{21}^\gamma\rangle$. The main closure hypothesis of Davis & Peebles (1977) concerns this term. They suppose that the tensor:

$$\left\langle\left(\mathbf{v}_{21}-\left\langle\mathbf{v}_{21}\right\rangle\right)^\alpha\left(\mathbf{v}_{21}-\left\langle\mathbf{v}_{21}\right\rangle\right)^\beta\left(\mathbf{v}_{21}-\left\langle\mathbf{v}_{21}\right\rangle\right)^\gamma\right\rangle=0$$

This implies:

$$\left\langle v_{21}^\alpha v_{21}^\beta v_{21}^\gamma\right\rangle=-2\left\langle v_{21}\right\rangle^3\frac{r^\alpha r^\beta r^\gamma}{r^3}+$$

$$\left\langle v_{21}\right\rangle\left[\frac{r^\alpha}{r}\left\langle v_{21}^\beta v_{21}^\gamma\right\rangle+\frac{r^\beta}{r}\left\langle v_{21}^\alpha v_{21}^\gamma\right\rangle+\frac{r^\beta}{r}\left\langle v_{21}^\alpha v_{21}^\gamma\right\rangle\right] \tag{5.10}$$

This equation represents a crucial point in the development, because this severe truncation hypothesis eliminates the need to deal with high-order velocity dispersion terms.

Another final major approximation concerns the three-point spatial correlation function $\zeta(1,2,3)$ which is approximated as:

$$\zeta(r_{12},r_{23},r_{31})=Q\left[\xi\left(r_{12}\right)\xi\left(r_{23}\right)+\xi\left(r_{23}\right)\xi\left(r_{31}\right)+\xi\left(r_{31}\right)\xi\left(r_{12}\right)\right] \tag{5.11}$$

This equation is actually the first of a series coming out of an hierarchical expansion hypothesis for the n-th order spatial correlation functions which has been hypothesized by Groth & Peebles (1977) and discussed later by many authors (Fry, 1982, 1984, 1984b, 1985; Bouchet & Pellat, 1984; Balian & Schaeffer, 1985; Lucchin & Matarrese, 1988; Hamilton, 1988; Bernardeau, 1992). It turns out that the evolution at least until the early nonlinear regime (i.e. $\xi\approx 1$) can be well described by this equation, so this approximation for the purposes stated in the introduction is well suited.

We will not continue with a detailed derivation of the final set of equations: the major details can be found in Davis & Peebles (1977). The set of equations we will consider is the following:

$$\frac{\partial\xi}{\partial t}+\frac{1}{ar^2}\frac{\partial}{\partial r}\left[r^2(1+\xi)\left\langle v_{21}\right\rangle\right]=0 \tag{5.12}$$

$$\frac{\partial \Sigma}{\partial t}+\frac{1}{ar^4}\frac{\partial}{\partial r}\left\{r^4\langle v_{21}\rangle\left[\Sigma+\frac{2}{3}(ma)^2\langle v_1\rangle^2\right]\right\}+$$

$$\frac{8\pi}{3}Gm^3na^3\left\{\frac{1}{r^3}\int_0^r dzz^3(1+\xi)\langle v_{21}\rangle+\int_r^\infty dz(1+\xi)\langle v_{21}\rangle\right\}=0 \qquad (5.13)$$

$$(1+\xi)\frac{\partial\langle v_{21}\rangle}{\partial t}+\langle v_{21}\rangle\frac{\partial}{\partial t}(1+\xi)-\frac{1}{a}\cdot\frac{1}{(ma)^2}\left\{\frac{2}{3}\frac{\partial}{\partial r}\left[(ma)^2\langle v_1\rangle^2+\Pi\right]+\frac{3}{2r}(\Pi-\Sigma)\right\}+$$

$$\frac{2Gm}{a^2r^2}(1+\xi)+\frac{8\pi G\rho_b a}{r^2}\int_0^r drr^2\xi+I[\xi]=-(1+\xi)\left[\frac{\dot{a}}{a}+\eta\right]\langle v_{21}\rangle+\frac{d\Phi}{dr} \qquad (5.14)$$

$$\frac{1}{2}\frac{d\langle v_1\rangle^2}{dt}=\frac{1}{a}\frac{d}{dt}(aU)-\frac{\dot{a}}{a}\langle v_1\rangle^2, \qquad (5.15)$$

$$I[\xi]=-\frac{2G\rho_b Q}{(ma)^2}\frac{r^\alpha}{r^4}\int_0^\infty dz\int_0^\pi d\theta\sin\theta\int_0^{2\pi}d\phi z^2z^\alpha\xi(|\mathbf{z}-\mathbf{r}|)[\xi(z)+\xi(r)] \qquad (5.16)$$

$$U=2\pi G\rho a^2\int_0^\infty drr\xi(r,t) \qquad (5.17)$$

Eqs. (5.12- 5.17) constitute a system of 4 differential equations in 5 unknowns, namely: $\xi, \Sigma, \Pi, \langle v_{21}\rangle, \langle v_1\rangle^2$. We then need one more equation and some boundary conditions to determine completely the problem. Davis & Peebles (1987) considered a second order (in time) equation obtained from the diagonal component of the general equation for the second order velocty moments. This equation contains two integral terms which, after some approximations, are reduced to differential terms. These approximations however are enough arbitrary: they involve hypotheses on the behaviour of the correlation function in the nonlinear regime. Moreover in the final solutions they find that the behaviour of Π is rather arbitrary and ultimatelt depends on some joining conditions fro the boundary value problem.

We will follow another path, namely we will specify the relationship between Σ and Π. This amounts to specify the amount of anisotropy of the structures we are considering, and we feel it can provide an useful test for the physical models of structure formation. In particular, we will check whether the hypothesis of **previrialization** (Davis & Peebles, 1977; Peebles, 1990) can provide results consistent with the observations and with the numerical simulations.

5.3 Self-similar Solutions.

We will now look for self-similar solutions of the above system of equations (5.12- 5.17). Before doing this, we will take the fluid limit $m \to 0, n \to \infty$ with

$\rho = mn = const.$ This is necessary to eliminate the fourth term in the left-hand side of eq.(5.14) which prevents the possibility of obtaining a consistent set of equations under the hypothesis of self-similarity. This choice was also implicitly followed by Davis & Peebles (1977). Let us introduce a new variable: $s = r/t^{\alpha}$, where α is a coefficient which will be determined later. Let us also suppose that the dependence of the correlation function depends on r and t enters only through this quantity: $\xi(r,t) \equiv \xi(s)$. Substituting into eq.(5.12) we obtain the equation:

$$-\alpha \frac{s}{t}\frac{d\xi}{ds} + \frac{1}{ar^2}\frac{\partial}{\partial r}\left[r^2\left(1+\xi\right)\langle v_{21}\rangle\right] = 0$$

This equation ultimately constrains the dependence of $\langle v_{21}\rangle$ on r and t. One can verify by direct substitution that it can be satisfied only if:

$$\langle v_{21}\rangle = ast^{\alpha-1}\frac{\langle u_{21}\rangle(s)}{1+\xi} \tag{5.18}$$

One then verifies by direct susbtitution that eq. (5.12) becomes an ordinary differential equation:

$$\frac{d\xi}{ds} - \frac{1}{\alpha s^3}\frac{d}{ds}\left[s^3\langle u_{21}\rangle\right] = 0 \tag{5.19}$$

Proceeding in a similar way, one finds that all the equations (5.12- 5.15) can be expressed as ordinary differential equations in the independent variable s in the fluid limit, and in addition to eq. (5.19) we get the equations:

$$-\alpha s\frac{d\Sigma'}{ds} + 2\left(\alpha+\frac{1}{3}\right)\Sigma' + \frac{1}{s^4}\cdot\frac{d}{ds}\left\{s^5\frac{\langle u_{21}\rangle}{1+\xi}\left[\Sigma' + \frac{2}{3}\langle u_1^2\rangle\right]\right\} +$$

$$\frac{8\pi G\rho_b}{3}\left\{\frac{1}{s^3}\int_0^s d\sigma\sigma^4\langle u_{21}\rangle + \int_s^{\infty} d\sigma\sigma\langle u_{21}\rangle\right\} = 0 \tag{5.20}$$

$$-\alpha s\frac{d}{ds}\langle u_{21}\rangle + \left(\alpha-\frac{1}{3}\right)\langle u_{21}\rangle - \frac{1}{m^2c_0^3}\cdot\frac{1}{s}\left\{\frac{d}{ds}\left[\frac{2}{3}\langle u_1\rangle^2 + \Pi'\right] + \frac{3}{2}\cdot\frac{\Pi'-\Sigma'}{s}\right\} +$$

$$\frac{8\pi G\rho_b}{c_0^2 s^3}\int_0^s d\sigma\sigma^2\xi(\sigma) - \frac{2G\rho_{b0}Q}{c_0^2}\cdot\frac{s^{\alpha}}{s^4}\int_0^{\infty} d\sigma\int_{\Sigma^2} d^2\Omega\sigma^2\sigma^{\alpha}\xi(|\sigma - s|)\left[\xi(\sigma)+\xi(s)\right] =$$

$$= -\left[\frac{2}{3} + \eta'\left(V^{(2)}\right)\right]\langle u_{21}\rangle \tag{5.21}$$

$$-\alpha s\frac{d}{ds}\langle u_1^2\rangle + 2\left(\alpha-\frac{1}{3}\right)\langle u_1^2\rangle = 0 \tag{5.22}$$

$$V^{(2)} = 4\pi\int_0^{\infty} d\sigma\sigma^2\xi(\sigma) \tag{5.23}$$

where the quantities with an apex depend only on s and are connected to the unprimed quatities through the relations:

$$\Sigma = at^{2\alpha}\Sigma'(s), \quad \langle v_1\rangle^2 = \frac{at^{2\alpha}}{m^2a^2}\langle u_1\rangle^2(s), \quad \eta' \equiv \eta\left(\xi\left(s\right)\right) \tag{5.24}$$

We have also adopted the definitions: $c_0 = a_0 t_0^{-2/3}$.
The integral terms in equation (5.20) can be more conveniently reformulated as a differential term by defining two new variables:

$$J(s) = \frac{1}{s^3}\int_0^s d\sigma\sigma^4\langle u_{21}\rangle + \int_s^\infty d\sigma\sigma\langle u_{21}\rangle$$

$$K(s) = \frac{1}{s^3}\int_0^s d\sigma\sigma^4\langle u_{21}\rangle \tag{5.25}$$

which are related through the equations:

$$\frac{dJ}{ds} = -\frac{3}{s}K(s) \tag{5.26}$$

$$\frac{dK}{ds} = -\frac{3}{s}K(s) + s\langle u_{21}\rangle \tag{5.27}$$

The coefficient α is fixed by the boundary conditions on the correlation function ξ, and is connected to the index of the power-spectrum n by the relation (Davis & Peebles, 1977, eq. (84)):

$$\alpha = \frac{4}{9+3n}$$

Apart for the fact that we did not use any second order equation, the main difference between our set of equations and those of Davis & Peebles lies in the term η', which depends explicitly on a volume integral of the correlation function (i.e. on $V^{(2)}$), as we saw already in chapter 4. This term describes the effect of the dynamical friction and its dependence on the correlation function. Our system of equations describes then the dynamics of structure formation in a completely self-consistent way. Observe that it is still a linear system of equations, because also the coefficient η' depends linearly on ξ (via $V^{(2)}$).
We notice immediately that eq.(5.22) can be solved exactly and the solution reads:

$$\langle u_1\rangle^2(s) = \begin{cases} \left(\langle u_1\rangle^2\right)(s_0)\left(\frac{s}{s_0}\right)^\gamma & \alpha \neq \frac{1}{3} \\ \\ \langle u_1\rangle^2(s_0) & \alpha = 1/3 \end{cases} \tag{5.28}$$

The set of equations (5.18- 5.27) must be complemented by a set of boundary conditions which describe the behaviour of the solutions at the extremes of the integration interval. At any fixed time the extreme of the integration interval (s_-, s_+) define two corresponding scales r_-, r_+. On small scales one can assume that the correlation function ξ describes a nonlinear regime, while on large scales one can assume that it is still in the linear regime. The asymptotic behaviour of the correlation function in the nonlinear regime can be predicted to be a power-law: $\xi(s) \propto s^{-\gamma}, \quad \gamma = 2/(\alpha + 2/3)$ (Davis & Peebles, 1977, eq. (86)); inserting this equation into eq.(5.19) one can verify that also $\langle u_{21} \rangle$ must have the same asymptotyic behaviour and one obtains the boundary condition:

$$\xi(s_-) + \frac{3}{4}(2+n)\langle u_{21} \rangle(s_-) = 0 \tag{5.29}$$

Analogously, also in the linear regimes the behaviour of ξ is predicted to be a power law, although with a different exponent: $\gamma = 3 + n$, so one obtains the second boundary condition:

$$\xi(s_+) - \frac{3n}{4}\langle u_{21} \rangle(s_+) = 0 \tag{5.30}$$

Another boundary condition can be obtained from eq.(5.25) and from the condition that at small separation the variable $\langle u_{21} \rangle$ changes as a power law; one then obtains:

$$K(s_-) - s_-^2 \langle u_{21} \rangle(s_-) = 0 \tag{5.31}$$

At large s_+ one can similarly exploit the power law behaviour of $\langle u_{21} \rangle$ to obtain:

$$K(s_+) - \frac{1}{n} s_+ \langle u_{21} \rangle(s_+) = 0 \tag{5.32}$$

At large s the last term in the equation for $J(s)$ (eq.(5.24)) can be considered very small w.r.t. the first, and one has:

$$J(s_+) = K(s_+) \tag{5.33}$$

Finally, under the assumption that the center of mass is at rest, one obtains:

$$\int_{s_-}^{s_+} d\sigma \sigma \langle u_{21} \rangle = 0$$

from which one obtains the boundary condition:

$$J(s_-) - J(s_+) = K(s_-) - K(s_+) \tag{5.34}$$

We have then obtained a closed system of 6 equations, namely eqs.(5.19, 5.20, 5.21, 5.23, 5.26, 5.27) and the associated boundary conditions given in eqs.(5.29- 5.34). In addition we have to specify the velocity anisotropy as a relation between Π and Σ.

5.4 Results.

We have solved numerically the system of equations considered in the precedinga section using an algorithm based on a relaxation method with 1000 grid points; the implementation is the one given by Press et al. (1986) in the routine SOLVDE. The integration interval (s_-, s_+) was chosen in such a way as to cover the distance interval 50 Kpc-100 Mpc by the present epoch. The initial guessed solutions satisfy the boundary conditions asymptotic behaviours, according to the preceding discussion. The initial guess for $\xi(s)$ was then chosen to be a power-law with two different exponents at small and large s, joining smoothly in the middle part. Substituting this into eq.(5.19) we then obtained the initial guess for $\langle u_{21} \rangle$, and proceeding this way we obtained all the other initial guesses.

Peebles (1990) suggested that torques induced by substructure could induce random motions inside primordial structure which ultimately could reach a virialized, quasi-relaxed state at an eopoch approximately coinciding with the epoch of turnaround, i.e. during the linear and early nonlinear stage. If the system is virialised, one expects the relation $\Pi = \Sigma$ to be approximately verified, and this is the assumption we are adopting.

Dynamical friction could well act as the source of previrialization, and if this happens already during the linear phase one should be able to observe the consequences on the pairwise velocity profile: one expects friction to reduce the mean pairwise velocity w.r.t. the unperturbed case. As one can see from Figure 14, this is precisely what happens: the pairwise velocity is lower at larger separations than in the case without dynamical friction. Here we have assumed a Cold Dark Matter spectrum, and the dependence of the dynamical friction coefficient on the correlation function is as specified in chapter 4. The difference is not very large, approximately 30 Km/sec: remember however that, as we said in the preceding chapter, the coefficient η is probably underestimated. Moreover, the shape of the plot shows that also also the pairwise velocity dispersion is diminished w.r.t the no-friction case, because the half-maximum width is smaller. It is also interesting

to observe that the correlation function is not very much affected by the dynamical friction (Figure 13): the crossing point at which $\xi > 1$ is identical in the two cases.

Our solutions cannot be directly compared to those of Davis & Peebles, because the system of equations and boundary conditions we considered are different. This explains some differences in the results: for example, our solutions for ξ and $\langle v_{21} \rangle$ decrease very fast after the maximum. This is a consequence of the hypothesis of complete isotropy $\Pi = \Sigma$, which imposes a clear truncation of the system if it has to have a finite total energy, while Davis & Peebles (1977) left the value of Π to vary freely and to compensate for the negative gradients of the other quantities.

We find a sharp decrease of the average pairwise velocity also in a set of numerical simulations we performed in order to gain more insights into the effects of dynamical friction. These simulations were run using a copy of the TREECODE, kindly provided to us by L. Hernquist, which we modifies as we are going to shortly describe. The TREECODE implements a tree algorithm for the calculation of forces and has been widely discussed elsewhere (e.g. Barnes & Hut, 1986; Hernquist, 1987). In short, the force acting on a given particle is written as the sum of two components: $\mathbf{F} = \mathbf{F}_{nn} + \mathbf{F}_{smooth}$, where $\mathbf{F}_{nn}$ is the force coming from the direct summation of the newtonian potential provided by the nearest neighboors (defined according to some "proximity" parameter), and $\mathbf{F}_{smooth}$ is the contribution coming from an expansion up to quadrupole terms of the gravitational potential of the distribution of all the other particles. However, in general, the fluctuating component of the gravitational field is badly reeproduced in N-body codes. This can be seen by comparing the average values of the fluctuating force in N-body simulations with the one predicted on the basis of the CDM model. From Kandrup (1980a) we know that in a discrete system composed of point-like objects of mass m having an average density n the average fluctuating force is given by (apart for some constant numerical factors): $\bar{F} \propto Gmn^{2/3}$. Suppose now that in the real system the fluctuating field is generated by a population of n_p peaks having characteristic mass $m_p = M_{tot} f^3$, f^3 being the fraction of the volume composed of peaks, while in the numerical simulation we have N_{sim} particles and the total mass of the system is M_{tot} within a radius R_{sys}. One then has: $m_{sim} = M_{tot}/N_{sim}$, $n_{sim} = N_{sim}/R_{sys}^3$, and taking for n_p the value given in

chapter 4, namely: $n_p = 1.6 \times 10^{-2} \cdot [(n+5)/6]^{3/2} f^{-3} R_{sys}^{-3}$, one finally gets:

$$\frac{\bar{F}_{sim}}{\bar{F}_p} \approx 15.75 \times \frac{6}{n+5} \cdot N_{sim}^{-1/3} f^{-1} \tag{5.35}$$

In a treecode one takes into account direct interaction only with a fraction of all the particles N_{sim}; typically if $N_{sim} = 50000$ an average particle "sees" by direct summation about 500 particles in the simulations we performed. Then from eq.(5.35) one has: $\bar{F}_{sim}/\bar{F}_p > 30.9$. This suggests that only the high-force, low probability component of the fluctuating field is actually taken into account: all the small fluctuations induced by the small scale substructure are simply not included.

To remedy the situation we modified the TREECODE by including a *small scale* force component $\mathbf{F}_{(ss)}$ in the treecode. This is generated by a Montecarlo generator which at fixed timesteps scans the probability distributions found in chapter 3 and adds this component to the force field. The duration of the force is computed after Kandrup (1980a), and the parameters of the distributions are those appropriated to the CDM spectrum. Essentially, our modified TREECODE is a combined N-body and Montecarlo code: the random process generated by the Montecarlo part reproduces the low-amplitude, high-frequency part of the fluctuating gravitational field.

The introduction of the Montecarlo process tends to worsen energy conservation. This is because one does not take into account the back reaction of the fluctuating force field on the total energy and angular momentum of the "invisible" peaks' population which induces the fluctuating field. We then arbitrarily reduced the average value of the stochastic force until at the end of the runs energy was conserved as in the original runs not including the fluctuating field, i.e. to approximately 5%. A more appropriate procedure would consist in taking into account the evolution of the low-density substructure, giving some prescription on the way how it evolves with the background density, and considering how it is transformed in larger mass substructure (i.e. in actual particles of the simulations). We implemented recently such an algorithm, but the raise in computational time did not allow us to run simulations with more than 5000 particles. Although the results are encouraging, we feel that they are not yet definitive and rather we prefer to show the results we obtained with the first procedure.

The results refer to numerical simulations performed with 50000 particles. CDM

initial condition were created according to the algorithm by West et al. (1987). The only difference is that the particles were initially distributed in a quasi-random way inside a spherical region having an initial radius corresponding to 21 Mpc at the actual epoch. The quasi-random initial position and velocity generator is based on the Sobolev algorithm (Press & Teukolsky, 1989), and generates initial positions which are strongly anticorrelated on small scales. The initial positions and velocities are then sligthly modified according to the Zeldovich solution. Our procedure should reduce the small-scale periodicities which are generated when the particles are initially put on a regular cubic lattice (Peebles, 1990), although one must allow a sufficient initial number of particles to reduce the Poisson noise. Our choice of $N_{sim} = 50000$ meets this condition.
In Figure 16 we show the variation of the average pairwise velocity with separation. This plot should be compared with the analogous plots from Efstathiou et al. (1988) (Figure 5). The main striking difference is the reduced discrepancy between the observed velocities and the Hubble prediction in our case. The interpretation is simple: dynamical friction reduces the average pairwise velocities among particles. Similar effects were also observed in the simulations by Carlberg & Dubinsky (1991), who prefer rather to speak of "velocity bias". Observe also the sharp decline with distance, in agreement with the solutions of the boundary value problem found in the preceding section. The effect of dynamical friction is evident also on the pairwise velocity distribution function (Figure 16) which is remarkably simmetric, while Efstathiou et al. (1988) find asymmetries generated by large bulk flows. We believe that these asymmetries are reduced when a small amount of dynamical friction is added.

5.5 Final Remarks.

Our main purpose in this chapter was to study the effects of a dynamical friction coefficient assumed to depend realistically on the correlation function on the evolution of clustering in CDM models. In chapter 4 we saw that the effects on the dynamics of shell were little but detectable, especially low δ, slowly evolving environments. We have confirmed this fact in this chapter in a twofold way: by looking for a self-similar solution of the BBGKY hiearchy with a proper truncation and by N-body simulations. The results are qualitatively comparable: we have not attempted a quantitative comparison because we made many hypothe-

ses to truncate the BBGKY hierarchy and it is not very clear whether hypotheses are verified in the numerical simulations.

It is tempting to try to compare our results with those recently obtained by Carlberg (1991) and Carlberg & Dubinsky (1991). The "velocity bias" of the highest density peaks in their numerical simulations, i.e. the tendency of high density peaks to have smaller pairwise velocities and velocity dispersions, could be explained as a dynamical friction effect, and in fact the above authors suggest this interpretation. High density peaks inside their numerical simulations are bounded regions which move within the field generated by the background particles: these latter produce the fluctuating field which exerts a drag on high density peaks. However, we have also shown that the average properties of the force probability distribution generated by the particles in a N-body code do not coincide with those one expects in a CDM scenario, where much more abundant and diffuse substructure cluster in a hierarchical way to produce the present-day observed structure. We have remedied to this situation by modifying a N-body code adding this small amplitude, gravitational force "noise" according to the probability distributions found in chapter 3, and the results have shown a better agreement with the predictions from the self-similar solutions of the BBGKY hierarchy.

One problem of the present work is that the evolution of small-scale substructure is not taken into account, i.e. the coefficient of dynamical friction do not depend explicitly on time. However, we took explicitly into account its dependence on the correlation function, and this produced a clear effect on the fact that the discrepancy between pairwise velocity and Hubble-law predictions in the numerical simulations tends to be reduced at small separation, i.e. where the correlation function is larger. We think it would be interesting to check whether this discrepancy will be similarly reduced when numerical simulations which take into account the temporal evolution of substructure will have been completed.

Figure Caption.

Figure 13.–Correlation functions. We plot the results for the case in which no dynamical friction is included ($\eta = 0$, *solid line*), and those with a coefficient $\eta(\xi) = \eta_{CDM}$ computed as described in the text (*dashed line*). The parameter s' depends on the assumed scaling of the configuration.

Figure 14.–Pairwise velocities. In ordinate the average pairwise velocity is displayed. $\eta = 0$: *solid line*, $\eta = \eta_{CDM}$: *dashed line*. Absolute value of the Hubble velocity ($\equiv -(2/3)s$): *dotted line*. The parameter s_0 is the scale at which the correlation function becomes nonlinear ($\xi = 1$)

Figure 15.–Average pairwise velocities from N-body simulations. The open stars are averages over 10 simulations, the dotted line is the Hubble profile.

Figure 16.–N-body Pairwise velocity distribution. The histogram shows the distribution of the relative frequency of particle numbers vs. the pairwise velocity.

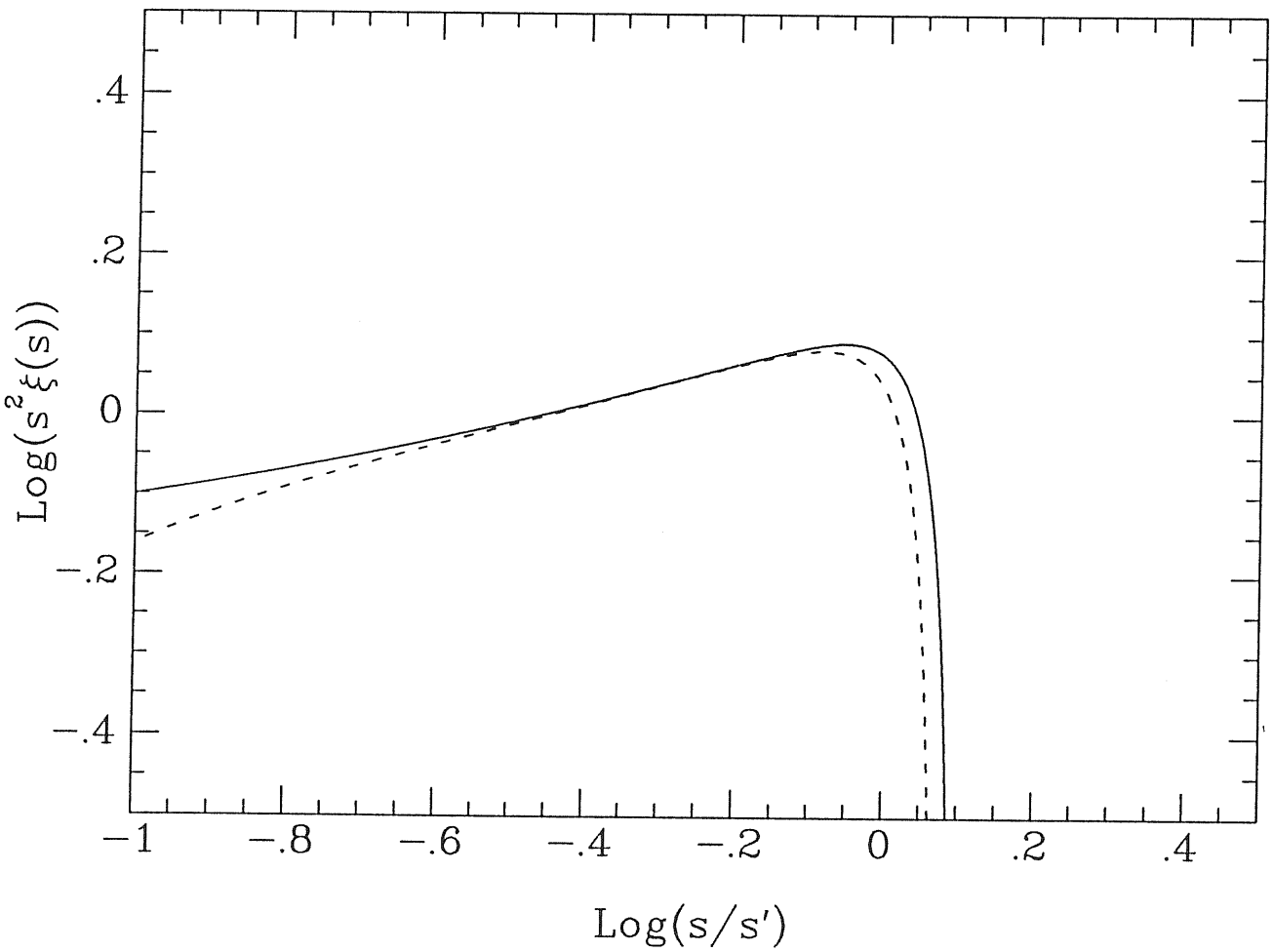

Fig. 13

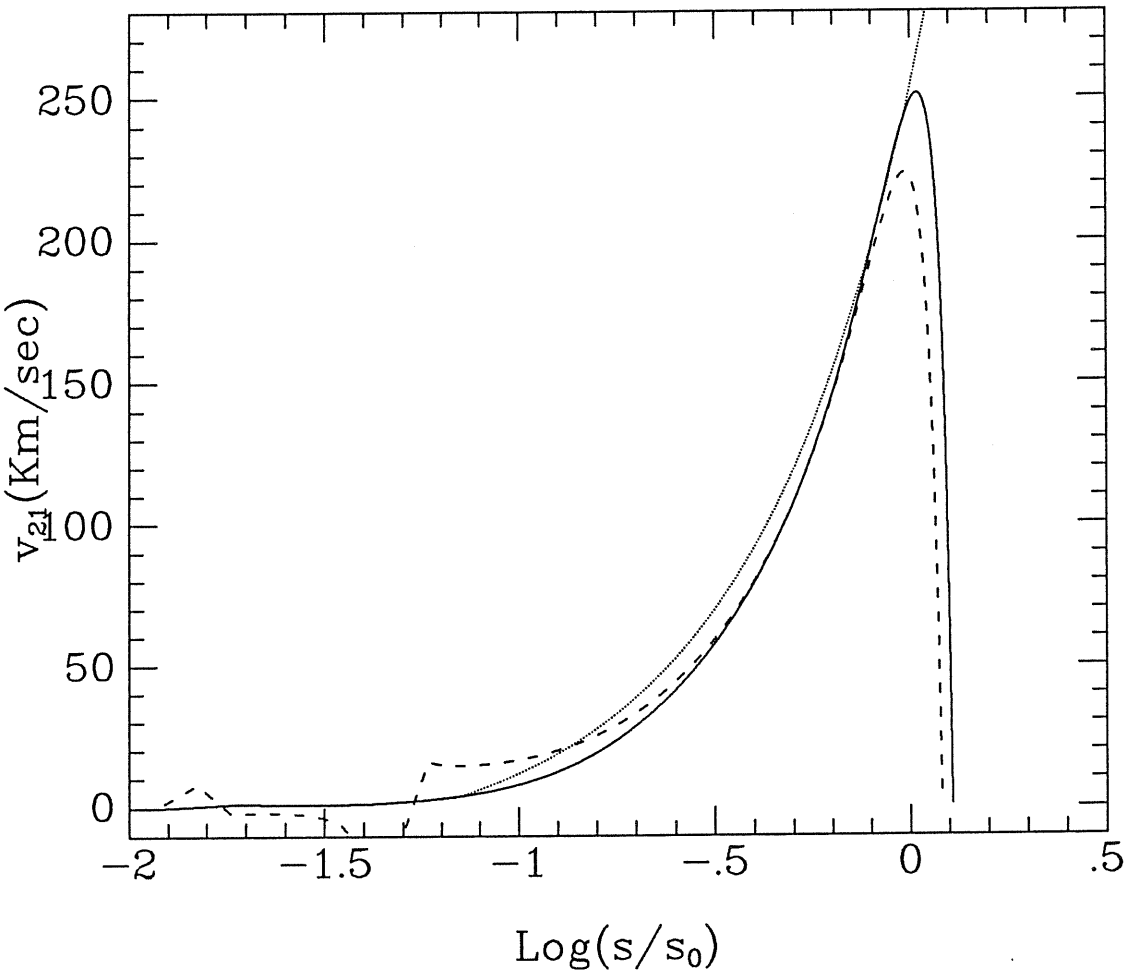

Fig. 14

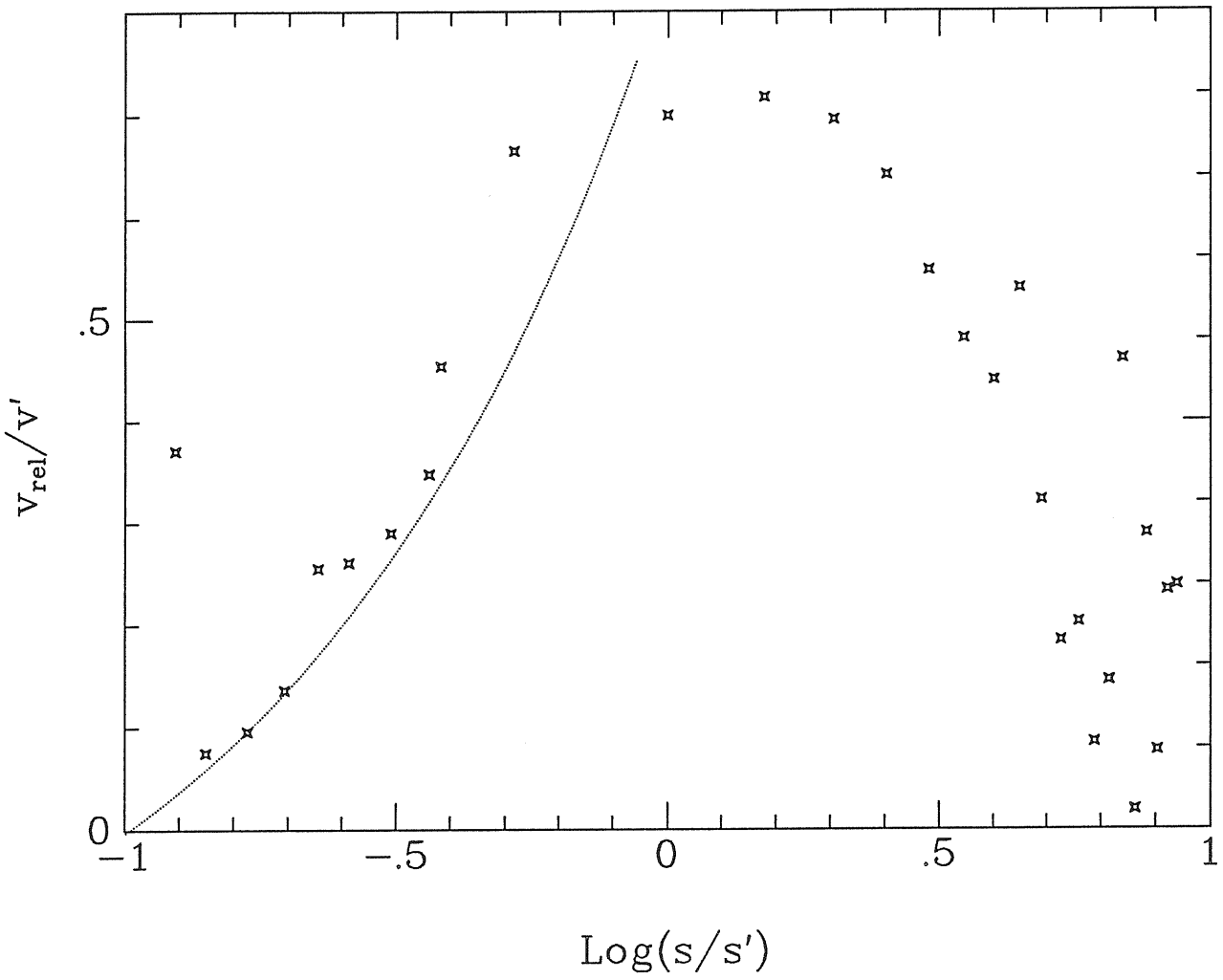

Fig. 15

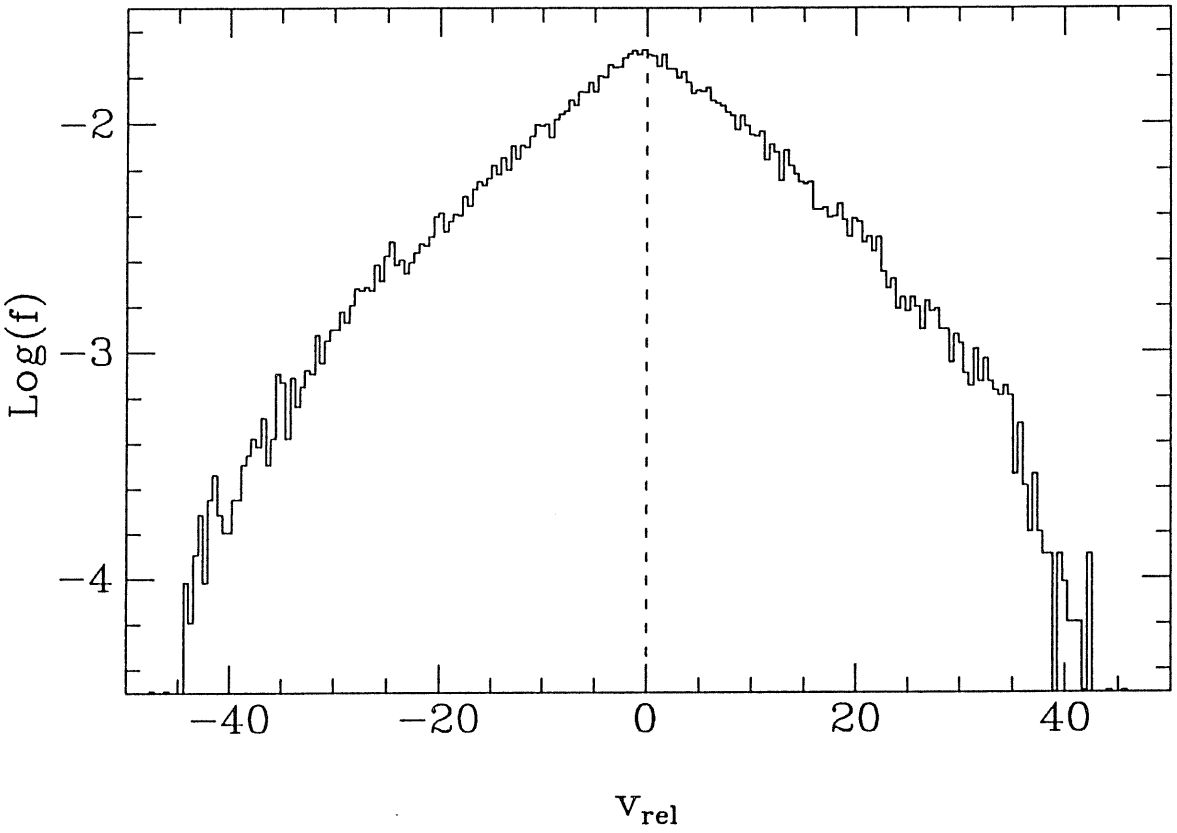

Fig. 16

Chapter 6

Concluding Remarks and Prospects for Future Work.

The main purpose of this thesis was to present some insights into the effect of dynamical friction on the dynamics of structures which form on cosmological time scales, like clusters of galaxies. The idea that dynamical friction can significantly affect the evolution of clusters has been studied by many authors, starting with the seminal paper by White (1977). Most of these studies have made use of the classical Chandrasekhar (1943) formula, or of some corrections to it which take into account the effect of inhomogeneities (Kandrup 1980a) and/or anisotropy of the matter distribution (Binney, 1977), but not the dependence of dynamical friction on clustering. Our purpose in this thesis was that of investigating better the theoretical foundations of a theory of dynamical friction inside a clustered medium, and to discuss some of its predictions. Our theory strictly applies only to the linear stages of evolution: however it can be extended to the early nonlinear stages, and non-gaussian terms can easily be included.

We also derived an equation for the torques' probability distribution which could be applied to predict the amount of previrialization induced by substructure. Despite recent efforts (Peebles, 1990), the issue of previrialization is still unsolved, and our results suggest that a key point could arise from the coupling between clustering and tidal torques' field.

One of the crucial issues is the comparison with observations. Our predictions apply to the outer infalling regions of clusters, and could then be checked against observations of infall patterns around rich clusters (Schechtman, 1982; Ostriker et al., 1988; Regös & Geller, 1989). The infall pattern of galaxies are used to

predict values of Ω by comparison with linear theory's predictions, and a detailed modelling of the motions of the outer shells is then necessary. One difficulty lies in the estimation of the tidal field originated from deviations of the inner distribution from spherical symmetry and from surrounding clusters. However, once a model for the density distribution is chosen, it is possible to predict in detail the velocity field around the cluster.

Some useful indications about the effect of dynamical friction on the structure of the innermost relaxed parts of clusters can come out of numerical simulations. In this respect, the outputs of extensive investigations using the modified TREECODE we described in chapter 5, which we are presently analyzing, could tell us something about the effect of a clustering-dependent dynamical friction coefficient on the relaxation processes acting inside clusters' cores: ultimately about the density and velocity dispersion profiles, and so on. This work is complementary to the self-similar solutions described in Chapter 5, and there is much to learn from a comparison between them.

Many more data about substructure in clusters and the outer infalling regions are becoming available (e.g. Briel et al., 1991). After the completion of the ROSAT survey it is reasonable to expect that the predictions of cluster formation theories, like the present one, could be tested and tell us much more about the formation of structure in the Universe.

6.1 Bibliography for Chapters 3, 4, 5 and 6.

Ahmad, A., and Cohen, L., *Ap. J.*, **179**, 885 (1973)

Ahmad, A., and Cohen, L., *Ap. J.*, **188**, 469 (1974)

Antonuccio–Delogu, V., and Atrio–Barandela, F., *Ap. J.* **392**, 403 (1992)

Bardeen, J. M., Bond, J. R., Kaiser, N. and Szalay, A.S., *Ap. J.* **304**, 15 (1986)

Bahcall, N., *Ap. J.***232**, 689 (1979)

Balian, R., and Schaeffer, R.J., *Ap. J.***335**, L43 (1988)

Barnes, J., and Hut, P., *Nature* **324**, 444 (1986)

Bernardeau, F., *Ap. J.* **392**, 1 (1992)

Bertschinger, E., *Ap. J. Supp.* **58**, 39 (1985)

Bertschinger, E. and Watts, P.N., *Ap. J.* **323**, 23 (1988)

Binggeli, B., Sandage, A. and Tammann, G. A., *Ann. Rev. Astron. Astrophys.* **26**, 509 (1988)

Binney, J., *M.N.R.A.S.* **181**, 735 (1977)

Bleistein, N., Handelsman., R. A., Asymptotic Expansions of Integrals, 2nd ed., (New York: Dover) (1986)

Bond, J. R., and Efstathiou, G., *Ap. J.* **285**, L45 (1984)

Bouchet, F. R., and Pellat, R., *Astron. Astrophys.* **141**, 77 (1984)

Bourland. F.J., and Haberman, R., *SIAM J. Appl. Math.*, **48**, 737 (1988)

Bourland. F.J., and Haberman, R., *SIAM J. Appl. Math.*, **50**, 1716 (1990)

Briel, U. G., Henry, J. P., Schwarz, R. A., Böhringer, H., Ebeling, H., Edge, A. C., Hartner, G. D., Schindler, S., Trümper, J. and Voges, W., *Astron. Astrophys.* **246**, L10 (1991)

Bower, R. G., *M.N.R.A.S.* **248**, 332 (1991)

Carlberg, R.G., *Ap. J.* **367**, 385 (1991)

Carlberg, R.G., and Dubinsky, J., *Ap. J.* **369**, 13 (1991)

Cavaliere, A., Colafrancesco, S., and Scaramella, R., *Ap. J.* **380**, 1 (1991)

Cavaliere, A., Colafrancesco, S., and Menci, N., invited lecture at the NATO ASI on "*Clusters and Superclusters of Galaxies*" (1991)

Chandrasekhar, S., *Ap.J.* **94**, 511 (1941)

Chandrasekhar, S., *Rev. Mod. Phys.* **15**, 1 (1943)

Chandrasekhar, S., and von Neumann, J.,*Ap. J.* **95**, 489 (1942)

Chandrasekhar, S., and von Neumann, J.,*Ap. J.* **97**, 1 (1943)

Davis, M., and Peebles, P.J.E.,*Ap. J.* **267**, 465 (1976)

Davis, M., and Peebles, P.J.E.,*Ap. J. Supp.* **34**, 425 (1977)

Efstathiou, G., in Physics of the Early Universe, Peacock, J. A., Heavens, A. F. and Davies, A. T. eds., p. 361, (Edinburgh: Scottish Universities Summer School in Physics Press) (1990)

Fall, M., and Saslaw, W.C.,*Ap. J.* **204**, 361 (1976)

Farouki, R.T., Hoffman, G.L. and Salpeter, E. E., *Ap. J.* **271**, 11 (1983)

Fitchett, M., and Merritt, D.,*Ap. J.* **335**, 18 (1986)

Fillmore, J. A. and Goldreich, P., *Ap. J.* **281**, 1 (1984)

Fry, J. N., *Ap. J.* **262**, 424 (1982)

Fry, J. N., *Ap. J.* **279**, 499 (1984)

Fry, J. N., *Ap. J.* **277**, L5 (1984b)

Fry, J. N., *Ap. J.* **289**, 10 (1985)

Fry, J. N., *Ap. J.* **308**, 171 (1986)

Geller, M.J., in *"Clusters of Galaxies"*, Oegerle, W.R., Fitchett, M. J. and Danly, L., eds., p.25 (Cambridge: Cambridge University Press) (1990)

Gioia, I.M., Henry, J.P., Maccacaro, T., Morris, S.L., Stocke, J.T., and Woltjer, A., *Ap. J.* **336**, L35 (1990)

Grinstein, and Wyse, M. B., *Ap. J.***310**, 19 (1986)

Groth, E.J. and Peebles, P.J.E., *Ap. J.***217**, 385 (1977)

Gunn, J. E., *Ap. J.* **218**, 592 (1977)

Gunn, J.E., and Gott, J.R., III, *Ap. J.* **176**, 1 (1972)

Gradshteyn, I. S., and Ryzhik, I. M., Tables of Integrals, Series, and Products, 4th. ed. (New York: Academic Press) (1968)

Hamilton, A. J. S., *Ap. J.* **332**, 67 (1988)

Hansel, D., Bouchet, F.R., Pellat, R., and Ramani, A., *Ap. J.* **310**, 23 (1986)

Heavens, A. F., and Peacock, J. A.,*M.N.R.A.S.* **232**, 339 (1988)

Henry, J.P., and Arnaud, K.A., *Ap. J.* **372**, 410 (1991)

Hernquist, L., *Ap. J. Supp.* **64**, 715 (1987)

Hoffmann, Y., *Ap. J.* **328**, 489 (1988)

Hoffmann, Y., *Comm. Astrophys.* **14**, 153 (1989)

Hoffmann, Y. and Shaham, J., *Ap. J.* **297**, 16 (1985)

Hoffmann, Y. Shaham, J., and Shaviv, G., *Ap. J.* **262**, 413 (1982)

Kandrup, H. E.,*Phys. Rep.* **63**, 1 (1980a)

Kandrup, H. E.,*Ap. J.* **244**, 1039 (1980b)

Kandrup, H. E.,*Ap. J.* **272**, 1 (1983)

Kashlinsky, A.,*Ap. J.* **306**, 374 (1986)

Kashlinsky, A.,*Ap. J.* **312**, 497 (1987)

Kashlinsky, A., and Jones, B. J. T., NORDITA preprint 90–45/A (1990)

Lucchin, F., and Matarrese, S,*Ap. J.* **330**, 535 (1988)

Ostriker, E.C., Huchra, J.P., Geller, M.J., and Kurtz, M.J., *A.J.* **96**, 1775 (1988)

Padmanabhan, T.,*Phys. Rep.* **188**, 285 (1990)

Peacock, J. A., and Heavens, A. F.,*M.N.R.A.S.* **217**, 805 (1985)

Peebles, P. J. E.,*Ap. J.* **189**, L51 (1974)

Peebles, P. J. E., The Large Scale Structure of the Universe, (Princeton: Princeton University Press) (1980)

Press, W.H., Flannery, B.T., Teukolsky, S.A. and Vetterling, W.T., *Numerical Recipes*, (Cambridge: Cambridge University Press) (1986)

Press, W.H., and Schechter, P., *Ap. J.* **187**, 425 (1974)

Press, W.H., and Teukolsky, S.A., *Computers in Physics* **3**, 76 (1989)

Regös, E., and Geller, M. J., *A. J.* **98**, 755 (1989)

Rozgacheva, I. K.,*Astrophysics* **28**, 368 (1988)

Ryden, B. S., *Ap. J.* **329**, 589 (1988a)

Ryden, B. S., *Ap. J.* **333**, 78 (1988b)

Ryden, B. S. and Gunn, J. E., *Ap. J.* **318**, 15 (1987)

Schechtman, S.A., *Ap. J.* **262**, 9 (1982)

Scherrer, R. J., Melott, A. L and Shandarin, S. F., *Ap. J.* **377**, 29 (1991)

Yepes, G., Domínguez-Tenreiro, R. and del Pozo-Sanz, R., *Ap. J.* **373**, 336 (1991)

West, M.J., in *"Clusters of Galaxies"*, Oegerle, W.R., Fitchett, M. J. and Danly, L., eds., p. 65 (Cambridge: Cambridge University Press) (1990)

West, M.J., Oemler Jr., A., and Dekel, A., *Ap. J.* **327**, 1 (1988)

White, S. D. M.,*M.N.R.A.S.* **174**, 19 (1976)

White, S. D. M.,*M.N.R.A.S.* **170**, 33 (1977)

Zwillinger, D., *Handbook of Differential Equations*, New York: Academic Press (1989)